2019 - 2020 年度报告 ANNUAL REPORT

CONTENTS 目录

ABOUT CSRC	中心简介	01 - 06
PEOPLE	人员情况	07 - 23
RESEARCH HIGHLIGHTS	科研亮点	24 - 72
RESEARCH PROJECTS	科研项目	73 - 83
PUBLICATIONS	发表论文	84 - 99
EVENTS	学术活动	100 - 108
COLLABORATIONS	合作交流	109
VISITORS	学术访问	110
CSRC HOME-BUILDING	科研大楼	111 - 113

本册所列所有信息为2019年8月1日至2020年7月31日学术年期间

北京计算科学研究中心（以下简称中心）是隶属于中国工程物理研究院的独立法人单位，是以计算科学为牵引的多学科基础研究机构。中心成立于2009年8月。中心的定位是开展计算科学研究，促进科技发展，打造一个国际一流的开展计算科学及相关学科交叉研究的综合平台。

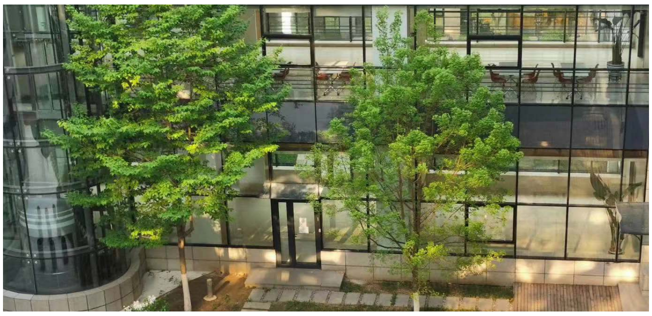

中心积极引进高层次人才，努力开展计算科学相关学科的交叉和创新研究，共有七个研究部：物理系统模拟研究部、量子物理与量子信息研究部、材料与能源研究部、复杂系统研究部、应用与计算数学研究部、力学研究部、计算方法研究部。截至2020年8月，中心的科研人才队伍包括17位讲座教授、1位教授、5位研究员、9位特聘研究员、5位特聘副研究员和2位工程师。另外，中心还有签约客座教授38位、博士后105位、博士/硕士研究生106位。他们的研究领域涵盖了数学、力学、物理学、化学、材料科学、计算机科学等多个基础、前沿领域。

2019-2020学术年期间，中心公开发表国际学术论文368篇，主办合办国内外学术会议8场，开设培训班6场，举办科技前沿讲座1期，邀请学术报告57期，接待来自10多个国家和地区的访问学者300余人次。中心还积极与国内外知名科研机构以合办会议、合带博士后、人员互访等丰富形式开展合作，努力推动学科交叉、加强学术交流。

作为一个基础性、跨学科、开放式的综合研究平台，中心将成为中物院在各个研究领域开展创新研究的重要支撑，开展对外科学技术交流合作的桥梁和纽带，高层次人才引进与培养的摇篮，同时填补我国计算科学相关学科交叉研究领域的空白。

中心定位与目标

1. 开展科学前沿研究

◇ 以计算科学研究为手段，以重大科学技术工程的实施和发展需求为牵引，积极引进海内外高层次人才，促进人才培养，开展基础性、前沿性、关键性和交叉性的研究工作；

◇ 加强对外学术技术交流，促进与国际知名科研机构的合作，搭建开放式、综合性、国际化的科研平台；

◇ 探索适于科研创新的管理体系，落实机制改革创新，提升我国科技自主创新能力，增强我国科技综合实力。

2. 发挥科学支撑效能

◇ 将科学前沿研究获取的新知识、新思想、新概念、新方法新手段通过多种方式转移到中物院其他研究机构；

◇ 与中物院其他机构合作，开展国家安全领域所需的新技术、新方法、新思路、新手段，乃至产生新工艺、新机理、新材料、新体系的研究；

◇ 拓展育新，根据中物院战略发展需求，布局和开展探索性、先导性研究，服务于院和国家未来发展的需要。

ABOUT CSRC

Beijing Computational Science Research Center (CSRC) is a multidisciplinary research organization under the auspices of the China Academy of Engineering Physics (CAEP). Established in August 2009, CSRC positions itself as a center of excellence in computational science research addressing current and critical issues in multidisciplinary of Mathematics, Mechanics, Physics, Chemistry, Materials Science, and Computational Science.

Mission of CSRC

◎ Carry out fundamental, frontier, critical, and multidisciplinary research with advanced computational approaches, thereby attract talents worldwide and train highly qualified research personnel, to support grand scientific development and technology innovation in China;

◎ Develop and maintain collaboration with research institutes elsewhere by building a comprehensive and internationalized research platform, to support academic and technological exchange and advancement;

◎ Innovate and reform organizational structures, management policies and methods for enabling creative and effective scientific research, to raise our national competence in technology innovation and enhance our comprehensive strength in science and technology.

Specifically, CSRC supports the development and implementation of grand challenging projects in natural science and engineering where computational modeling and simulation play a key role. CSRC also encourages its members to engage in the development of computational algorithms and software.

As of August 2020, CSRC has 37 faculty members, 2 engineers, 38 associate members, 105 postdoctoral fellows and 106 students. With its talented research staff, CSRC has established the following seven divisions: Simulation of Physical Systems, Quantum Physics and Quantum Information, Materials and Energy, Complex Systems, Applied and Computational Mathematics, Mechanics, and Algorithms. In research performance, CSRC has published 368 papers, organized 8 academic conferences and workshops, 6 tutorials, 1 colloquium on scientific frontiers, and 57 CSRC seminars. CSRC has also forged partnerships with many prestigious universities and research institutes around the world.

ORGANIZATION 中心组织构架

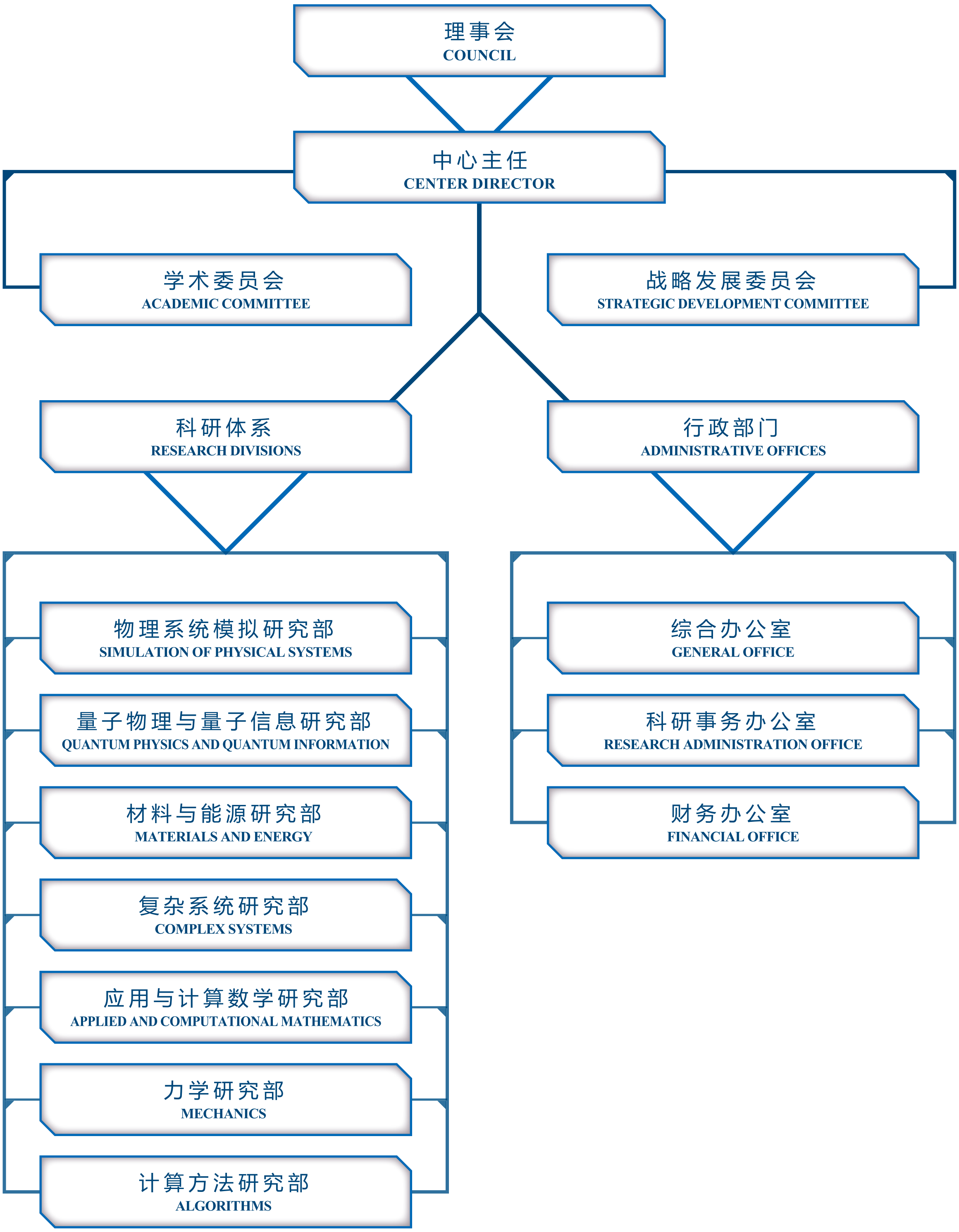

PLASMON-ENABLED ROOM-TEMPERATURE VALLEYTRONIC TRANSISTOR [25
等离激元辅助的室温工作能谷电子学器件 [26

LARGE OUT-OF-PLANE PIEZOELECTRICITY OF OXYGEN FUNCTIONALIZED MXENES FOR ULTRATHIN PIEZOELECTRIC CANTILEVERS AND DIAPHRAGMS [27
超薄压电悬臂和隔膜的氧官能化二维过渡金属碳化物的大外平面压电效应 [28

PLASMON-ENABLED TWO-DIMENSIONAL MATERIALS-BASED OPTOELECTRONIC DEVICES [29
等离激元增强二维材料光电器件综述 [30

FAST ENANTIO-CONVERSION OF CHIRAL MIXTURES BASED ON A FOUR-LEVEL DOUBLE-Δ MODEL [31
基于四能级双Δ型模型的快速手性转化 [32

MAGNETIC NOISE ENABLED BIOCOMPASS [33
基于磁噪音的生物指南针 [34

NON-HERMITIAN BULK-BOUNDARY CORRESPONDENCE IN QUANTUM DYNAMICS [35
量子动力学中非厄米系统的体边对原理 [36

REALISTIC DIMENSION-INDEPENDENT APPROACH FOR CHARGED-DEFECT CALCULATIONS IN SEMICONDUCTORS [37
与维度无关的半导体带电缺陷的实用计算方法 [38

PLASMON-INDUCED ELECTRON−HOLE SEPARATION AT THE $AG_{20}/TIO_2(110)$ INTERFACE [39
等离激元的衰变和热电子空穴对空间分离动力学研究 [40

ELASTIC AVALANCHES REVEAL MARGINAL BEHAVIOR IN AMORPHOUS SOLIDS [41
基于弹性雪崩研究揭示非晶固体中的边缘行为 [42

FIRST REALIZATION OF LIEB LATTICE IN REAL MATERIAL SYSTEMS [43
Lieb Lattice在实际材料系统中的首次实现 [44

PHONON-ASSISTED HOPPING THROUGH DEFECT STATES IN MOS_2 [45
等离激元辅助的室温工作能谷电子学器件 [46

3D MODEL RECONSTRUCTIONS FROM 1D SAXS CURVES USING MACHINE LEARNING METHODS [47
应用机器学习的方法从一维SAXS数据准确重构三维模型 [49

WHY FRACTIONAL DERIVATIVES WITH NON-SINGULAR KERNELS SHOULD NOT BE USED [51

RESONANT PHOTOVOLTAIC EFFECT IN DOPED MAGNETIC SEMICONDUCTORS [52
掺杂磁性半导体中的共振光伏效应 [52

ANALYTICAL TRANSIENT DISTRIBUTION AND DYNAMIC PHASE DIAGRAM FOR AUTOREGULATED BURSTY GENE EXPRESSION [53
自调控突发性基因表达的解析瞬时分布与动力学相图 [55

A CONVERGENT LINEARIZED LAGRANGE FINITE ELEMENT METHOD FOR THE MAGNETO-HYDRODYNAMIC EQUATIONS IN 2D NONSMOOTH AND NONCONVEX DOMAINS [57
非光滑区域上磁流体力学方程的线性化拉格朗日有限元法 [58

SUPPLEMENTARY VARIABLE METHOD FOR STRUCTURE-PRESERVING APPROXIMATIONS TO PARTIAL DIFFERENTIAL EQUATIONS WITH DEDUCED EQUATIONS [59
补充变量方法构造带有导出方程的PDE系统的保结构算法 [61

TUNABLE PHOTORESPONSE BY GATE MODULATION IN BILAYER GRAPHENE NANORIBBON DEVICES [63
通过门电压调制实现的双层石墨烯纳米带器件的可调光响应 [64

PHOTONIC BAND STRUCTURE CALCULATION FOR DISPERSIVE MATERIAL [65
色散材料的光子带隙结构计算 [66

SWIMMING OF THE MOSQUITO LARVA: PRINCIPLES AND TRICKS OF LOCOMOTION AT INTERMEDIATE REYNOLDS NUMBERS [67
蚊子幼虫的游动：中雷诺数流体中运动的原理和技巧 [68

REGULARIZED 13-MOMENT EQUATIONS FOR INVERSE POWER LAW MODELS [69

CONTROLLING THE EMISSION FREQUENCY OF GRAPHENE NANORIBBON EMITTERS BASED ON SPATIALLY EXCITED TOPOLOGICAL BOUNDARY STATES [71
通过激发石墨烯纳米带不同位置处的拓扑边界态实现发光频率可调控的量子发光器件 [72

PLASMON-ENABLED ROOM-TEMPERATURE VALLEYTRONIC TRANSISTOR

(By Lingfei Li, **Lei Shao**, Xiaowei Liu, Anyuan Gao, **Hao Wang**, Binjie Zheng, Guozhi Hou, Khurram Shehzad, Linwei Yu, Feng Miao, Yi Shi, Yang Xu, Xiaomu Wang)

Valleytronics, based on the valley degree of freedom rather than charge, is a promising candidate for next-generation information devices beyond complementary metal–oxide–semiconductor (CMOS) technology. Although many intriguing valleytronic properties have been explored based on excitonic injection or the non-local response of transverse current schemes at low temperature, demonstrations of valleytronic building blocks like transistors in electronics, especially at room temperature, remain elusive. Plasmonic structures can strongly boost the interaction between light and 2D materials and therefore modify the device optoelectronic properties greatly, opening new possibilities for novel applications [1,2]. Here, we report a solid-state device that enables a full sequence of generating, propagating, detecting, and manipulating valley information at room temperature [3]. Chiral nanocrescent plasmonic antennae are used to selectively generate valley-polarized carriers in MoS2 through hot-electron injection under linearly polarized infrared excitation. These long-lived valley-polarized free carriers can be detected in a valley Hall configuration even without charge current and can propagate over 18 μm by means of drift. In addition, electrostatic gating allows us to modulate the magnitude of the valley Hall voltage. The electrical valley Hall output could drive the valley manipulation of a cascaded stage, rendering the device able to serve as a transistor free of charge current with pure valleytronic input/output. Our results demonstrate the possibility of encoding and processing information by valley degree of freedom and provide a universal strategy to study the Berry curvature dipole in quantum materials.

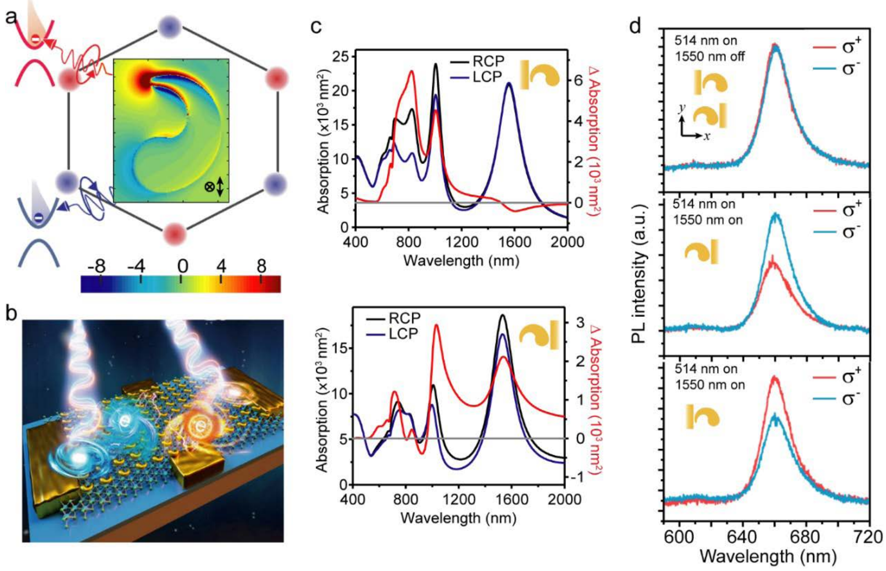

Fig. 1. Plasmon-enabled room-temperature valleytronic transistor. a) The calculated local enhancement of the optical chirality. The incident source is a 1,550 nm linearly polarized monochromatic light, with the polarization direction along the long axis of the nanocrescent antenna (indicated by the black arrow). The color bar represents the enhancement of optical chirality. b) Schematics and operation mechanism of the room-temperature valleytronic transistor. The device comprises a standard MoS2 transistor, two lateral Hall probes (named probe a and probe b, with the voltage drop between them VH) and a purposely aligned chiral plasmonic antennae array. c) Circular dichroism spectra obtained as the difference between the RCP and LCP absorption spectra for nanoantennae coupled with the electrode at different manners. d) Circular-polarization-resolved photoluminescence (PL) results. With infrared-excited nanoantennae, an obvious circular-polarized helicity of the PL signal was achieved, even when pumped by a linearly polarized 514 nm laser, in stark contrast to the circular-unpolarized cases of pristine MoS2 and infrared OFF-excitation (top panels). The polarized PL is due to the doping-level-dependent PL quantum yield and unbalanced doping levels in the K and K’ valleys. NPs, nanoparticles (referring to the gold nanoantennae).

等离激元辅助的室温工作能谷电子学器件

（中心作者：邵磊#、汪浩）

电子具有两个内禀自由度，即电荷和自旋。对电子内禀自由度的控制是现代电子信息器件的核心。近来对一类具有特殊对称性的半导体的研究表明布洛赫电子能带的最高处或最低处，也即能谷，可以是一个新颖的自由度。如果电子的能谷状态可以被选择性的极化和探测，则可用于编码和处理信息。目前对能谷性质的研究还受限于需要低温或强磁场等苛刻的实验条件，实现室温工作的能谷电子学器件仍然是一大挑战。等离激元可以通过各种机制显著增强光与二维半导体材料的相互作用，从而诱导二维半导体材料中新的物理效应，并带来崭新的应用前景[1,2]。在这篇工作中，我们利用等离激元纳米天线实现了室温下对单层二维半导体材料光电器件中能谷信息的产生、传输、探测以及操纵[3]。我们利用具有手性性质的等离激元金纳米天线，实现了线偏振的红外光激发下热电子对单层MoS_2能谷的选择性注入。这些能谷极化的自由载流子在即便没有电荷流（无外加电压）的情况下，仍然可以被能谷霍尔效应实验所探测。另外，在外加栅极电压的条件下，能谷霍尔电压可以被相应地调制。由此我们实现了一类单纯能谷输入（光注入）、能谷输出（能谷霍尔电压）的室温能谷电子学器件。

References:

[1] L. F. Li, W. Liu, A. Gao, Y. L. Zhao, Q. Lu, J. Z. Wang, L. Shao,* F. Miao, Y. Shi, Y. Xu,* X. M. Wang,* Plasmon excited ultrahot carriers and negative differential photoresponse in vertical graphene van der Waals heterostructure, *Nano Lett.* 19: 3295-3304 (2019).

[2] H. Wang, S. S. Li, R. Q. Ai, H. Huang, L. Shao,* J. F. Wang,* Plasmonically enabled two-dimensional materials-based optoelectronic devices, *Nanoscale* 12: 8095-8108 (2020).

[3] L. F. Li,# L. Shao,#(equal contribution) X. W. Liu, A. Y. Gao, H. Wang, B. J. Zheng, G. Z. Hou, K. Shehzad, L. W. Yu, F. Miao, Y. Shi, Y. Xu,* X. M. Wang,* Room-temperature valleytronic transistor, Nat. *Nanotechnol.* DOI: 10.1038/s41565-020-0727-0 (2020).

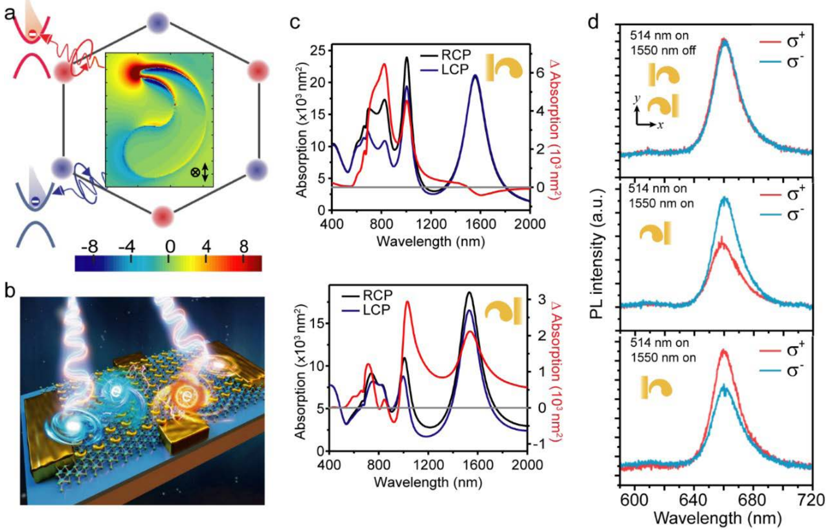

图 1　等离激元辅助的室温工作能谷电子学器件 a)手性金纳米结构在1550 nm线偏振激光激发下周围的光学手性密度计算。b)室温工作能谷电子学场效应管示意图。c)计算得到的不同等离激元耦合条件下手性金纳米结构的圆二色吸收光谱。d)手性金纳米结构-单层MoS_2复合体系的圆偏振分辨的光致发光谱。

LARGE OUT-OF-PLANE PIEZOELECTRICITY OF OXYGEN FUNCTIONALIZED MXENES FOR ULTRATHIN PIEZOELECTRIC CANTILEVERS AND DIAPHRAGMS

(By Jie Tan, **Yunhua Wang**, Zongtan Wang, Xiujie He, Yulan Liu, Biao Wang, Mikhail I. Katsnelson, **Shengjun Yuan**)

The piezoelectric effect is intensively applied in sensors, transducers and energy harvesting devices, by virtue of its high response sensitivity, efficient transformation capability between electrical and mechanical signals, and simple technical feasibility. The appearance of piezoelectricity in 2D materials has shed new light on atomically thin piezotronics and energy conversion system. Hundreds of 2D materials are found to be in-plane piezoelectric. However, an out-of-plane piezoelectric effect in 2D materials is also important for some piezoelectric devices. A recent paper [1] including Yunhua Wang and Shengjun Yuan from CSRC, Jie Tan, Zongtan Wang, Xiujie He, Yulan Liu and Biao Wang from Sun Yat-sen University, and Mikhail Katsnelson from Radboud University reports the out-of-plane piezoelectric effect in 2D M_2CO_2 MXenes with M = Sc, Y, and La in Fig. 1(a) and 1(b) and also performs corresponding piezoelectric device simulations.

The density-functional perturbation theory calculations show that, M_2CO_2 MXenes have a remarkable flexibility, an in-plane piezoelectricity comparable to that of 2H-MoS_2 and a large out-of-plane piezoelectricity enabled by the broken inversion symmetry and semiconducting features in this system. The piezoelectric response analyses are also developed in a MXene diaphragm device by virtue of the mechanical plate theory. The simulated results indicate that the nonuniform positive and negative charges produced by the in-plane piezoelectricity mainly concentrate in six regions near the clamped circular boundary but the out-of-plane piezoelectric charges are located inside the bubble, as shown in Fig. 1(c) and 1(d). These observations propose a realistic way to collect the piezoelectricity-induced charges, making these systems very promising for energy harvesting and piezoelectric sensing.

Fig. 1. Crystal structures of M2CO2 MXene from (a) top and (b) side views. The calculated charge density induced by the in-plane piezoelectricity in (c) and the out-of-plane piezoelectricity in (d).

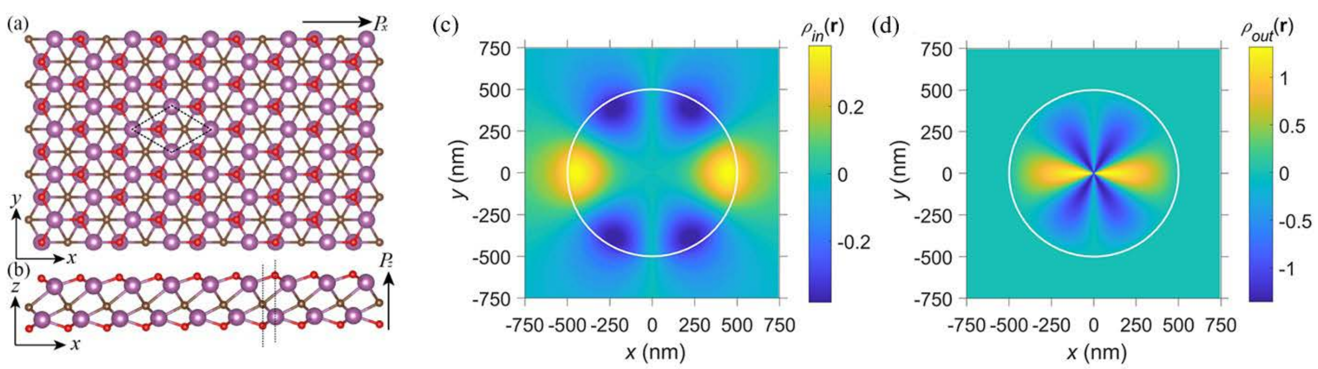

超薄压电悬臂和隔膜的氧官能化二维过渡金属碳化物的大外平面压电效应

（中心作者：王云华）

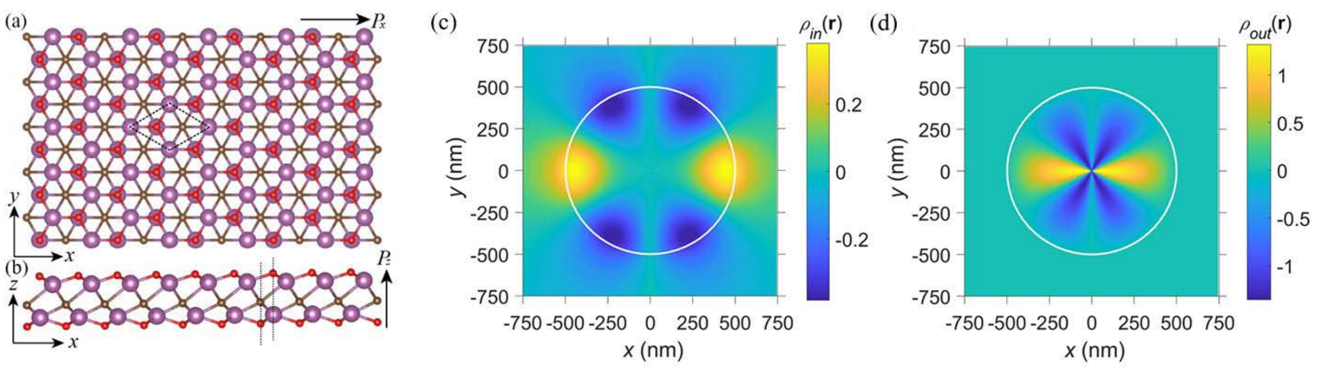

图 1　M_2CO_2 MXene 晶体结构的（a）顶视图和（b）侧视图。（c）面内（d）面外压电感应电荷密度的计算结果

压电效应因其高的灵敏响应度、有效的力电转换能力和简单的技术可行性而被广泛用作传感器、信号转换器和能量俘获器。二维材料压电性的出现为实现原子层尺度的超薄压电电子和微纳机电器件提供了新的机遇。目前，理论和实验已预报有数百种的二维压电材料，它们中的大多数具有面内压电性。然而一些压电薄膜器件常要求在垂直于二维材料平面的方向上也具有压电性，因此搜寻和设计具有平面外压电性的二维材料具有重要意义。我们目前的工作[1]报道了二维过渡金属碳化物M_2CO_2（M = Sc, Y, La）具有大的平面外压电性，其结构如图1(a)和1(b)所示。

密度泛函微扰理论计算结果显示，二维过渡金属碳化物M_2CO_2（M = Sc, Y, La）有明显的柔韧性，和2H相二硫化钼的压电性相当的平面压电特性，以及大的平面外压电性。基于弹性平板理论，我们也发展了二维过渡金属碳化物隔膜的压电响应理论模型。压电模拟结果表明：对于一个具有圆形夹住边缘的压电隔膜器件而言，平面内压电产生的电荷密度主要分布在夹住边缘，而平面外压电产生的电荷集中在隔膜中间区域。这些理论结果为真实压电膜器件的设计和实验提供了重要参考。

References:

[1] Jie Tan, Yunhua Wang, Zongtan Wang, Xiujie He, Yulan Liu, Biao Wang, Mikhail I. Katsnelson, Shengjun Yuan, Nano Energy 65, 104058 (2019).

PLASMON-ENABLED TWO-DIMENSIONAL MATERIALS-BASED OPTOELECTRONIC DEVICES

(By **Hao Wang**, **Shasha Li**, Ruoqi Ai, He Huang, **Lei Shao**, Jianfang Wang)

Two-dimensional (2D) materials, such as graphene, transition metal dichalcogenides, black phosphorus and hexagonal boron nitride, have been intensively investigated as building blocks for optoelectronic devices in the past few years. Very recently, significant efforts have been devoted to the improvement of the optoelectronic performances of 2D materials, which are restricted by their intrinsically low light absorption due to the ultrathin thickness. Making use of the plasmonic effects of metal nanostructures as well as intrinsic plasmon excitation in graphene has been shown to be one of the promising strategies. Recently, we are invited to review the recent progresses in plasmon enabled 2D material-based optoelectronic applications. We have highlighted the integration of various metallic plasmonic nanostructures, such as random metal nanostructures, coupled metal nanostructure antennas and other plasmonic nanostructures, with graphene and other 2D materials. The plasmon-enhanced light–matter interactions can greatly enhance the photoresponse of 2D materials. We have also discussed the underlying enhancement mechanisms in detail. In addition, we have introduced the development in optoelectronic applications powered by graphene plasmons. Finally, we point out some unanswered questions and possible improvements for future research studies in this emerging field. This review article will facilitate the research on plasmon-enhanced two-dimensional material-based optoelectronic applications and generate long-term impact in the fields of both plasmonics and two-dimensional materials. This work is selected as the Front Cover of Issue 15, 2020 of *Nanoscale*.

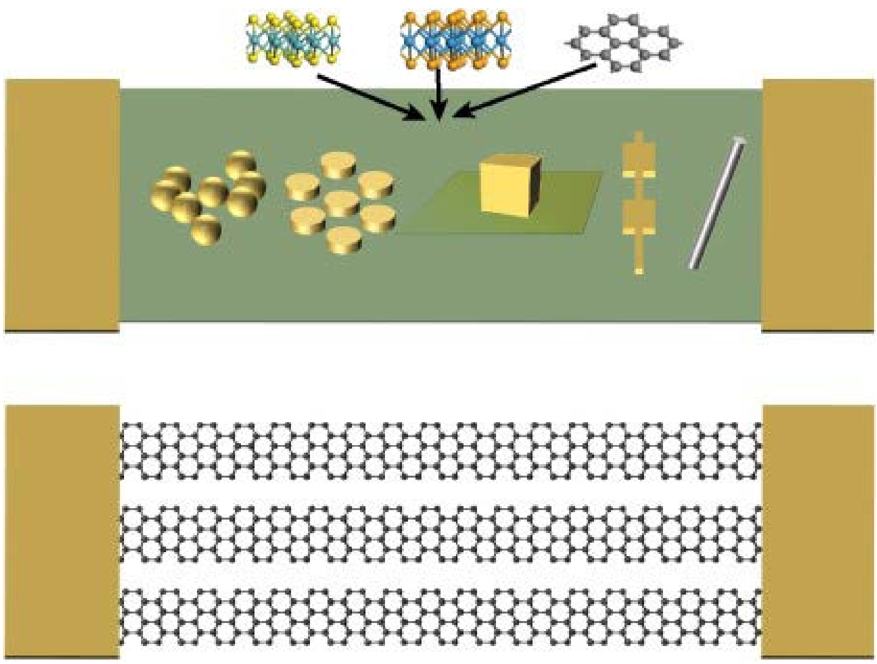

Fig. 1. Schematic of 2D materials-based optoelectronic devices integrated with various metallic plasmonic nanostructures as well as graphene nanostructures. The plasmon resonances supported by various metallic plasmonic nanostructures, such as random metal nanostructures, coupled metal nanostructure antennas, and structured metal films, can enhanced the optoelectronic response of 2D materials-based devices. In addition, the optoelectronic properties of graphene-based devices can also be improved by graphene plasmons.

等离激元增强二维材料光电器件综述

（中心作者：汪浩、李莎莎、邵磊*）

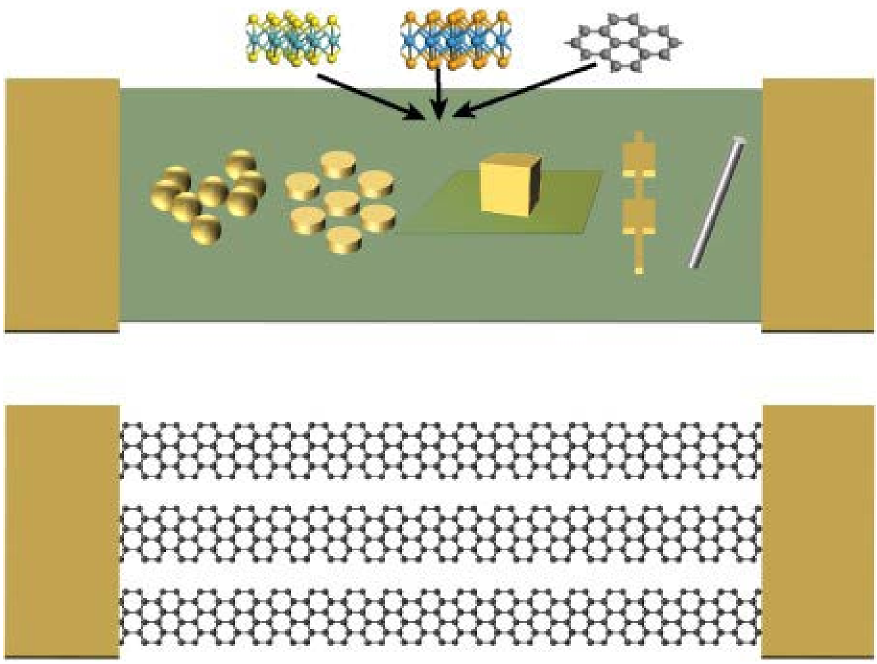

图 1　不同等离激元纳米结构对二维材料光电器件的性能增强示意图

石墨烯、过渡金属硫族化合物、黑磷、六方氮化硼这些二维材料可以由于构筑新型光电器件，是近年来的研究热点。但由于其原子级别的超薄厚度，上述二维材料的对光的吸收较弱，导致其光电响应性能提高受限。金属纳米结构或者石墨烯纳米结构的等离激元激发带来的物理效应可以用于增强光与物质的相互作用，对提高二维材料光电性能十分有前景。在这篇综述文章中我们总结了利用不同金属纳米结构的等离激元激发、以及石墨烯等离激元来提升二维材料光电响应性能的方法。我们详细讨论了其中等离激元增强的机制，包括吸收增强、近场效应、能量传输以及热载流子注入。文章指出了当前研究中亟待回答的科学问题，为进一步的研究提供相应的思路。这篇工作被选为当期（2020年第15期）Nanoscale杂志的封面工作。

References:

[1]　H. Wang, S. S. Li, R. Q. Ai, H. Huang, L. Shao,* J. F. Wang,* Plasmonically enabled two-dimensional materials-based optoelectronic devices, *Nanoscale* 12: 8095-8108 (2020).

FAST ENANTIO-CONVERSION OF CHIRAL MIXTURES BASED ON A FOUR-LEVEL DOUBLE-Δ MODEL

(By **Chong Ye**, **Quansheng Zhang**, **Yu-Yuan Chen**, and **Yong Li**)

Laser-assisted enantio-separation [1-3] and enantio-conversion [4,5] have important applications due to the chirality-dependence in most chemical, biological, and pharmaceutical processes. They both devote to get enantiopure samples of the wanted chirality from chiral mixtures with the help of optical operations. Since the laser-assisted enantio-conversion converts the unwanted enantiomer, which may be inefficient or even cause serious side effects, to the wanted enantiomer, it has more promising features than the laser-assisted enantio-separation. Two decades ago, an original theoretical work [4] was introduced to realize enantio-conversion based on a four-level double-Δ model of chiral molecules. However, due to the requirement of relaxation step and repeated operations, the original enantio-conversion method is time-consuming. This greatly prevents the realization of the enantio-conversion in the reality when the total operation time is limited due to the racemization and/or experimental conditions.

Here, Li's team proposes a fast method for achieving enantio-conversion within the four-level double-Δ model. In our method, the applied fields are well designed so that the four-level model can be simpified to two two-level subsystem in dressed state basis. Based on this, with only three coherent operations, the highly efficient enantio-conversion can be achieved. This method can be three order of magnitude faster than the original work [4] since this method do not require the time-consuming relaxation step and repeated operations. Accordingly, this work plays an important role in bringing laser-assisted enantio-conversion to reality.

For more information, please see the paper C. Ye, Q. Zhang, Y.-Y. Chen, Y. Li, Phys. Rev. Research, **2**, 033064 (2020).

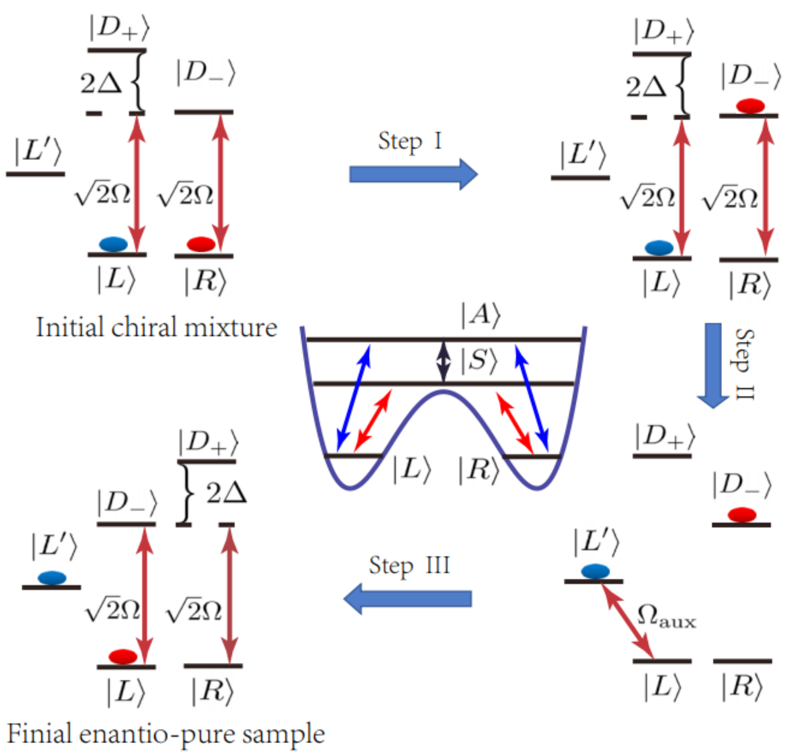

Fig. 1. Fast enatio-conversion from the initial chiral mixture with $\rho_0 = \frac{1}{2}(|L\rangle\langle L| + |R\rangle\langle R|)$ to final enatio-pure sample with $\rho_f = \frac{1}{2}(|L\rangle\langle L| + |L'\rangle\langle L'|)$ via coherent operations of three steps based on the four-level double-Δ model of chiral molecules (center panel).

基于四能级双Δ型模型的快速手性转化

（中心作者：叶冲、张全省、陈煜远、李勇）

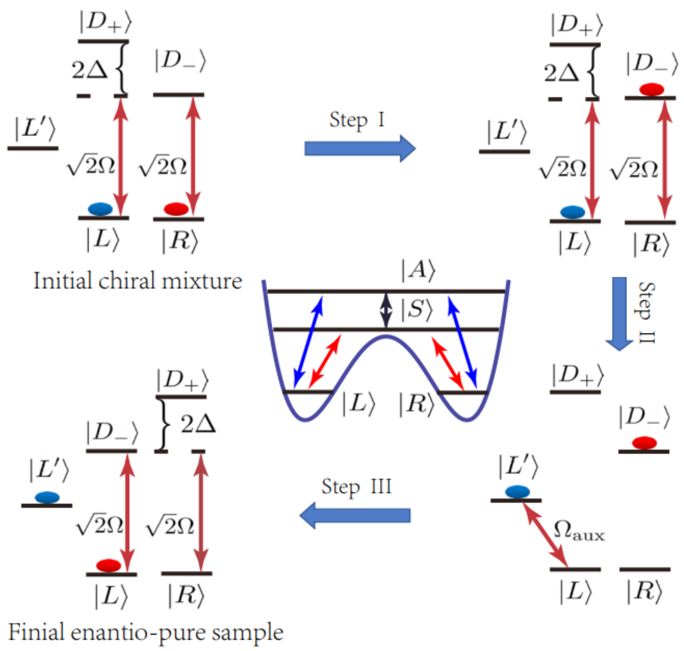

图 1　从初态 $\rho_0 = \frac{1}{2}(|L\rangle\langle L| + |R\rangle\langle R|)$ 到末态 $\rho_f = \frac{1}{2}(|L\rangle\langle L| + |L'\rangle\langle L'|)$ 的快速手性转化示意图。图中给出了每一步的初末态，以及工作的模型。中间的能级图为原始的四能级模型。

激光辅助的手性分离[1-3]和手性转化[4,5]在很多化学、生物和制药过程中具有重要的应用。它们都致力于借助光学操作从手性混合物中获得所需手性的单一对映体样品。激光辅助的手性转化能将不需要的对映体转化为需要的对映体。由于在药理上不需要的对映体无效，甚至会产生严重的副作用，因此激光辅助的手性转化相比激光辅助的手性分离具有更诱人的前景。二十年前，基于手性分子的四能级双Δ模型被提出，以实现手性对映体的转化。然而，最初的手性转化方案中涉及耗时较长的弛豫过程和需要多次重复操作。这些要求使得最初的手性转化方案耗时较长。实际系统中由于外消旋化和/或实验条件，总操作时间会受到限制。这极大地阻碍了手性转化的实现。

为此，李勇研究团队提出了一种基于四能级双Δ模型的实现手性转化的快速方法。该方法对驱动光场进行了优化设计，使四能级模型可以简化为两个二能级子系统。在此基础上，只需三次相干的光学操作，就可以实现高效的手性转化。因为不需要耗时的弛豫过程和重复操作过程，此方法可以比原工作快三个数量级。这将极大地促进激光辅助的手性转化的实验实现。

详见 C. Ye, Q. Zhang, Y.-Y. Chen, and Y. Li, Phys. Rev. Research 2, 033064 (2020).

References:

[1] P. Král and M. Shapiro, Phys. Rev. Lett. **87**, 183002 (2001).

[2] Y. Li, C. Bruder, and C. P. Sun, Phys. Rev. Lett. **99**, 130403 (2007).

[3] N. V. Vitanov and M. Drewsen, Phys. Rev. Lett. **122**, 173202 (2019).

[4] M. Shapiro, E. Frishman, and P. Brumer, Phys. Rev. Lett. **84**,1669 (2000).

[5] P. Král, I. Thanopulos, M. Shapiro, and D. Cohen, Phys. Rev. Lett. **90**, 033001 (2003).

MAGNETIC NOISE ENABLED BIOCOMPASS

(By **Da-Wu Xiao**, **Wen-Hui Hu**, Yunfeng Cai, and **Nan Zhao**)

The discovery of magnetic protein [1] provides a new understanding of a biocompass at the molecular level. However, the mechanism by which magnetic protein enables a biocompass is still under debate [2], mainly because of the absence of permanent magnetism in the magnetic protein at room temperature. In a recent work [3], based on a widely accepted radical pair model of a biocompass, Prof. Nan Zhao's group proposes a microscopic mechanism that allows the biocompass to operate without a finite magnetization of the magnetic protein in a biological environment. With the structure of the magnetic protein, they show that the magnetic fluctuation, rather than the permanent magnetism, of the magnetic protein can enable geomagnetic field sensing.

Experiments have shown that migrating birds employ the geomagnetic field for orientation and navigation. To understand the physical origin of the navigation of animals, several physical models have been proposed. A widely accepted model is the radical pair model, which assumes that the navigation process is governed by radical pairs, with each pair consisting of an unpaired electron spin. The pairs are usually created via photon excitation and form a spin singlet state. In the geomagnetic field and the magnetic field provided by the local molecular environment, the spin singlet state undergoes a transition to spin triplet states. The radical pair is metastable and eventually produces different chemical products according to the spin states of the radical pair, and the chemical products determine the subsequent navigation behavior.

In the radical pair model, a geomagnetic field sensor plays a crucial role. In 2016, Prof. Can Xie and his collaborators reported a new magnetic receptor (MagR) protein and showed that the MagR forms a rod-like magnetosensor complex with the radical pair in the photoreceptive cryptochromes [1]. The MagR consists of an Fe-S cluster protein, with the *d* electrons in the Fe atom contributing the electron spins.

However, the microscopic role of the magnetic protein is under debate. In Ref. [2], the author pointed out that electron spins are hardly polarized at room temperature and cannot produce a significant single-triplet transition process. Therefore, it is crucial to elucidate what makes the biocompass possible in the absence of a finite magnetization in the MagR.

In their recent work[3], Prof. Nan Zhao's team solved this challenging problem in a very different way. They started from the microscopic structure of the MagR spins and pointed out the essential role of the magnetic noise due to the MagR protein. With a semiquantitative analysis of a radical pair coupling to an electron spin bath in the geomagnetic field, they found two necessary intuitive requirements for the local magnetic field that need to be satisfied: (i) the strength of the noise magnetic field must be comparable to the geomagnetic field ($\sim 10^{-1}$ Gauss), and (ii) the local magnetic field should have directional dependence. Then, they made theoretical analysis and numerical calculations, and found that the singlet fidelity of the radical pair can exhibit a sensitive geomagnetic field direction dependence. This work provides new insights into the understanding of the biocompass mechanism.

For more information, please see Ref. [3].

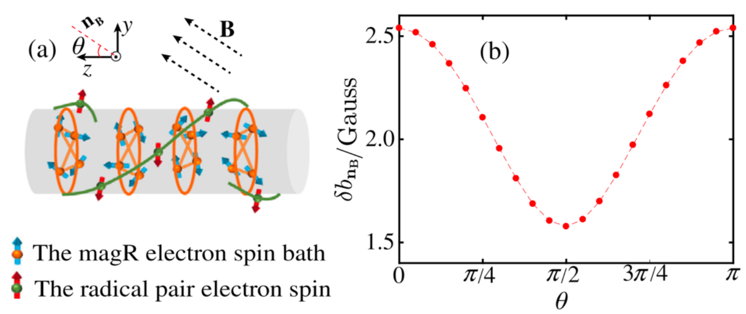

Fig. 1. (a) Illustration of the structure of the bath electron spins and the radical pair. The spins are fixed in the proteins. (b) Magnetic field fluctuation along the geomagnetic field direction δb_{nB} as a function of the geomagnetic field direction θ.

基于磁噪音的生物指南针

（中心作者：肖大武、胡文辉、赵楠）

新发现的磁蛋白[1]为在分子层面上理解生物指南针提供了新的角度。但是，磁蛋白使得生物指南针能够工作的机制受到很大的争议[2]，主要是因为在室温下，磁蛋白没有永久磁性。在最近的一个工作中[3]，基于一个被广泛接受的自由基对模型，赵楠教授研究组提出了一个微观机制，使得生物指南针能够在磁蛋白没有永久磁矩的情况下工作。通过磁蛋白的结构，他们发现，磁蛋白的磁噪音而非磁蛋白的永久磁矩，使得地磁场辅助的生物指南针能够工作。

实验表明，迁徙鸟类会利用地磁场进行导航。为了理解动物导航的物理机制，人们提出了很多物理模型。一个广为接受的模型是自由基对模型，它假设生物的导航都是由一些自由基对决定的，每个自由基对包含一对未配对电子。光的激发会使得自由基对形成自旋单态。在地磁场以及自由基对周围的分子环境的影响下，自旋单态会向自旋三态转化。自由基对是亚稳的，最终会根据自由基对的自旋状态产生不同的生化产物，这些生化产物会进一步决定生物的行为。

分子层面的地磁场探测器是自由基对模型的核心。在2016年工作中，谢灿教授和他的合作者报道了一种新型的磁蛋白（MagR），他们发现，感光的隐花色素中的自由基对包裹着了一个棒状的磁敏感的蛋白质[1]。这个蛋白质由Fe-S集团组成，Fe中的d壳层电子会有净的电子自旋。

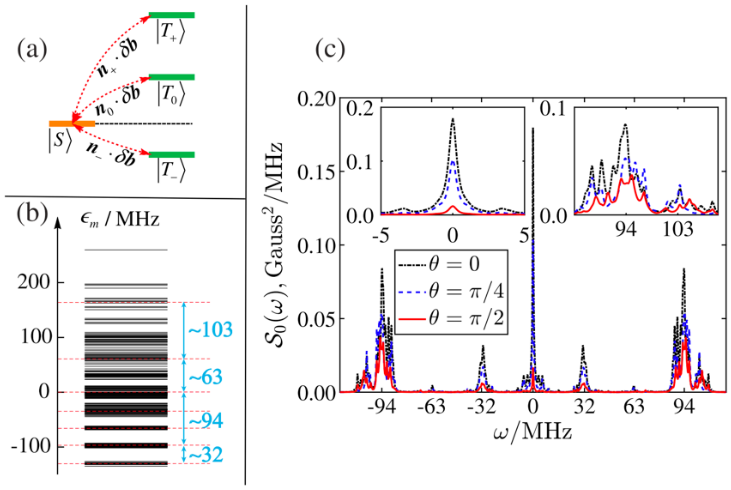

Fig. 2. (a) Illustration of the radical pair's energy spectrum and the corresponding noise component during the transition. (b) The energy spectrum of the spins in the MagR. (c) The noise spectrum S0(ω) for the two rings in different geomagnetic field directions.

但是，微观层面上，这个磁蛋白在生物指南中的角色受到很大的质疑。在文献[2]中，作者提出，电子自旋在室温下几乎没有极化，并不能引起显著的单三态转化。因此，如何理解这个没有平均磁化的磁蛋白如何使得生物指南针正常工作是一个非常重要的科学问题。

在他们最新的工作中[3]，赵楠教授的研究组通过另一种方式解决了这个挑战的问题。他们从磁蛋白电子的微观结构出发，指出了磁蛋白中磁噪音的重要作用。通过对一个自由基对与一个电子自旋库相互作用模型在地磁场下的半定量分析，他们发现自由基对感受到的局域磁场所需要满足的两个必要的条件：首先噪音磁场的强度必须与地磁场相匹配，也就是说量级在0.1高斯；其次这个局域磁场在地磁场方向上的投影必须依赖于空间指向。然后，通过理论分析和数值计算，他们发现在一定条件下，自由基对的单态产率会非常敏感的依赖于地磁场的方向。这个工作为理解生物指南针的微观机制提供了很好的理解角度。

更进一步的详细讨论，见[3]。

References:

[1] S. Qin, H. Yin, C. Yang, Y. Dou, Z. Liu, P. Zhang, H. Yu, Y. Huang, J. Feng, J. Hao, J. Hao, L. Deng, X. Yan, X. Dong, Z. Zhao, T. Jiang, H.-W. Wang, S.-J. Luo, and C. Xie, *Nat. Mater*. **15**, 217 (2015).

[2] M. Meister, *Elife* **5**, 1 (2016).

[3] D.-W. Xiao, W.-H. Hu, Y. Cai, and N. Zhao, *Phys. Rev. Lett*. **124**, 128101 (2020).

NON-HERMITIAN BULK-BOUNDARY CORRESPONDENCE IN QUANTUM DYNAMICS

(By **L. Xiao**, T. S. Deng, **K. K. Wang**, Z. Wang*, W. Yi*, and **P. Xue***)

Bulk–boundary correspondence, a guiding principle in topological matter, relates robust edge states to bulk topological invariants. Its validity, however, has so far been established only in closed systems. Recent theoretical studies indicate that this principle requires fundamental revisions for a wide range of open systems with effective non-Hermitian Hamiltonians. Therein, the intriguing localization of nominal bulk states at boundaries, known as the non-Hermitian skin effect, suggests a non-Bloch band theory in which non-Bloch topological invariants are defined in generalized Brillouin zones, leading to a general bulk–boundary correspondence beyond the conventional framework. Here, we experimentally observe this fundamental non-Hermitian bulk–boundary correspondence in discrete-time non-unitary quantum-walk dynamics of single photons. We demonstrate pronounced photon localizations near boundaries even in the absence of topological edge states, thus confirming the non-Hermitian skin effect. Facilitated by our experimental scheme of edge-state reconstruction, we directly measure topological edge states, which are in excellent agreement with the non-Bloch topological invariants. Our work unequivocally establishes the non-Hermitian bulk–boundary correspondence as a general principle underlying non-Hermitian topological systems and paves the way for a complete understanding of topological matter in open systems.

Recently, the research team led by Prof. Peng Xue at Beijing Computational Science Research Center, reported an experiment on non-Hermitian bulk-boundary correspondence in quantum dynamics was published Nature Physics (2020, 16: 761).

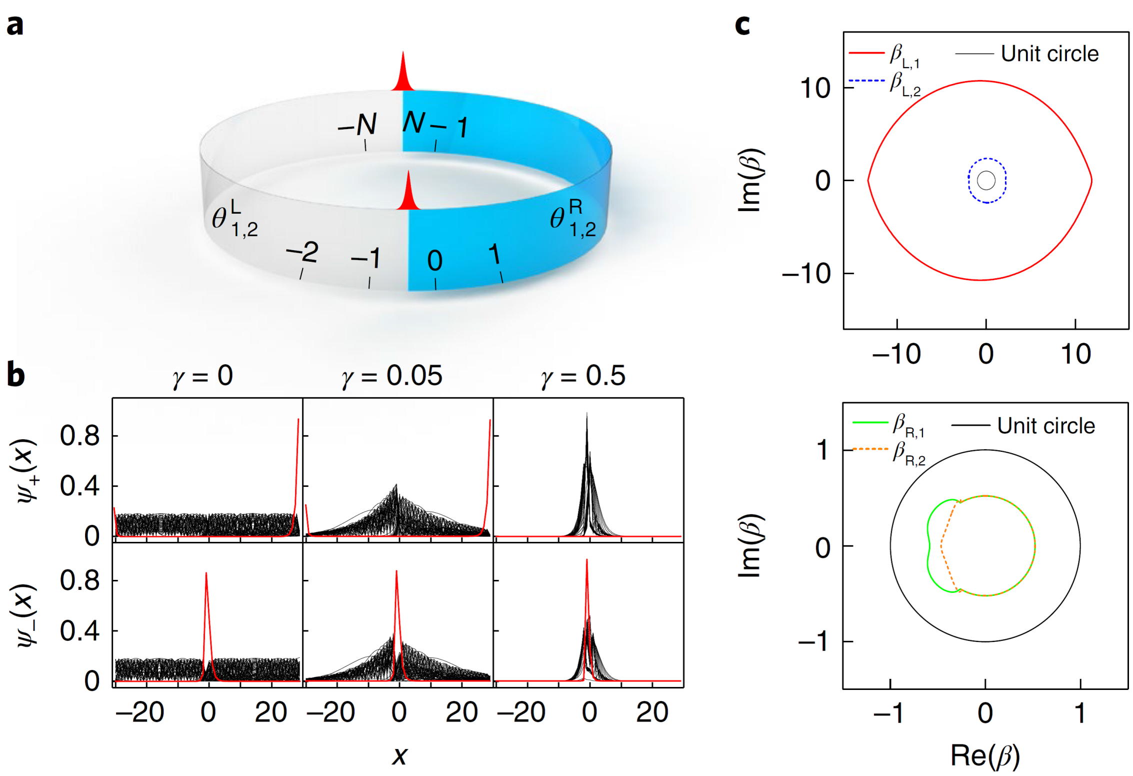

量子动力学中非厄米系统的体边对原理

（中心作者：肖磊、王坤坤、薛鹏*）

体边对应原理是固态拓扑材料中的基本原理，它把定义于拓扑物质体态的拓扑不变量与出现在其边界的稳定的边界态联系了起来。然而，到目前为止对体边对应原理有效性的讨论都是在封闭的体系中。最近，随相关研究表明将封闭的厄米系统拓展到非厄米系统，由于趋肤效应的存在，体态的主要性质无法在标准的拓扑能带理论框架下描写，需要将其扩展到非布洛赫的能带理论，在非布洛赫能带理论中，非布洛赫拓扑不变量由一般情况下的布里渊区得到，从而得到更为普适的一般情况下的体边对应原理。

这里，我们用单光子的离散时间量子行走观测到这种更为基础的非厄米体边对应原理。我们发现了在没有拓扑边界存在的情况下也会出现光子局域在边界的趋肤效应。基于实验对演化量子态的重构我们直接测量到在非布洛赫拓扑不变量预言下的边界态的存在。我们明确了非厄米系统下更为普适的体边对应原理，为完全理解拓扑物理和开放系统开辟了道路。

北京计算科学研究中心的薛鹏教授领导的课题组完成了该项工作的研究，相关成果《Non-Hermitian bulk-boundary correspondence in quantum dynamics》于2020年3月发表在《自然·物理》上。

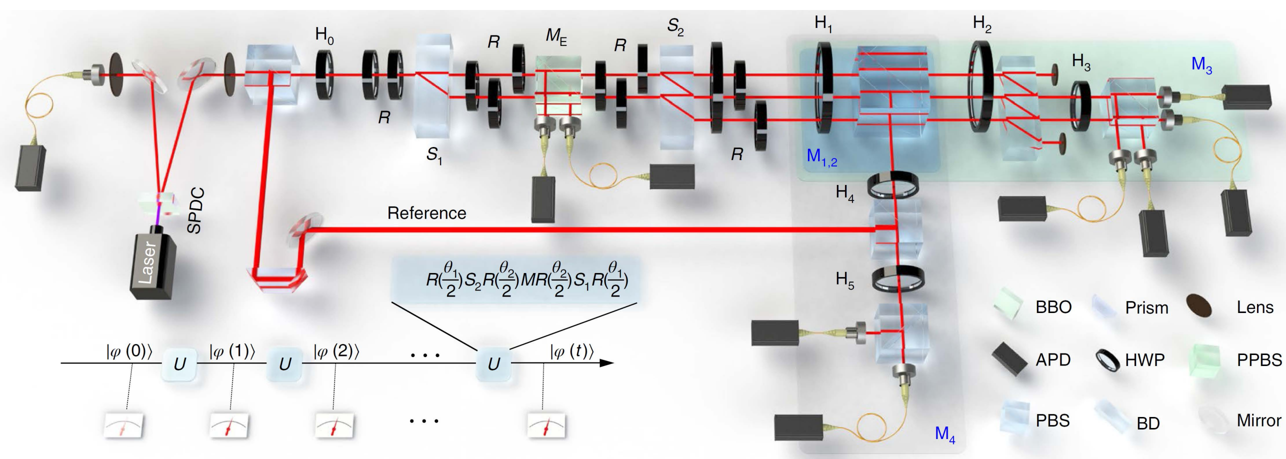

REALISTIC DIMENSION-INDEPENDENT APPROACH FOR CHARGED-DEFECT CALCULATIONS IN SEMICONDUCTORS

(By J. Xiao, K. Yang, D. Guo, T. Shen, J.-W. Luo, S.-S. Li, **S.-H. Wei**, and H.-X. Deng)

First-principles calculations of charged defects have become a cornerstone of research in semiconductors and insulators by providing insights into their fundamental physical properties. But current standard approach using the so-called "jellium model" has encountered both conceptual ambiguity and computational difficulty, especially for low-dimensional semiconducting materials. Recently, Su-Huai Wei at CSRC, in collaboration with Hui-Xiong Deng's group from Institute of Semiconductors, proposed a more physical and straightforward transfer-to-real-state (TRSM) model to calculate the formation energies of charged defects in both three-dimensional (3D) and low-dimensional semiconductors [1]. Within this universal model, the ionized electrons or holes are placed on the realistic host band-edge states instead of the virtual jellium state; therefore, rendering it not only naturally keeps the supercell charge neutral, but also has clear physical meaning, thus can be easily extended to study other physical properties such as exciton binding energy, free carrier bound to the defect in low-dimensional systems. This realistic model reproduces the same accuracy as the traditional jellium model for most of the 3D semiconducting materials, and remarkably, for the low-dimensional structures, it can cure the divergence caused by the artificial long-range electrostatic energy encountered in the jellium model, and hence gives meaningful formation energies of defects in charged-state and transition-energy levels of the corresponding defects. Our realistic method, therefore, will have significant impact for the study of defect physics in all low-dimensional systems.

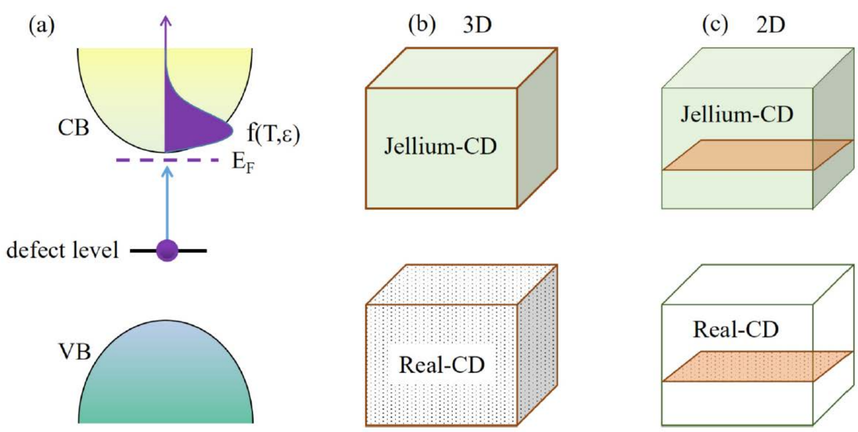

Fig. 1. (a) Schematic plot of occupations of the ionized electronic states above the CBM with a statistical distribution for a given Fermi energy EF at the finite temperature from the donor level. (b), (c) Schematic plots of charge distributions of jellium charge distribution (Jellium-CD) and real state with a certain statistical charge distributions (Real-CD) in the 3D and 2D semiconductors, respectively.

与维度无关的半导体带电缺陷的实用计算方法

(中心作者：魏苏淮)

通过第一性原理计算提供有关带电缺陷的基本物理特性已成为半导体和绝缘体研究的基石。但是，当前使用的所谓“jellium”模型的标准方法既有概念上的模糊性，在实际计算上也遇到了困难，特别是对于低维半导体材料而言。北京计算中心的魏苏淮教授与半导体所邓惠雄等人合作，提出了一种物理上更直观的“转移到真实状态”（TRSM）模型，用以计算三维（3D）和低维半导体中带电缺陷的形成能。在这个通用模型中，电离的电子或空穴被放置在真实的电子边缘态上，而不是虚拟的“jellium”态。因此，使其不仅自然地保持超胞的电荷中性，而且具有清晰的物理含义，因此可以很容易地扩展以研究其他物理性质，例如激子结合能，自由载流子与低维系统中的缺陷的结合能等。对于大多数3D半导体材料来说，使用这个更真实的模型计算的结果和传统的“jellium”模型计算的结果非常类似，但是非常重要的是，对于低维结构，它可以治愈在“jellium”模型中遇到的人为造成的远距离静电能引起的发散，因此，这个新方法可以被用来计算带电缺陷的形成能和相应的跃迁能级并提供有意义的数值。因此这个实用的方法将对研究低维系统中的缺陷物理产生重大影响。

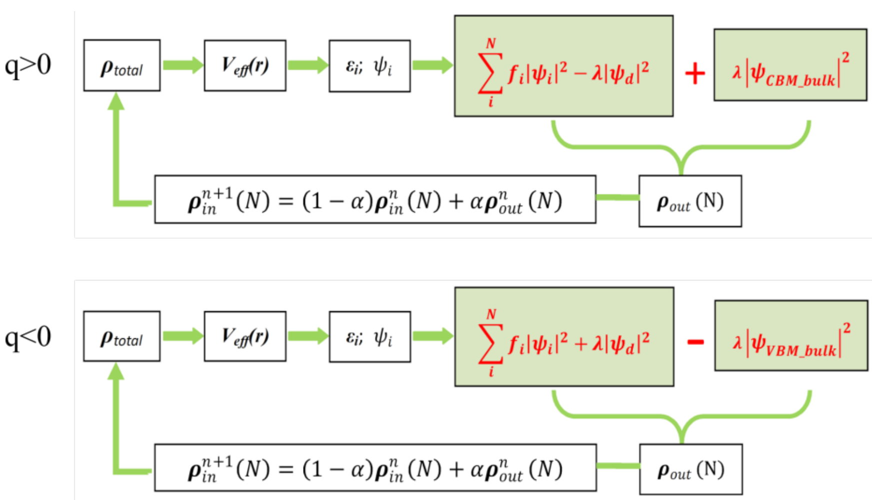

图 1　TRSM方法中针对（a）施主和（b）受主带电缺陷总能量计算的自洽计算流程示意图。

References:

[1] J. Xiao, K. Yang, D. Guo, T. Shen, J.-W. Luo, S.-S. Li, S.-H. Wei, and H.-X. Deng, Phys. Rev. B. **101**, 165306 (2020).

PLASMON-INDUCED ELECTRON−HOLE SEPARATION AT THE $AG_{20}/TIO_2(110)$ INTERFACE

(By J. Ma and **Shiwu Gao***)

The decay of surface plasmon of nanoparticles generates hot electron-hole pairs, which can separate at metal-semiconductor interfaces and lead to charge transfer across the interfaces. It is one of the key issues of fundamental plasmonics and is promising for applications in photovoltaics, surface photochemistry, and optoelectronic rectifications. Recently, the plasmon induced electron-hole separation has been investigated using time-dependent density functional theory (TDDFT) and atomistic model simulating the $Ag_{20}/TiO_2(110)$ interface. It has been found that the charge separation dynamics consists of two processes: during the first 10 fs an initial charge separation resulting from the direct plasmon−electron coupling at the interface and a subsequent charge redistribution governed by the sloshing motion of the charge-transfer plasmon (CTP). The interplay between the two processes determines the charge separation and leads to the inhomogeneous layer-dependent distribution of hot carriers. The hot electrons are more efficient than the hot holes in the charge injection, resulting in the charge separation. Over 40% of the hot electron−hole pairs are separated spatially from the interface. These results reveal the mechanism and dynamics of the plasmon induced charge separation and have broad implications. This work has been published at ACS Nano[1] and highlighted by the Perspective feature articles[2].

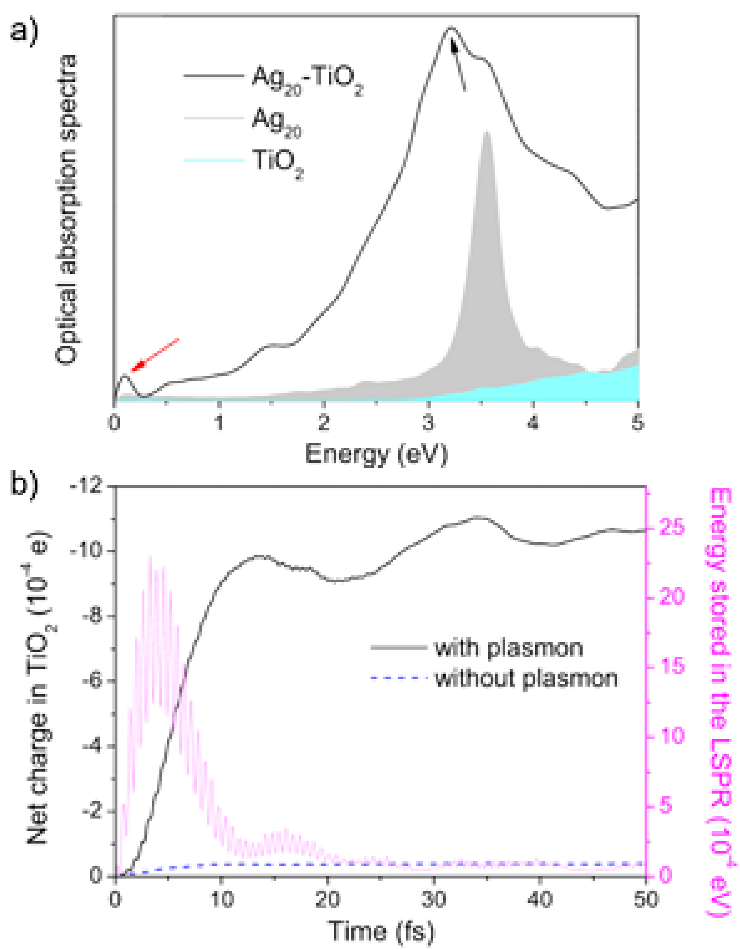

Fig. 1. (a) The calculated absorption spectrum of an $Ag_{20}/TiO_2(110)$ structure. (b) Net charge transferred into TiO_2 and the energy stored in the surface plasmon as a function of time.

等离激元的衰变和热电子空穴对空间分离动力学研究

（中心作者：高世武）

纳米颗粒表面等离激元的衰变产生热电子空穴对，可以在金属-半导体界面发生分离并导致电荷在界面上转移。它是基础等离激元学的基本问题之一，在光电、表面光化学和光电整流等领域有着广阔的应用前景。利用含时密度泛函理论（TDDFT）和模拟$Ag_{20}/TiO_2(110)$界面的原子模型，高世武和马杰（北理工）在前期工作上对等离激元诱导的电子空穴分离进行了计算研究。研究发现，电荷分离动力学包括两个过程：在前10fs期间，界面上的直接等离子激元-电子耦合而产生的初始电荷分离，以及随后由电荷转移等离激元（CTP）的低频运动控制的电荷重新分布。这两个过程之间的相互作用决定了电荷分离效率和空间发表，并导致热载流子在半导体内的不均匀分布。在电荷注入中，热电子比热空穴更有效，从而导致电荷分离。超过40%的热电子-空穴对在空间上与界面分离。这些结果揭示了等离子体诱导电荷分离的机理和动力学，具有广泛的意义。这个工作在ACS Nano发表[1]并且得到编辑的Perspective文章highlight[2].

References:

[1] J. Ma and Shiwu Gao, ACS Nano 13, 13658-13667 (2019).

[2] D. C. Ratchford, ACS Nano 13, 13610-13614 (2019).

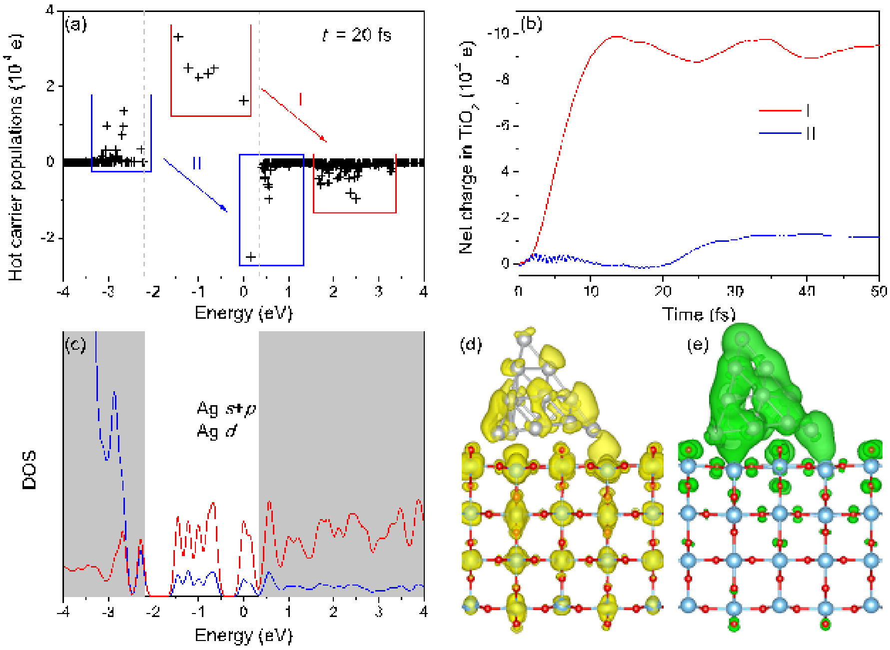

图 1　t=20 fs时的本征态上的布居数。正值表示热空穴，负值表示热电子。根据共振条件，热电子和空穴可分为两个激发群，以红色（I组）和蓝色（II组）矩形标记。灰色虚线表示TiO_2的导带最小值和价带最大值。（b） 两个电子空穴激发基团对TiO_2中净电荷的贡献。（c） Ag_{20}/TiO_2系统的分波态密度。红线代表Ag s和p态，蓝线表示Ag d态，灰色区域表示TiO_2的导带和价带。（d，e）t=20 fs时的热电子密度（黄色）和热空穴密度（绿色）。

ELASTIC AVALANCHES REVEAL MARGINAL BEHAVIOR IN AMORPHOUS SOLIDS

(By B.S. Shang, **P. F. Guan** and Jean-Louis Barrat)

At large strains, glassy systems deform through a series of elastic loading phases followed by energy and stress drops without a characteristic scale, similar to earthquakes. Less is known about the small deformation case, which is related to the structure of the energy landscape close to an energy minimum. Recently, Prof. Pengfei Guan and Dr. Baoshuang Shang at CSRC, in collaboration with Prof. Jean-Louis Barrat from Universit ´e Grenoble Alpes, France, investigated numerically this regime and show that even at very small strains the deformation proceeds through avalanches that are power-law distributed, with a universal exponent that corresponds to the predictions of mean field theory for a hierarchical phase space structure. These avalanches reveal marginal stability in the amorphous solid, which is intrinsically inelastic. By investigating the preparation and size dependence, we infer that the effect persists in the thermodynamic limit. As a result, it can be expected that in very well-annealed systems the size needed for observing large-scale avalanches at small strains could be prohibitively large, so that observed excitations are limited to localized defects. The need to use larger sizes to properly describe the scaling behavior in the response of highly annealed systems. Whether or not there is an actual transition is an issue that cannot be addressed here, although this may be consistent with the idea of a sharp change from ductile to brittle behavior in amorphous materials.

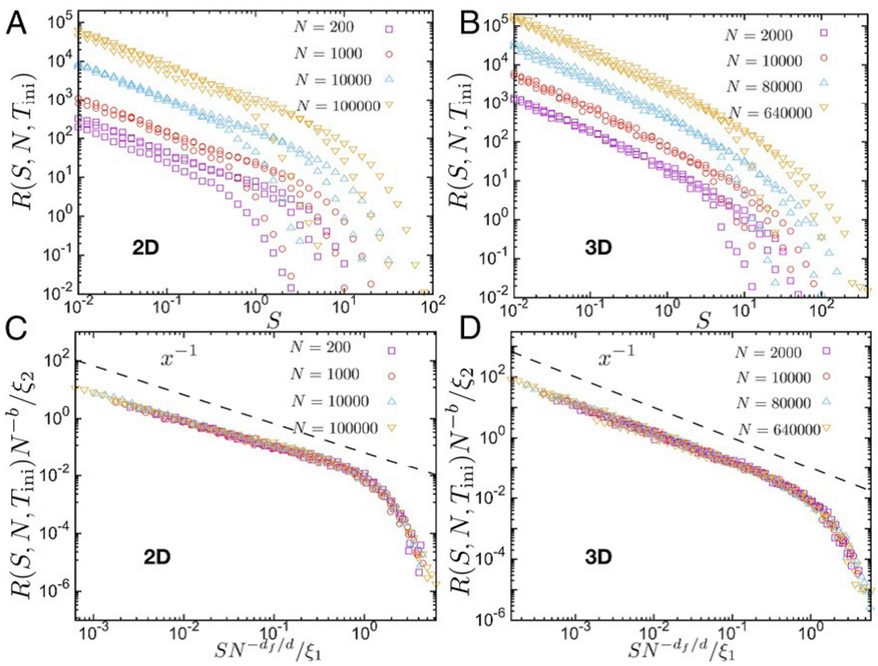

Fig. 1. Avalanche number density versus avalanche size. (A and B) Avalanche number density for different system sizes and thermal histories in 2D and 3D, respectively. (C and D) Data collapse using 2 exponents, df =d and b for the scaling as a function of system size. The dashed line shows the avalanche exponent -1 predicted by mean-field theory near the ground state.

基于弹性雪崩研究揭示非晶固体中的边缘行为

（中心作者：尚宝双、管鹏飞）

在大应变下，非晶体系的变形是通过一系列没有特征尺度的伴随着能量和应力下降的弹性形变过程实现的，和地震的行为十分相似。但人们对于小变形情况的了解却较少，这与能量图景中接近能谷能量最小值附近的势能曲面形貌密切相关。北京计算科学研究中心的管鹏飞教授、尚宝双博士与法国Grenoble Alpes大学Jean-Louis Barrat教授人合作，运用原子尺度数值模拟研究了非晶固体小变形下的形变行为，研究结果表明，即使在非常小的应变下，变形过程中的雪崩行为依然符合幂律分布，并且其幂律指数符合基于平均场理论的分级相空间结构的预测。这一雪崩行为特征揭示了非晶固体的边缘稳定性，即非晶固体本质上是非弹性的。通过对制备热历史和尺寸依赖关系的研究，我们推断这种行为在热力学极限内都普遍存在。可以预期，在深退火的非晶体系中，观察小应变下大规模雪崩所需的尺寸可能会大得令人望而却步，因此观察到的激励发仅限于局部缺陷。因而，可能需要使用更大的尺寸系统去理解该雪崩行为特征与非晶固体韧脆断裂特性之间存在的关联。

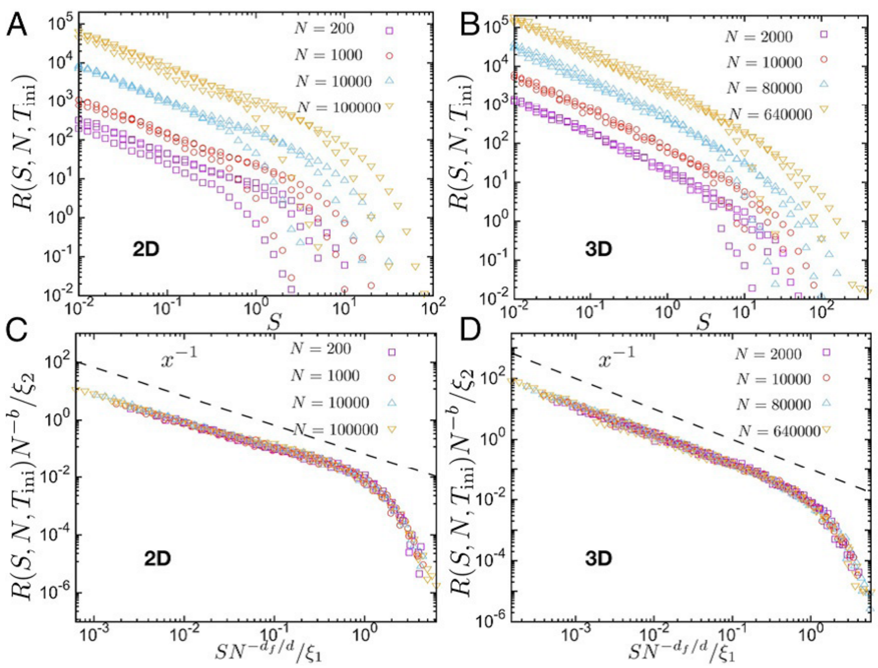

图 1　雪崩数密度与尺度之间的关联。无论是二维还是三维的雪崩都符合相同的幂率关系。

References:

[1] B. Shang, **P. Guan***, J. L. Barrat*, *Proc. Natl Acad. Sci*. 117, 86 (2020)

FIRST REALIZATION OF LIEB LATTICE IN REAL MATERIAL SYSTEMS

(By Bin Cui, **J. F. Wang**, S. J. Xie, **Bing Huang**)

The electronic properties of a crystal are determined by its crystalline lattice symmetry. Lieb lattice, a two-dimensional (2D) edge-depleted square lattice, can be regarded as the reduced 3D perovskite lattice. As one of the most important frustrated lattices, the ideal Lieb lattice can host exotic electronic structures, which is featured by the Dirac cone intersected by a flat band (Dirac-flat bands). Interestingly, various physical phenomena, *e.g.*, topological Mott insulator, superconductivity, ferromagnetism, and fractional quantum Hall (FQH) effects, have been predicted to exist in the ideal Lieb lattice systems. However, until now only a few Lieb lattices have been realized in artificial lattice systems, *e.g.*, molecular patterning lattices on metal substrates, photonic and cold-atom lattices, rather than a real material system, which significantly prevent the realization of these unusual physical properties of Lieb lattice for practice applications.

Recently, a joint research team from Beijing Computational Science Research Center (CSRC) and Shandong University, leaded by Dr. Bing Huang, has discovered the first real example in the world that can achieve Lieb lattice bands around the band edges. Based on tight-binding modeling, the authors find that the lattice distortion can significantly determine the electronic and topological properties of a Lieb lattice. Importantly, based on first-principles calculations, the authors predict that the two existing covalent organic frameworks (COFs), *i.e.,* sp^2C-COF and sp^2N-COF, are actually the first two material realizations of organic-ligand-based Lieb lattice. Interestingly, the sp^2C-COF can experience the phase transitions from a paramagnetic state to a ferromagnetic one and then to a Néel antiferromagnetic one, as the carrier doping concentration increases.

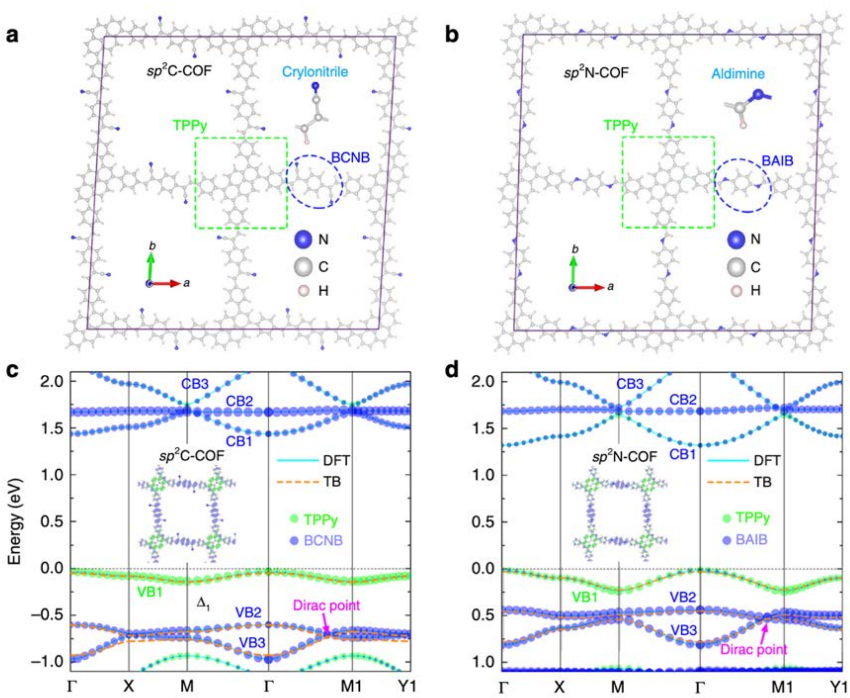

Fig. 1. Realization of distorted Lieb lattices in COFs.

Lieb Lattice在实际材料系统中的首次实现

（中心作者：王建峰、黄兵）

晶体的电子性质取决于其晶格对称性。Lieb晶格是一种二维正方形晶格，可以视为单层的3D钙钛矿晶格。作为最重要的阻挫晶格之一，理想的Lieb晶格可以实现各种奇特的电子结构，其特征是狄拉克锥与平带相交。有趣的是，各种物理现象，例如拓扑Mott绝缘体，超导性，铁磁性和分数量子霍尔效应，已被预测存在于理想的Lieb晶格系统中。但是，到目前为止仅仅在人工晶格系统中仅实现了少数Lieb晶格，例如金属衬底上的二维分子晶体，光子和冷原子晶格。而在实际的材料系统中Lieb晶格非常难以实现，这大大阻止了这些异常物理特性在真实材料的实现和应用。

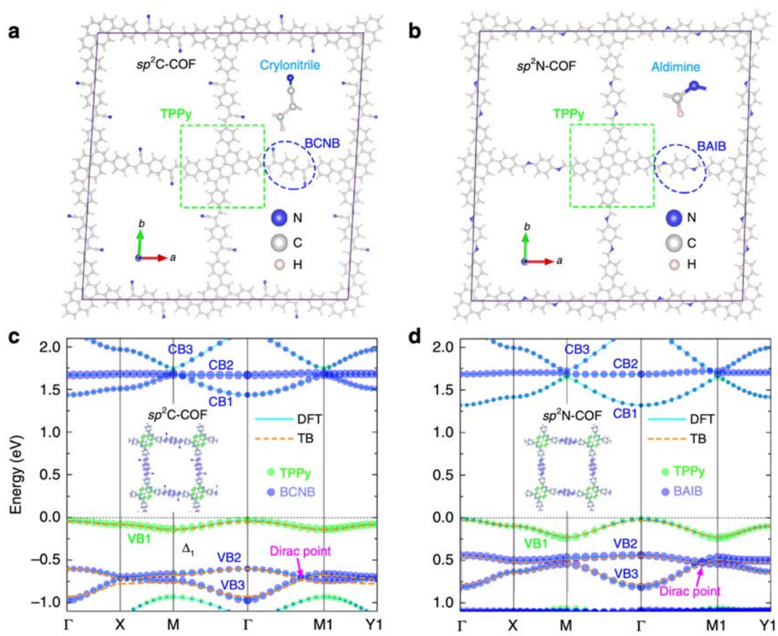

图 1　a和b: Lieb lattice在两种真实COF中材料的实现；c和d: 它们的能带结构。

最近，由黄兵博士领导的北京计算科学研究中心（CSRC）和山东大学的联合研究小组发现了世界上第一个可以在能带带边实现Lieb晶格带的真实材料系统，从而破解了长久以来的疑惑。基于紧密绑定模型，作者发现晶格畸变可以调控Lieb晶格的电子态和拓扑特性。重要的是，基于第一性原理的计算，作者预测了两个现有的共价有机框架（COF），即sp^2C-COF和sp^2N-COF，可以实现基于有机配体的Lieb晶格的真实系统。有趣的是，随着载流子掺杂浓度的增加，sp^2C-COF可以经历从顺磁态到铁磁态的相变，然后到Néel反铁磁态的相变。

References:

[1] B. Cui, X. Zheng, J. Wang, D. Liu, S. Xie, and B. Huang, Realization of Lieb lattice in covalent-organic frameworks with tunable topology and magnetism, Nat. Comm. 11, 66 (2020).

PHONON-ASSISTED HOPPING THROUGH DEFECT STATES IN MOS_2

(By J. Kang)

Understanding the carrier transport mechanism in transition metal dichalcogenides (TMDs) is essential for their device application. Experiments demonstrated that at low carrier density and room temperature, the conductivity in 2D MoS_2 is dominant by activation hopping transport through localized S-vacancy states. However, the underlying mechanism remains unclear, and a microscope model including atomic structural details to qualitatively predict the hopping mobility is still missing. In this work, combining ab initio calculation and the Marcus theory, a multiscale model which covers length scale of 0.1 nm to 1 µm is developed to study such transport [1]. Among several possible mechanisms, phonon-assisted hopping (PAH) is identified as the most possible mechanism for the activation hopping. It is found that the macroscopic conductivity is mainly contributed by a few microscopic percolation paths. Analysis on the hopping distance indicated nearest-neighbor hopping behavior. The calculated PAH mobility using the model is consistent with experiment, whereas ignoring atomic structure details leads to large overestimation. The mobility increases as the defect concentration and the temperature increase, and as the energy mismatch between defect sites decreases. It is also proposed that alloying can be an efficient way to tune the PAH mobility due to increased energy mismatch effect. This work indicates atomistic multiscale simulations are necessary to correctly model the hopping transport in defective TMDs. It also shed light on the microscopic mechanism and modulation of such transport, which is important to the optimization of TMD-based devices.

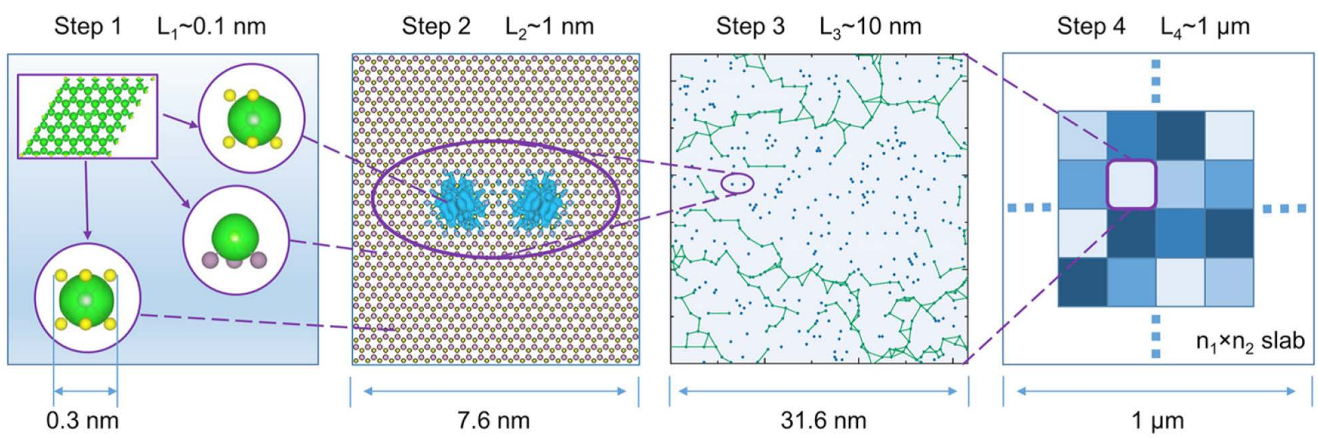

Fig. 1. Schematic of the multiscale model used to study the PAH transport in defective MoS2. Step 1: Ab initio calculation of the charge density in a small supercell and generation of charge motifs for inequivalent atoms. Step 2: Defect states in a large supercell calculated by charge patching method. Step 3: Random defect network (dots) and an illustration of relevant current paths (lines). Step 4: Continuum system simulation. The length scale of the model covers 0.1 nm to 1 µm.

等离激元辅助的室温工作能谷电子学器件

（中心作者：康俊）

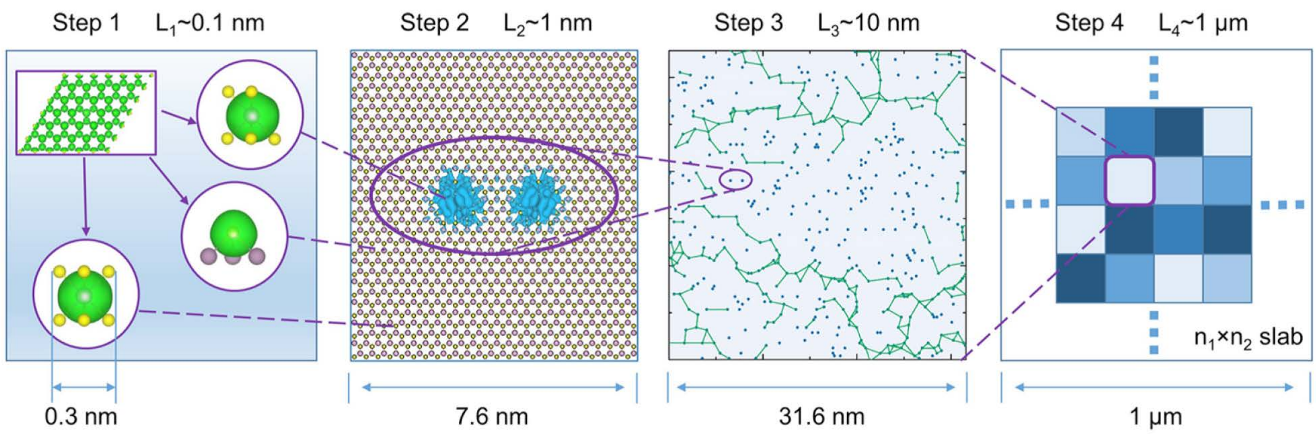

图 1　模拟MoS2中声子辅助缺陷态间输运的多尺度模型示意图。步骤1：第一性原理计算电荷基元。步骤2：利用电荷补缀方法计算缺陷态间耦合。步骤3：构建随机分布的缺陷格点，求解电导网络。步骤4：连续介质模型计算。各步骤覆盖了0.1 nm至1 μm尺度。

理解过渡金属硫化物中的输运性质对于相关的器件应用具有重要意义。多个实验研究表明当载流子浓度较低时，二维MoS_2中的输运主要由缺陷态决定。然而具体的输运机制一直未得到明确，目前也没有一个比较好的包含原子尺度细节的模型来定量计算这类输运的迁移率。通过对量子隧穿、直接热激发、声子辅助等多种输运机制的分析，本工作提出声子辅助跃迁是主导的输运机制。结合大规模电子结构第一性原理计算和Marcus理论，构建了一个涵盖0.1纳米至1微米范围的多尺度模型，实现对迁移率的定量模拟，结果与实验相符 [1]。计算表明，声子辅助跃迁主要发生于最近邻缺陷位点之间，体系电导仅由少数跃迁路径所决定。通过该模型进一步研究了缺陷浓度、温度、能级失配等因素对于迁移率的影响，发现迁移率随着缺陷浓度和温度的增加，或能级失配的减少而升高。由于合金可以显著改变缺陷间的能级失配，因而是有效调控迁移率的手段。这些结果对于深入理解二维材料中的输运行为及相关电子器件性能优化都具有重要意义。

References:

J. Kang, J. Phys. Chem. Lett. 11, 3615 (2020).

3D MODEL RECONSTRUCTIONS FROM 1D SAXS CURVES USING MACHINE LEARNING METHODS

(Hao He, Can Liu, Haiguang Liu*)

Small-angle X-ray scattering (SAXS) method is widely used in investigating protein structures in solution, but high-quality 3D model reconstructions are challenging. This is mainly due to the ill-posed question to reconstruct 3D models from 1D data that is rotationally averaged representation of the corresponding model. To cope with this information deficiency, researchers from CSRC developed a new algorithm based on a deep learning method for model reconstruction from SAXS data.

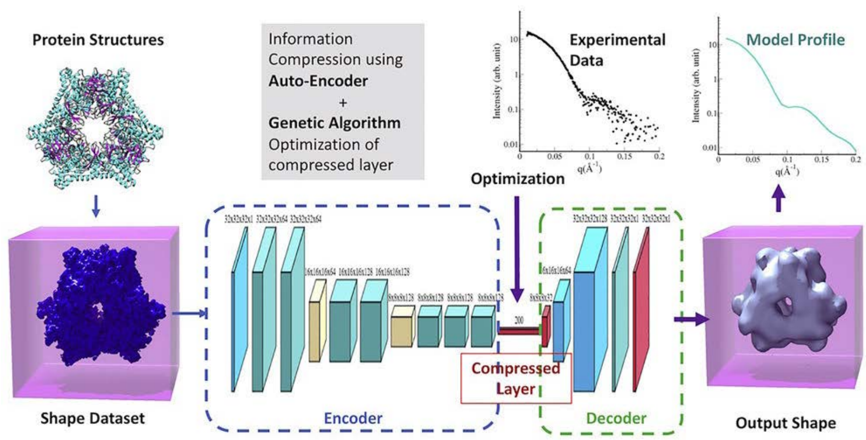

Fig. 1. DecodeSAXS design principle and implementations. A neural network is designed to encode 3D model information to a compressed representation and then decode to an approximation of the original 3D models. After training the CNN auto-encoder, the decoder part is integrated to a genetic algorithm optimization workflow to produce 3D models based on 1D SAXS data (right panel).

The project was carried mainly by two intern students from the University of Science and Technology China (USTC), under the supervision of Dr. Haiguang Liu. The first student, Can Liu, started the project in 2017 and demonstrated the feasibility of compressing 3D shape information to low dimensional vector representations. Specifically, an auto-encoder for protein 3D models was trained to compress 3D shape information into vectors of a 200-dimensional latent space (Figure 1). The structures in the Protein Databank (PDB) were converted to voxel objects to represent protein shapes. In real space representation, it takes 32,768 voxels with binary values (0 or 1) to code a shape on a 3D grid of 32 x 32 x 32. By reducing this parameter space to a 200-d vector space, it is possible to use optimization algorithm to refine these parameters, such that the decoded 3D shape has a model profile matching the experimental SAXS data. In 2018, Hao He followed the progress and improved the auto-encoder neural networks so that the information compression is more efficient. The statistical distributions of the parameters for the 200-d vectors are saved for model optimizations using genetic algorithms. The motivation is that protein shapes have their own characteristics, such as continuity and positivity, which are intrinsically encoded into the 200-d vectors. In the second stage, the decoder part is connected to a genetic algorithm that generates and selects those 200-d vectors representing the shapes with matching SAXS profiles.

The program has been tested on >500 experimental SAXS datasets, demonstrating the robustness of accurate model reconstruction. Furthermore, the model size information can be optimized using this algorithm, enhancing the automation in model reconstruction directly from SAXS data (Figure 2). The program was implemented using Python within TensorFlow framework, with source code and webserver available from http://liulab.csrc.ac.cn/decodeSAXS (Figure 3).

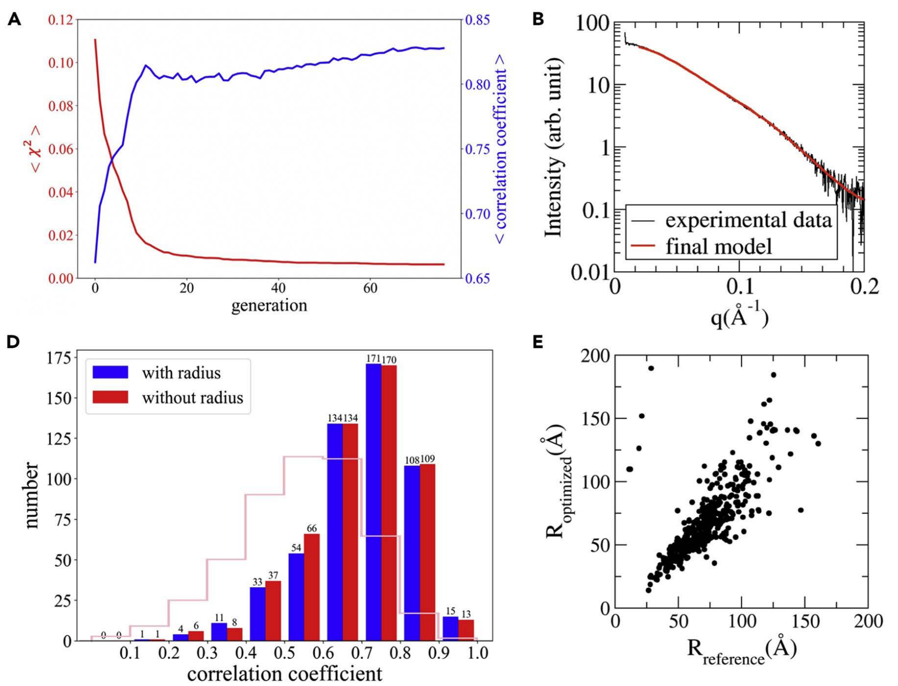

Fig. 2. The model reconstruction examples and quality statistics. (A) the progression of the optimization, showing the improvement of fitting to SAXS data is correlated to the model accuracy. (B) The final model SAXS profile matches experimental data. (C) Reconstructed model (blue envelopes) superimposed to the atomic model. (D) Statistics of real space correlation between reconstructed models and known models. (E) The model size can be refined along the shape parameters. (F) Two examples showing the refined model sizes (Ropt) are consistent with prior knowledge (Rref).

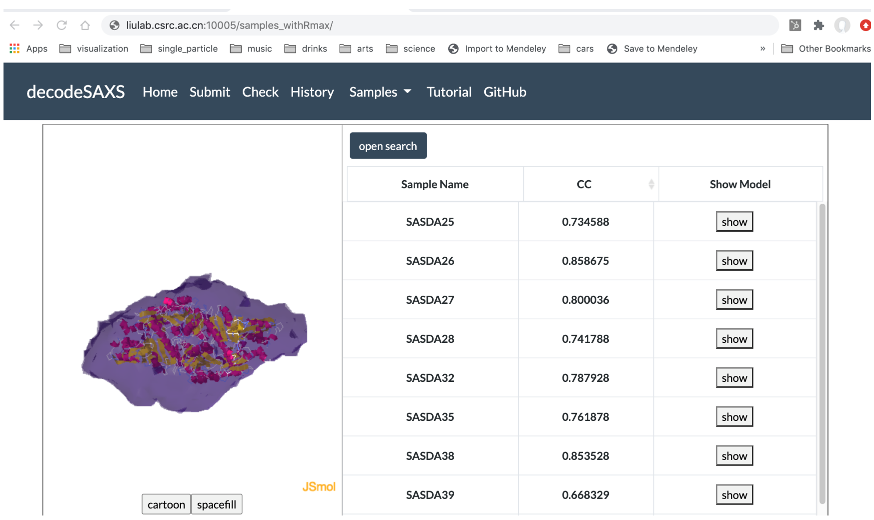

Fig. 3. Reconstruction online server. Users can upload the experimental SAXS data and the model will be automatically generated and compared to provided protein structures.

References:

Hao He; Can Liu; Haiguang Liu. Model Reconstruction from Small-Angle X-Ray Scattering Data Using Deep Learning Methods. iScience 23(3) 100906 (2020). https://doi.org/10.1016/j.isci.2020.100906

Acknowledgement:

The National Natural Science Foundation of China award to H. Liu (#11575021, U1530401) .

应用机器学习的方法从一维SAXS数据准确重构三维模型

（中心作者：刘海广*）

X射线小角散射方法被广泛应用于水溶液环境中的蛋白质分子结构和动力学研究，但是基于一维的散射谱准确重构对应的三维结构一直是个有挑战性的问题。这个困难主要在于小角散射数据测量的是三维物体旋转平均的信号，在没有其他渠道的信息来源的限制下，一维散射数据包含的信息量不足以直接重构唯一的三维结构。针对这个难题，北京计算科学研究中心的刘海广研究员率领的团队开发了基于深度学习框架的模型重构方法。该方法经过实验数据的测试，发现能够在不引入其他信息的情况下，能够自动优化模型的尺寸以及形状信息，优于其他方法。

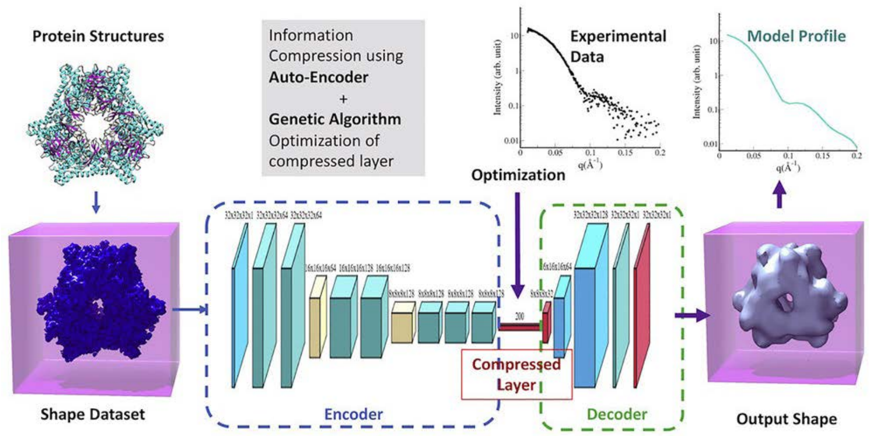

图 1　DecodeSAXS的设计和实现方案。自动编码器的神经网络用于对三维模型进行编码和解码，并且获得压缩层的表述形式。通过对卷积神经网络进行训练，优化得出的参数可以把任意200维参数解码为三维空间的模型。这些200维的向量则通过遗传算法进行优化，进而获得与实验数据一致的三维模型。

这个研究项目主要是由两名中国科学技术大学软件学院的研究生在北京计算科学研究中心实习期间完成的。2017年，刘灿同学通过努力搭建了第一个版本，证实用自动编码器的方式可以把蛋白质分子对应的三维形状信息压缩到很小的空间，再通过解码器就可以还原为形状信息。自动编码器的框架如图1所示。蛋白质分子的结构信息被抽象为三维格点的密度信息，之后再压缩到200维的向量空间（压缩层）。这200维的向量就包含了蛋白质分子的三维形状信息，并且这些参数的分布反应了蛋白质分子形状的内在属性。 在此基础上，2018年，何皓同学继续开发自动编码器模型，并且与遗传算法结合，通过迭代优化200维的向量，找到与X射线散射实验数据对应的三维空间模型。

这个重构的方法通过对500多组实验数据进行测试，展示出良好的可靠性和正确性。利用这个方法重构的模型与数据库中的模型或者结构进行比较，发现大多数的相似度都很高（图2）。尤其是，这个方法的表现显著优于其他被广发使用的方法，为解释X射线散射数据提供了新的思路。

基于这个方法，刘海广研究组开发了decodeSAXS程序，主要是用Python语言基于TensorFlow架构实现的，并且将decodeSAXS部署到中心的服务器供实验人员免费使用： http://liulab.csrc.ac.cn/decodeSAXS (图3).

References:

Hao He; Can Liu; Haiguang Liu. Model Reconstruction from Small-Angle X-Ray Scattering Data Using Deep Learning Methods. iScience 23(3) 100906 (2020). https://doi.org/10.1016/j.isci.2020.100906

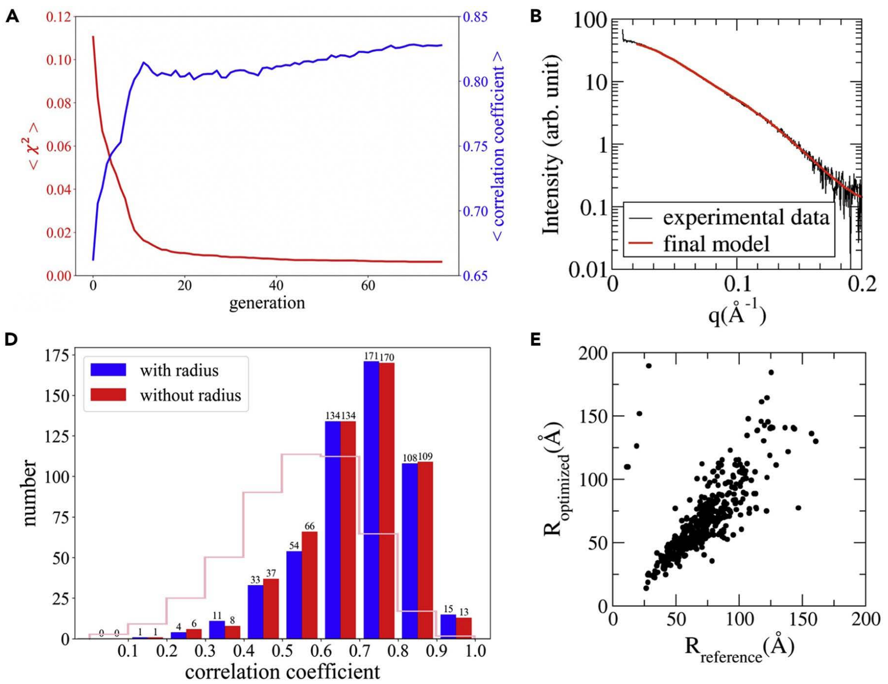

图 2 模型重构示例以及重构模型品质的统计分析。 (A) 参数优化的进程与模型品质的提升展示出良好的关联性。(B) 最终获得的模型对应的理论散射曲线与实验数据的比较。(C) 重构的模型（蓝色）与晶体衍射方法获得的结构（卡通）比较。(D) 500组实验数据重构的模型与正确模型相关性的分布。 (E) 模型的尺寸（半径）也可以自动优化。(F)两个示例展示自动优化的模型尺寸与给定参考值的模型重构结果.

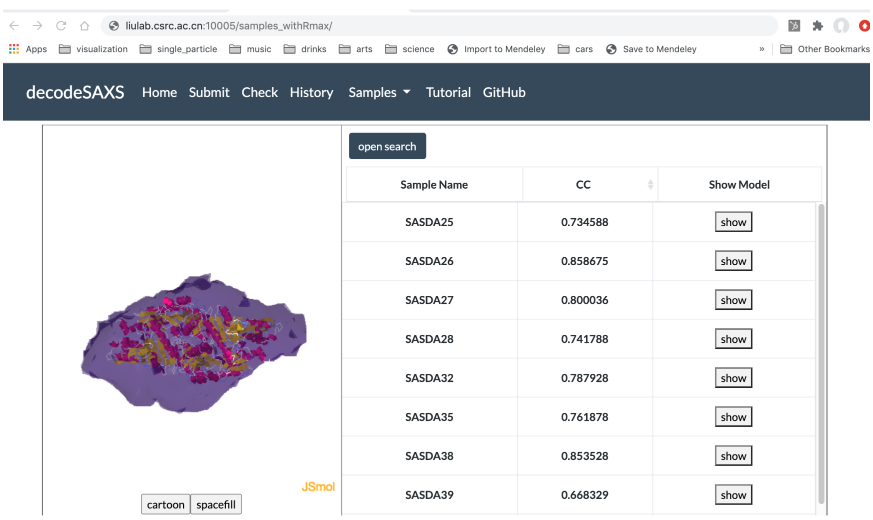

图 3 decodeSAXS网络服务器。 用户仅需要上传一维的实验数据，就可以获得重构的三维模型。

致谢: 感谢中国自然科学基金的资助(#11575021, U1530401) .

WHY FRACTIONAL DERIVATIVES WITH NON-SINGULAR KERNELS SHOULD NOT BE USED

(By Kai Diethelm, Roberto Garrappa, Andrea Giusti, **Martin Stynes***)

The use of Fractional Derivatives (FD) in the modelling of various physical processes has grown spectacularly in the last 10 years. Consequently the mathematical analysis and numerical solution of these models has also attracted significant attention, but differential equations that use the standard Caputo and Riemann-Liouville FD typically have solutions that exhibit weak singularities, which cause analytical and numerical difficulties.

Some authors have attempted to eliminate these difficulties by modifying the standard FD definitions: they replace the singular kernels of the Caputo and Riemann-Liouville FD by some nonsingular (i.e., bounded) approximation of those kernels. The best-known examples of this approach are the Caputo-Fabrizio (CF) and Atangana-Baleanu (AB) derivatives.

Example: The Caputo derivative of order $\alpha \in (0,1)$ is $D_C^\alpha f(t) = \frac{1}{\Gamma(1-\alpha)} \int_0^t (t-\tau)^{-\alpha} f'(\tau) d\tau$, while the CF derivative is $D_{CF}^\alpha f(t) = \frac{M(\alpha)}{1-\alpha} \int_0^t \exp\left(-\frac{\alpha}{1-\alpha}(t-\tau)\right) f'(\tau) d\tau$, where $M(\alpha)$ is a normalization factor such that $M(0)=M(1)=1$.

Our paper [1] shows several unpleasant and unexpected pitfalls that result from this naive attempt to simplify fractional models.

1st pitfall: The Caputo and Riemann-Liouville derivatives obey the fundamental theorem of calculus. Thus for (e.g.) the Caputo derivative D_C^α of order α with $0 < \alpha < 1$, there exists an integral operator J^α such that $D_C^\alpha J^\alpha f = f$ for all continuous functions f. But for the CF and AB derivatives, we prove that one cannot construct an integral operator with this property unless one imposes the extra (and unnatural) requirement that $f(0) = 0$.

2nd pitfall: If one does impose the condition $y(0) = 0$ of the previous paragraph in order to obtain a fundamental theorem of calculus, then we show that any fractional differential equation of the form $D^\alpha y(t) = g(t, y(t))$, where D^α is a CF or AB derivative, can be easily transformed into a classical first-order differential equation with the same solution $y(t)$, so the use of fractional derivatives in the differential equation is completely unnecessary.

3rd pitfall: For time-fractional partial differential equations of parabolic type (e.g., $D^\alpha u - \Delta u = f(x,t)$ with $0 < \alpha < 1$), where D^α is a CF or AB derivative, we prove that the given initial data $u(x,0) = u_0(x)$ must satisfy the differential equation $-\Delta u_0 = f(\cdot, 0)$, which with standard Dirichlet boundary conditions means that the initial condition u_0 is determined uniquely by the other data of the problem — a thoroughly unnatural constraint on the problem.

4th pitfall: One can integrate by parts the definitions of the CF and AB derivatives, obtaining formulas that express these derivatives of a function f in terms of values of f and a certain weighted integral of f — thus these "derivatives" are not really derivatives. (A similar calculation is impossible for the Caputo and Riemann-Liouville derivatives because of the singularities appearing in their kernels.)

References:

[1] K.Diethelm, R.Garrappa. A.Giusti, M.Stynes*[corresponding author], Why fractional derivatives with nonsingular kernels should not be used, Fract. Calc. Appl. Anal. 23 (2020), no. 3, 610–634. DOI: 10.1515/fca-2020-0032.

RESONANT PHOTOVOLTAIC EFFECT IN DOPED MAGNETIC SEMICONDUCTORS 掺杂磁性半导体中的共振光伏效应

(By Pankaj Bhalla, Allan H. MacDonald, Dimitrie Culcer)

The nonlinear optical response of a doped semiconductor to an oscillating electric field is investigated and a new second-order phenomenon known as resonant photovoltaic effect (RPE) is discovered on the breaking of Kramers degeneracy. This work was co-led primarily by Pankaj Bhalla from Beijing Computational Science Research Center, Allan H. MacDonald from University of Texas, USA and Dimitrie Culcer from University of New South Wales, Australia. The authors reported that due to the oscillation in the Bloch state anomalous velocities and the Fermi surface a resonance appears in the second-order current at the interband absorption threshold in the magnetized topological insulator. For the hexagonally warped topological insulator, the strength of this effect increases with larger warping that distort the Fermi surface and the in-plane magnetization that breaks both the time reversal and mirror symmetry.

References:

[1] Pankaj Bhalla, Allan H. MacDonald, Dimitrie Culcer Phys. Rev. Lett. 124, (2020) 087402.

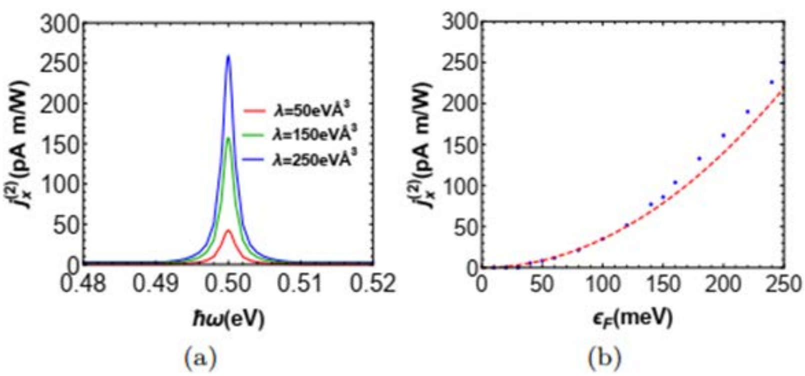

Fig. 1. RPE for magnetized TI surface states with different warping coefficients λ using εF = 250meV, A = 2.55eVÅ, T = 1K, M = 10meV, τ = 1ps. Blue: experimental value of λ for Bi_2Te_3. (b). Blue: peak value of RPE for λ = 250eVÅ^3 as a function of εF in Bi_2Te_3. Red: quadratic fit.

我们研究了掺杂半导体对振荡电场的非线性光学响应，发现了破坏Kramers简并导致的一种新的二阶现象：共振光伏效应（RPE）。这项工作主要由北京计算科学研究中心的Pankaj Bhalla、美国德克萨斯大学的Allan H.MacDonald和澳大利亚新南威尔士大学的Dimitrie Culcer共同完成。本文报道了由于Bloch态反常速度和费米面的振荡，在磁化拓扑绝缘体的带间吸收阈值处，二阶电流出现共振。对于六边形翘曲的拓扑绝缘体，这种效应随着翘曲的以及面内磁化强度的增大而增强。

图 1　不同六角翘曲参数的化拓扑绝缘体表面的共振光伏效应，参数：εF = 250meV, A = 2.55eVÅ, T = 1K, M = 10meV, τ = 1ps. 蓝色线：实验测得的Bi_2Te_3的六角翘曲参数. (b). 蓝色：λ = 250eVÅ^{3}时，共振光伏效应的峰值随Bi_2Te_3的费米能εF 的变化。红线：抛物线拟合。

ANALYTICAL TRANSIENT DISTRIBUTION AND DYNAMIC PHASE DIAGRAM FOR AUTOREGULATED BURSTY GENE EXPRESSION

(By **Chen Jia**, Ramon Grima)

Autoregulation is one of the most common and important network motifs in gene regulatory systems. In previous papers, three different stochastic models of autoregulation have been proposed and solved in steady-state conditions based on different implicit assumptions. Hornos et al. [1] ignored both binding fluctuations and translational bursting. Grima et al. [2] considered the former but ignored the latter. Kumar et al. [3] considered the latter but ignored the former. Thus far, there is no model of autoregulation that considered both the former and the latter.

A recent work [4,5] by Chen Jia from CSRC and Ramon Grima from University of Edinburgh proposed a more realistic stochastic model of autoregulation that takes into account both binding fluctuations and translational bursting and proved that this new model can be derived from a classical three-stage gene expression model using a multiscale model simplification technique called decimation [6]. Moreover, the authors obtained both the steady-state and time-dependent analytical solutions for the protein copy number distribution using the techniques of generating functions, special functions, and complex analysis. **From the mathematical perspective, it is the first time that complex analysis is applied to solve the chemical master equations of gene regulatory networks**.

The authors further investigated multimodality for an autoregulated gene and found that autoregulated bursty gene expression can display four different types of stochastic dynamics: (i) the protein distribution is unimodal at all times (unimodality), (ii) the protein distribution is unimodal at small and large times and is bimodal at intermediate times (transient bimodality), and (iii) the protein distribution is unimodal at small times and is bimodal at large times (stationary bimodality). Each type of dynamic behavior can be further divided into two phases according to whether the deterministic model shows monostability or bistability. Hence the dynamic behavior of autoregulated bursty gene expression can be classified into six possible phases.

Using the analytical transient distribution, the authors further obtained the dynamical phase diagram for autoregulated bursty gene expression. In the positive feedback case, there is a triple point separating the three phases of the stochastic model (unimodality, transient bimodality, and stationary bimodality) — this is similar to the triple point in the phase transition between solid, liquid, and gaseous states of a substance due to the effects of temperature and pressure. Finally, the authors showed that transient bimodality is a noise-induced phenomenon that occurs when protein expression is sufficiently bursty and they used theory to estimate the observation time window when it is manifest.

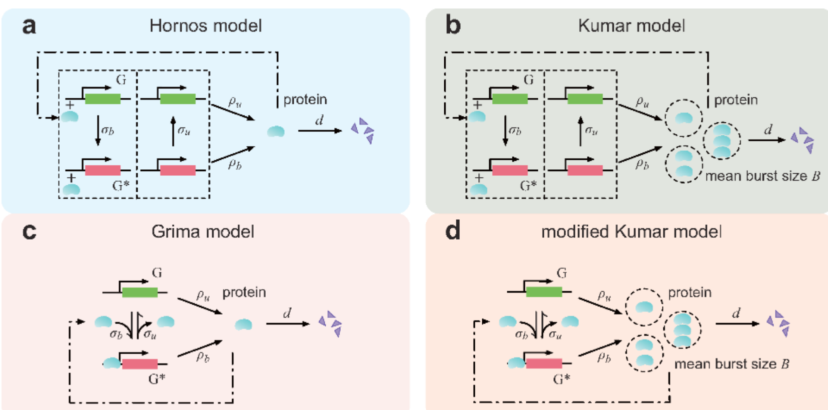

Fig. 1. Four different models of autoregulation. (a) Hornos model that ignored both binding fluctuations and translational bursting. (b) Kumar model that considered translational bursting but ignored binding fluctuations. (c) Grima model that considered binding fluctuations but ignored translational bursting. (d) Modified Kumar model that considered both binding fluctuations and translational bursting.

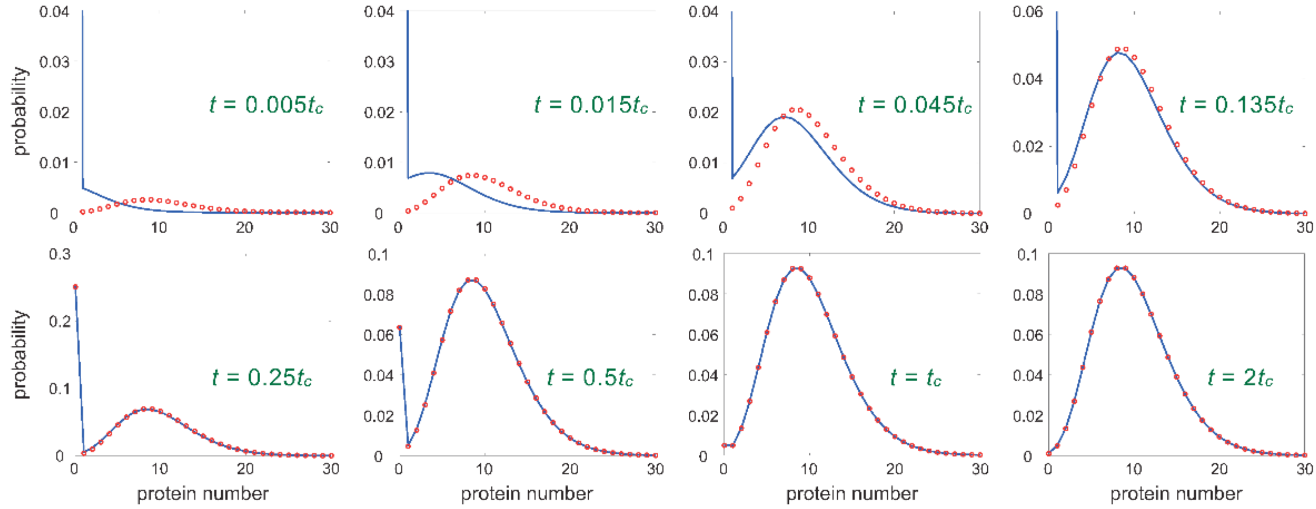

Fig. 2. Transient bimodality. The protein distribution is unimodal at small and large times and is bimodal at intermediate times.

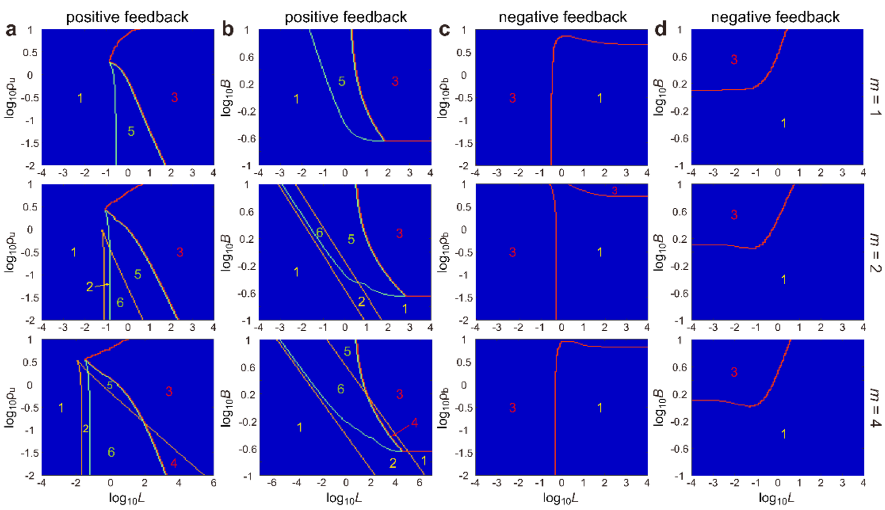

Fig. 3. Dynamical phase diagrams for autoregulated bursty gene expression. (a) L-ρu phase diagram for positive feedback loops. (b) L-B phase diagram for positive feedback loops. (c) L-ρb phase diagram for negative feedback loops. (d) L-B phase diagram for negative feedback loops.

References:

[1] Hornos, J. et al. Self-regulating gene: an exact solution. Phys. Rev. E 72, 051907 (2005).

[2] Grima, R., Schmidt, D. & Newman, T. Steady-state fluctuations of a genetic feedback loop: An exact solution. J. Chem. Phys. 137, 035104 (2012).

[3] Kumar, N., Platini, T. & Kulkarni, R. V. Exact distributions for stochastic gene expression models with bursting and feedback. Phys. Rev. Lett. 113, 268105 (2014).

[4] C. Jia, R. Grima. Dynamical phase diagram of an auto-regulating gene in fast switching conditions. J. Chem. Phys. 152(17):174110, 2020.

[5] C. Jia, R. Grima. Small protein number effects in autoregulated bursty gene expression. J. Chem. Phys. 152(8):084115, 2020.

[6] C. Jia. Kinetic foundation of zero-inflated negative binomial models for single-cell RNA sequencing data. SIAM J. Appl. Math. 80(3), 1336-1355, 2020.

自调控突发性基因表达的解析瞬时分布与动力学相图

（中心作者：贾晨）

自调控是基因调控系统中最常见且最重要的网络元件。先前的文章中提出了三种不同的随机自调控模型，并得到了相应模型的稳态解析解。这三个模型基于三种不同的隐含假设：Hornos等人[1]提出的模型同时忽略了蛋白的结合涨落与翻译突发性，Grima等人[2]提出的模型考虑了前者但忽略了后者，而Kumar等人[3]提出的模型考虑了后者但忽略了前者. 截至目前为止，现有文献中仍然缺乏一个同时考虑前者与后者的自调控基因网络模型。

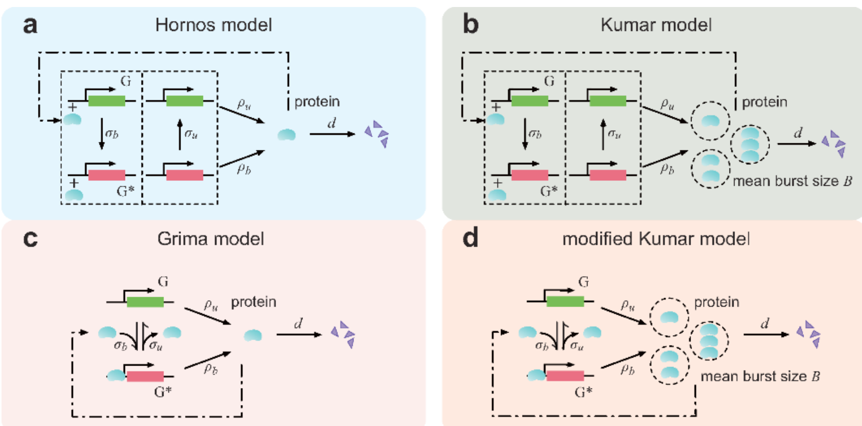

图 1　四种不同的自调控基因网络模型：(a) Hornos模型，该模型同时忽略了蛋白的结合涨落与翻译突发性；(b) Kumar模型，该模型考虑了翻译突发性但忽略了蛋白的结合涨落；(c) Grima 模型，该模型考虑了蛋白的结合涨落但忽略了翻译突发性；(d) 改良的Kumar模型，该模型同时考虑了蛋白的结合涨落与翻译突发性.

在最近的一项工作中[4,5]，北京计算科学研究中心的贾晨与英国爱丁堡大学的Ramon Grima同时考虑了蛋白的结合涨落与翻译突发性，提出了一个更加实际的随机自调控模型. 作者利用马氏过程的多尺度模型简化技术[6]，从经典的三阶段基因表达模型中完全推导出了这个新模型，因而验证了该模型的普适性与真实性. 此外，作者利用概率母函数，特殊函数以及复分析的方法，得到了蛋白拷贝数分布的稳态以及瞬时解析解。在数学方面，该工作首次将复分析方法应用于基因调控网络化学主方程的求解，具有高度的创新性。

作者进一步研究了自调控基因网络的多峰性，并发现自调控突发性基因表达可以呈现出四种不同的随机动力学：(1) 蛋白数量分布对于所有时间点都是单峰的，简称为单峰性，(2) 蛋白数量分布对于短时间点和长时间点是单峰的，但对于中间时间点是双峰的，简称为瞬时双峰性，(3) 蛋白数量分布对于短时间点是单峰的，但对于长时间点是双峰的，简称为平稳双峰性. 根据相应的确定性模型产生单稳态还是双稳态，这三种随机动力学的每一种又可以被进一步分为两种不同的动力学相。因此，自调控突发性基因表达的动力学行为可以被分为六种不同的动力学相。

利用蛋白瞬时分布的解析解，作者进一步得到了自调控突发性基因表达的动力学相图。在正反馈情形下，动力学相图具有一个三相点。该三相点分割了随机模型的三种不同的动力学相，即单峰性，瞬时双峰性与平稳双峰性. 该现象类似于当温度与压强变化时，物质在固态、液态以及气态间进行相变所产生的三相点。作者进一步发现暂态双峰性是一种由噪声诱导的现象，且该现象只有当蛋白表达的突发性足够强时才会发生。最后，作者利用他们所发展的解析理论估计了暂态双峰性的观测时间窗口。

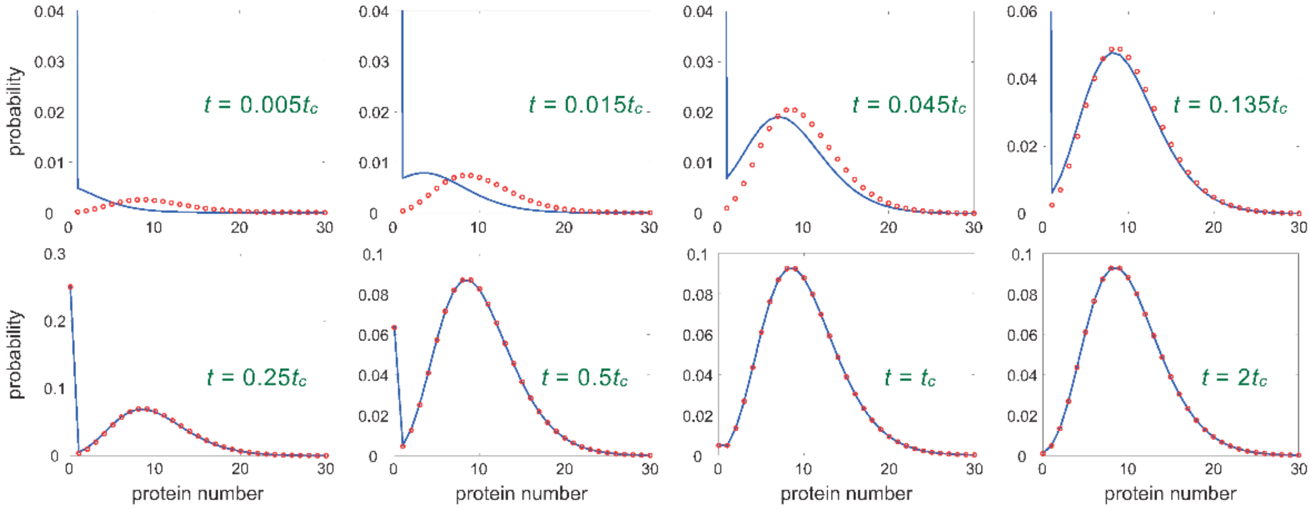

图 2　瞬时双峰性：蛋白数量分布对于短时间点和长时间点是单峰的，但对于中间时间点是双峰的。

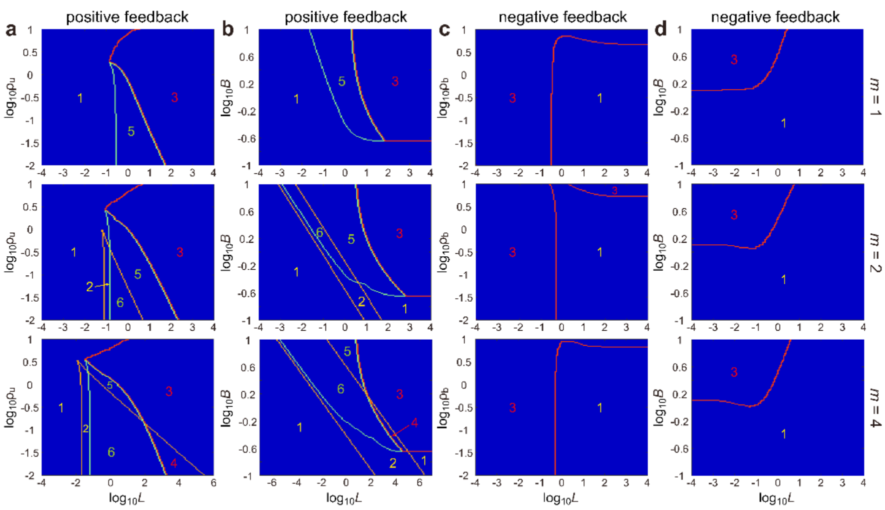

图 3　自调控突发性基因表达的动力学相图：(a) 正反馈环的L-ρu相图；(b) 正反馈环的L-B相图；(c) 负反馈环的L-ρb相图；(d) 负反馈环的L-B相图。

References:

[1] Hornos, J. et al. Self-regulating gene: an exact solution. Phys. Rev. E 72, 051907 (2005).

[2] Grima, R., Schmidt, D. & Newman, T. Steady-state fluctuations of a genetic feedback loop: An exact solution. J. Chem. Phys. 137, 035104 (2012).

[3] Kumar, N., Platini, T. & Kulkarni, R. V. Exact distributions for stochastic gene expression models with bursting and feedback. Phys. Rev. Lett. 113, 268105 (2014).

[4] C. Jia, R. Grima. Dynamical phase diagram of an auto-regulating gene in fast switching conditions. J. Chem. Phys. 152(17):174110, 2020.

[5] C. Jia, R. Grima. Small protein number effects in autoregulated bursty gene expression. J. Chem. Phys. 152(8):084115, 2020.

[6] C. Jia. Kinetic foundation of zero-inflated negative binomial models for single-cell RNA sequencing data. SIAM J. Appl. Math. 80(3), 1336-1355, 2020.

A CONVERGENT LINEARIZED LAGRANGE FINITE ELEMENT METHOD FOR THE MAGNETO-HYDRODYNAMIC EQUATIONS IN 2D NONSMOOTH AND NONCONVEX DOMAINS

(By Buyang Li, **Jilu Wang**, Liwei Xu)

The magneto-hydrodynamics (MHD) equations describe the interaction between a magnetic field and a viscous incompressible conducting fluid flow. For time-dependent MHD equations, many different numerical methods have been developed and analyzed, e.g., the H^1-conforming FEMs, Galerkin least square FEM, divergence-free preserving methods, and finite difference methods. Overall, the existing H^1-conforming FEMs for the MHD equations were proved to be convergent only in convex or smooth domains. In more general domains the mixed FEM with curl-conforming Nédélec elements is more suitable for approximating the magnetic field directly, while existing proofs for the convergence of numerical solutions either require mesh restriction $\tau = O(h^3)$ or yield only weak- or weak*-convergence of the numerical solutions.

Recently, Buyang Li (The Hong Kong Polytechnic University), Jilu Wang (CSRC), and Liwei Xu (University of Electronic Science and Technology) investigate the numerical approximation of the incompressible MHD equations [3]

$$\mu\partial_t \boldsymbol{H} + \sigma^{-1}\nabla\times(\nabla\times\boldsymbol{H}) - \mu\nabla\times(\boldsymbol{u}\times\boldsymbol{H}) = \sigma^{-1}\nabla\times J$$
$$\partial_t\boldsymbol{u} + \boldsymbol{u}\cdot\nabla\boldsymbol{u} - \nu\Delta\boldsymbol{u} + \nabla p = \boldsymbol{f} - \mu\boldsymbol{H}\times(\nabla\times\boldsymbol{H})$$
$$\nabla\cdot\boldsymbol{u} = 0$$

in a two-dimensional polygonal type domain $\Omega = \Omega_0\backslash(\cup_{j=1}^m \Omega_j) \subset \mathbb{R}^2$, where both Ω_0 and $\Omega_j \subset \Omega_0, j = 1,\cdots,m$, are polygons (thus the domain is possibly nonconvex and multi-connected, e.g., see the following figure).

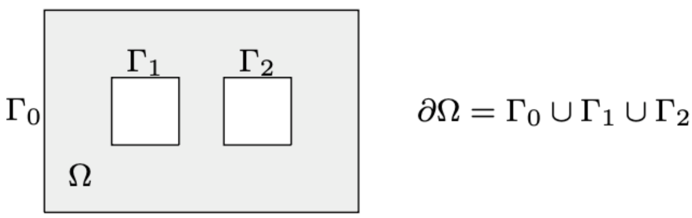

The most important applications of the MHD model considered in the paper [3] occur in metallurgy and liquid-metal processing [1,5]. In that context, consideration of general polygonal yet nonconvex and multi-connected domains is very relevant. In [3], the authors develop a new fully discrete linearized H^1-conforming Lagrange FEM for the two-dimensional MHD equations based on a magnetic potential formulation such that the numerical solutions would converge not only in convex and smooth domains but also in nonconvex and nonsmooth domains. In the magnetic potential formulation, the magnetic potential $\boldsymbol{A}$ would naturally has H^1 regularity and therefore can be solved correctly by using H^1-conforming finite element methods. Then the magnetic field is obtained through taking partial derivatives, i.e., $\boldsymbol{H} = \nabla\times A + \sum_{j=1}^m \beta_j \nabla\times\varphi_j$, where β_j and φ_j are some time-independent constants and functions, depending on the geometry of the computational domain. Similarly as [2,4], the proof of convergence of the numerical solutions in [3] is only based on the regularity of the initial conditions and source terms, without extra assumptions on the regularity of the solution. Strong convergence of subsequences in $L^2\left(0,T;\boldsymbol{L}^2(\boldsymbol{\Omega})\right)$ as $(\tau_n, h_n) \to (0,0)$ is proved for the numerical solutions of $\boldsymbol{u}$ and $\boldsymbol{H}$ without mesh restrictions.

非光滑区域上磁流体力学方程的线性化拉格朗日有限元法

（中心作者：王冀鲁）

磁流体力学是结合流体力学和电动力学的方法，研究导电流体在外磁场中的运动规律及相互作用。对于时间相关的磁流体力学方程，人们已经发展和分析了许多不同的数值方法，如H^1协调有限元法、Galerkin最小二乘有限元法、保持散度为零的数值方法、有限差分法。总的来说，现有的适用于求解磁流体力学方程的H^1协调有限元法仅在凸区域或光滑区域被证明收敛。在更一般的区域中，具有旋度协调的Nédélec元的混合有限元法更适合于直接近似磁场强度，而现有的数值解的收敛性证明要么要求时空网格比约束条件$\tau = \mathcal{O}(h^3)$，要么只能得到数值解的弱收敛或弱*收敛。

最近，李步扬（香港理工大学）、王冀鲁（北京计算科学研究中心）和徐立伟（电子科技大学）在二维多边形区域$\Omega = \Omega_0 \backslash (\cup_{j=1}^{m} \Omega_j) \subset \mathbb{R}^2$中研究了不可压磁流体力学方程的数值逼近 [3]

$$\mu \partial_t \boldsymbol{H} + \sigma^{-1} \nabla \times (\nabla \times \boldsymbol{H}) - \mu \nabla \times (\boldsymbol{u} \times \boldsymbol{H}) = \sigma^{-1} \nabla \times J$$
$$\partial_t \boldsymbol{u} + \boldsymbol{u} \cdot \nabla \boldsymbol{u} - \nu \Delta \boldsymbol{u} + \nabla p = \boldsymbol{f} - \mu \boldsymbol{H} \times (\nabla \times \boldsymbol{H})$$
$$\nabla \cdot \boldsymbol{u} = 0$$

其中，Ω_0 和 $\Omega_j \subset \Omega_0, j = 1, \cdots, m,$ 都是多边形（因此该区域可能是非凸或多连通的，如下图所示）。

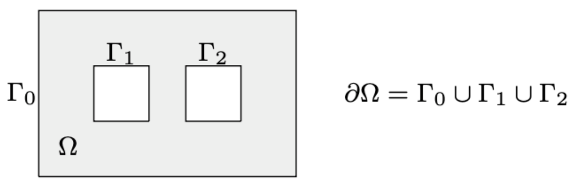

文章[3]中考虑的磁流体力学模型很重要的应用包括在冶金和液态金属加工中[1,5]。在这种情况下，人们常在更一般的多边形区域（比如非凸或多连通的）考虑该问题。在文章[3]中，作者基于磁势公式，对二维磁流体力学方程提出了新的全离散线性化H^1协调拉格朗日有限元法，使得数值解不仅在凸区域和光滑区域中收敛，而且在非凸区域和非光滑区域中也收敛。在磁势公式中，磁势A具有H^1正则性，因此可以使用H^1协调有限元法正确地求解。然后通过对其求偏导数得到磁场强度，即 $\boldsymbol{H} = \nabla \times A + \sum_{j=1}^{m} \beta_j \nabla \times \varphi_j$，这里 β_j 和 φ_j 是一些与时间相关的常数和函数，这取决于计算域的几何结构。与文献[2,4]类似，文章[3]中数值解的收敛性证明仅基于初始条件和右端源项的正则性，而没有对真解的正则性作额外的假设。同时，在不需要借助时空网格比约束的情况下，作者在文章[3]中证明了数值解子序列的 $L^2\left(0, T; \boldsymbol{L}^2(\boldsymbol{\Omega})\right)$ 强收敛性。

References:

[1] S. Asai: *Electromagnetic Processing of Materials*, Fluid Mechanics and Its Applications 99, 2012, Springer Netherlands.

[2] R. Hiptmair, L. Li, S. Mao, and W. Zheng: A fully divergence-free finite element method for magneto-hydrodynamic equaitons, *Math. Models Methods Appl. Sci.*, 28 (2018), pp. 659-695.

[3] B. Li, J. Wang, and L. Xu, A convergent linearized Lagrange finite element method for the magneto-hydrodynamic equations in two-dimensional nonsmooth and nonconvex domains, *SIAM J. Numer. Anal.*, 58 (2020), pp. 430-459.

[4] A. Prohl: Convergent finite element discretizations of the nonstationary incompressible magnetohydrodynamics system, ESAIM: Math. Model. Numer. Anal., 42 (2008), pp. 1065-1087.

[5] Y. Unger, M. Mond, and H. Branover: *Liquid Metal Flows*: Magnetohydrodynamics and Application, American Institute of Aeronautics and Astronautics, 1988.

SUPPLEMENTARY VARIABLE METHOD FOR STRUCTURE-PRESERVING APPROXIMATIONS TO PARTIAL DIFFERENTIAL EQUATIONS WITH DEDUCED EQUATIONS

(By **Qi Hong**, **Jun Li** and **Qi Wang**)

We present a supplementary variable method (SVM) for developing structure-preserving numerical approximations to a partial differential equation system with deduced equations [3]. The PDE system with deduced equations constitutes an over-determined, yet consistent and structurally unstable system of equations. We augment a proper set of supplementary variables to the over-determined system to make it well-determined with a stable structure. We then discretize the modified system to arrive at a structure-preserving numerical approximation to the over-determined PDE system. We illustrate the idea using a dissipative network generating partial differential equation model by developing an energy-dissipation-rate preserving scheme. We then simulate the network generating phenomenon using the numerical scheme. This numerical method is so general that it applies literally to any PDE systems with deduced equations.

Many partial differential equation systems have deduced equations that have physical significance. For example, in a thermodynamically consistent partial differential equation (TCPDE) system together with a deduced time evolutional equation of the energy functional that has a negative time rate of change. The energy functional and its time evolutionary equation has a profound physical and mathematical implication to the physical process that the TCPDE describes. All the non-equilibrium thermodynamical models derived from principles of non-equilibrium thermodynamics such as the Onsager principle belong to this class of equations [6,7,8].

When we augment the PDE system by including the deduced equations, the extended system is over-determined and yet consistent. A structure-preserving approximation to the extended system simply means that an approximation to the PDE system is consistent with a corresponding approximation to the deduced equations. If the approximations are carried out respectively on each equation, the chance to arrive at a consistent approximation to the two sets of equations is extremely small.

Traditionally, one relies on clever techniques with meticulous attentions to details to achieve the desired consistency by exploiting the structure of each individual PDE system. So, the development of structure-preserving approximation becomes highly equation-type dependent and technically challenging. In this letter, we present a new idea to achieve the structure-preserving purpose for any PDE systems with deduced equations. We augment the over-determined system with a proper set of supplementary variables to make it well-determined and structurally stable in the meantime. We note that the modified system reduces to the original one when the supplementary variables take on certain specific values. This can be viewed as an embedding of the original dynamical system into a modified dynamical system in a higher dimensional phase space whose solution set includes the solution of the original PDE system as a subset. Since the perturbation is done in such a way that the modified system is structurally stable. This requirement ensures the solution of the supplementary variable exists near the specific values and is unique locally. We illustrate the idea using the network generating TCPDE as an example.

We briefly recall the dissipative, network-generating PDE model proposed in [1,2,4,5]. Consider a bounded domain Ω with a smooth boundary $\partial\Omega$ and a time-independent source term $S(x)$. Here we use p to represent the scalar pressure of the fluid transported within the network and for the vector-valued conductance. The dissipative network-generating PDE system consists of two equations

$$-\nabla\cdot\left((r\mathbf{I}+\mathbf{mm})\nabla\mathbf{p}\right)=\mathbf{S},$$
$$\mathbf{m}_t-\mathbf{K}\Delta\mathbf{m}-\mathbf{a}^2(\mathbf{m}\cdot\nabla\mathbf{p})\nabla\mathbf{p}+\boldsymbol{\alpha}\,|\,\mathbf{m}\,|^{2(\gamma-1)}\,\mathbf{m}=\mathbf{0},$$

subject to homogeneous Dirichlet boundary conditions for $\mathbf{m}$ and p at $\partial\Omega$:

$$\mathbf{m}(t,\mathbf{x})=0,\quad p(t,\mathbf{x})=0,\quad \forall\ \mathbf{x}\in\partial\Omega,\quad t\geq 0.$$

Here the model parameters are diffusivity $K\geq 0, r, \gamma, \alpha>0$, and

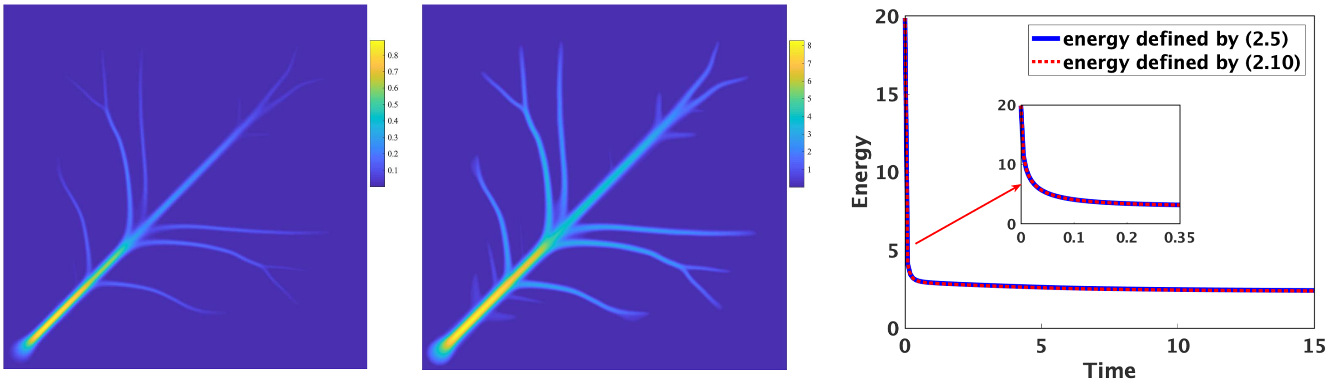

Fig. 1. The norm of conductance vector $\|\mathbf{m}\|$ (left), fluid velocity $\|\mathbf{v}\|$ (center) and the energy with $K = 0.005^2$ at $t = 15$ (right). The right sub-figure shows that two types of energy decay with time using the SVM scheme.

activation parameter $\alpha > 0$. One deduces from the model the following energy production rate equation

$$\frac{d\mathrm{E}}{dt} = -\int_\Omega \|\partial_t \mathbf{m}\| dx,$$

where the energy functional is defined by

$$\mathrm{E} = \frac{1}{2}\int_\Omega \left(K\,|\nabla \mathbf{m}|^2 + \frac{\alpha}{\gamma}|\mathbf{m}|^{2\gamma} + a^2\,|\mathbf{m}\cdot\nabla p|^2 + a^2 r\,|\nabla p|^2\right)\mathrm{dx}.$$

We apply the SVM to this PDE model together with its energy dissipation equation to develop a second order scheme in space and time on a staggered grid in space. The scheme performs well and captures the solution with good resolution. Figure 1 depicts a numerical simulation of the network formation using the model. The numerical results clearly demonstrate the capability of SVM scheme in capturing the network structure.

References:

[1] G. Albi, M. Artina., M. Foransier, and P. Markowich. Biological transportation networks: Modeling and simulation. Anal. Appl., 16:185-206, 2016.

[2] Jan Haskovec, Peter Markowich, and Benoit Perthame. Mathematical analysis of a PDE system for biological network formation. Comm. Partial Di_ erential Equations, 40:918-956, 2015.

[3] Qi Hong, Jun Li and Qi Wang, "Supplementary Variable Method for Structure-Preserving Approximations to Partial Differential Equations with Deduced Equations." Applied Mathematics Letter, 110:106576, 2020.

[4] D. Hu and D. Cai. An optimization principle for initiation and adaptation of biological transport networks. Commun. Math. Sci., 17:1427-1436, 2019.

[5] Dan Hu and David Cai. Adaptation and optimization of biological transport networks. Phys. Rev. Lett., 111:8701, 2013.

[6] L. Onsager. Reciprocal relations in irreversible processes. I. Phys. Rev., 37:405-426, 1931.

[7] L. Onsager. Reciprocal relations in irreversible processes. II. Phys. Rev., 38:2265-2279, 1931.

[8] X. Yang, J. Li, G. Forest, and Q. Wang. Hydrodynamic theories for flows of active liquid crystals and the generalized onsager principle. Entropy, 18:202, 2016.

补充变量方法构造带有导出方程的PDE系统的保结构算法

（中心作者：洪旗、王奇）

本文提出了一种补充变量方法 (SVM), 用于研究带有导出方程的PDE系统的保结构数值逼近[3]。原始偏微分方程和导出方程构成了一个超定、一致但结构不稳定系统。我们对这个超定系统补充一些合适的变量，使得它是一个适定且结构稳定的系统。然后，我们离散这个修正的系统，以便得到超定PDE系统的保结构数值逼近。为了说明该方法的主要思想，本文以具有耗散性质的Network增长模型为例，首先对模型设计保能量耗散率的数值格式，再利用该格式模拟Network增长现象。这种保结构数值算法具有普适性，它适用于任何带有导出方程的偏微分方程系统。

带有导出方程的偏微分方程系统有重要的物理意义。例如，在热力学一致偏微分方程（TCPDE）系统中, 能量泛函的演化方程关于时间变化率为负值。能量泛函及其时间演化方程对TCPDE所描述的物理过程具有深刻的物理和数学意义。所有由非平衡态热力学原理 (例如Onsager原理) 推导出的非平衡态热力学模型都属于这一类方程 [6,7,8]。

当我们通过导出方程来增广原始PDE系统时，得到的扩展系统是超定的，但仍是一致的. 扩展系统的保结构数值逼近意味着原始PDE系统的近似与导出方程的近似是一致的。如果分别对每个方程作相应的数值逼近，很少能得到两组方程的一致逼近。

传统做法需要采用一些技巧，通过研究每个独立的PDE系统的结构来达到预期的一致性。因此, 构造保结构数值逼近严重依赖方程的类型和技巧的选择。本文对任何具有导出方程的PDE系统的保结构算法设计提出了一个新的思路。我们使用一组适当的补充变量来扩充超定系统，使得它同时具有适定性和结构稳定。当补充变量选取某些特定值时，修正后的系统将退化为原始系统。这可以看作将原始动力学系统嵌入到一个高维相空间中的修正的动力学系统中，该系统的解集包含原始PDE系统的解。以此方式进行扰动可以保正修正系统在结构上是稳定的. 这需要确保补充变量方法的解存在于特定值附近，且局部唯一。本文以网络增长TCPDE模型为例来说明这一思想。

我们简要回顾文献 [1,2,4,5] 中提出的具有耗散性质的Network增长模型。考虑具有光滑边界的有界区域和不依赖时间的源项 $S(x)$, 这里使用标量 p 表示在网络内传输的流体压力, 和 $\mathbf{m}$ 表示向量电导值。耗散网络增长PDE系统由下面两个方程组成:

$$
\begin{aligned}
&-\nabla\cdot\big((r\mathbf{I}+\mathbf{mm})\nabla\mathbf{p}\big)=\mathbf{S},\\
&\mathbf{m}_{\mathbf{t}}-\mathbf{K}\Delta\mathbf{m}-\mathbf{a}^{2}(\mathbf{m}\cdot\nabla\mathbf{p})\nabla\mathbf{p}+\boldsymbol{\alpha}\,|\,\mathbf{m}\,|^{2(\gamma-1)}\,\mathbf{m}=\mathbf{0},
\end{aligned}
$$

其中，p 和 $\mathbf{m}$ 在边界 $\partial\Omega$ 上满足齐次Dirichlet边界条件:

$$
\mathbf{m}(t,\mathbf{x})=0,\quad p(t,\mathbf{x})=0,\quad \forall\ \mathbf{x}\in\partial\Omega,\quad t\geq 0.
$$

这里的模型参数是扩散系统 $K\geq 0, r, \gamma, \alpha > 0$, 激活参数 $\alpha > 0$。该模型有如下的能量耗散率方程:

$$
\frac{d\mathrm{E}}{dt}=-\int_{\Omega}\|\,\partial_t\mathbf{m}\,\|\,dx,
$$

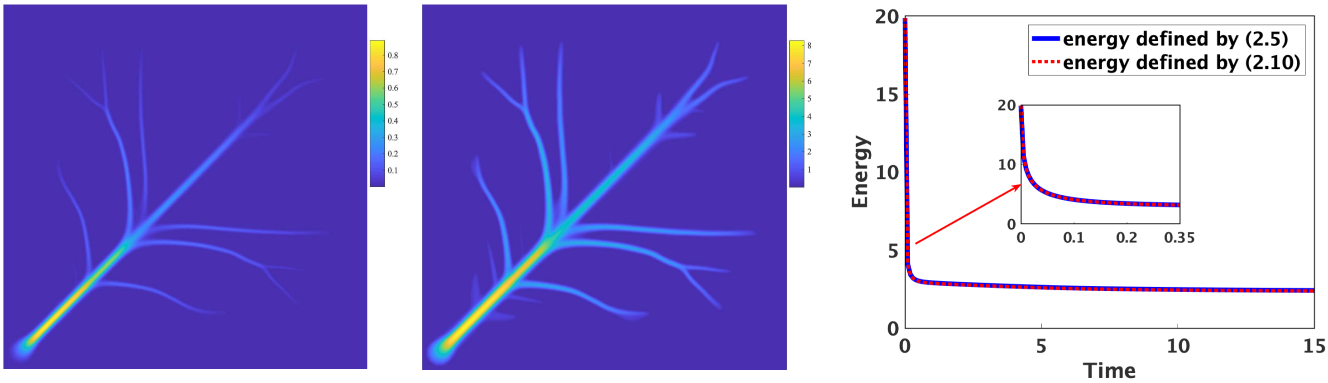

其中，能量泛函 **E** 定义为:

$$\mathrm{E}=\frac{1}{2}\int_{\Omega}\left(K\,|\nabla \mathbf{m}|^{2}+\frac{\alpha}{\gamma}|\mathbf{m}|^{2\gamma}+a^{2}\,|\mathbf{m}\cdot\nabla p|^{2}+a^{2}r\,|\nabla p|^{2}\right)\mathrm{dx}.$$

图 1　电导向量范数 $\|\mathbf{m}\|$ (左), 流体速度 $\|\mathbf{v}\|$ (中) 和能量 (右), 其中 $K=0.005^2$. 右边子图表明这种不同形式的能量随着时间是递减的。

我们将SVM方法应用于该模型和它的能量耗散率方程组成的系统，在空间交错网格上构造时空二阶保结构数值格式。该格式数值表现优异，并且数值解具有很好的精度。图1描述了使用该模型的网络增长的数值模拟结果, 它清晰地表明了SVM方法模拟Network结构的能力。

References:

[1] G. Albi, M. Artina., M. Foransier, and P. Markowich. Biological transportation networks: Modeling and simulation. Anal. Appl., 16:185-206, 2016.

[2] Jan Haskovec, Peter Markowich, and Benoit Perthame. Mathematical analysis of a PDE system for biological network formation. Comm. Partial Di_erential Equations, 40:918-956, 2015.

[3] Qi Hong, Jun Li and Qi Wang, "Supplementary Variable Method for Structure-Preserving Approximations to Partial Differential Equations with Deduced Equations." Applied Mathematics Letter, 110:106576, 2020.

[4] D. Hu and D. Cai. An optimization principle for initiation and adaptation of biological transport networks. Commun. Math. Sci., 17:1427-1436, 2019.

[5] Dan Hu and David Cai. Adaptation and optimization of biological transport networks. Phys. Rev. Lett., 111:8701, 2013.

[6] L. Onsager. Reciprocal relations in irreversible processes. I. Phys. Rev., 37:405-426, 1931.

[7] L. Onsager. Reciprocal relations in irreversible processes. II. Phys. Rev., 38:2265-2279, 1931.

[8] X. Yang, J. Li, G. Forest, and Q. Wang. Hydrodynamic theories for flows of active liquid crystals and the generalized onsager principle. Entropy, 18:202, 2016.

TUNABLE PHOTORESPONSE BY GATE MODULATION IN BILAYER GRAPHENE NANORIBBON DEVICES

(By Rulin Wang, Fuzhen Bi, Wencai Lu, and **ChiYung Yam**)

For optical-to-electrical conversion, separation of photo-excited electron-hole pairs is an essential step for generation of photocurrent. For the p-n junction, a built-in electric field around the junction interface can provide the separating force for the electron-hole pairs. And the use of an external electric field, provided, for example, by a source-drain bias voltage or a split gate voltage, has also been considered as a mean to drive the separation of electron-hole pairs. Recently, a tunable band gaps has been realized for bilayer graphene by applying an external electric field.1 This tunable band gap allows adjustment of the absorption range of photon energy and have potential application for the design of photoelectric devices.

ChiYung Yam *et al*. at Beijing Computational Science Research Center take advantage of the continuously tunable band gap and separation of electron-hole pairs by a gate voltage and investigate the controllability of the photocurrent in a bilayer armchair graphene nanoribbon (GNR).[2] They employed the nonequilibrium Green's function (NEGF) method together with a quantum description of the electron-photon interaction to model the photoelectric conversion proces.[3] The results demonstrate that the photoresponse of a bilayer graphene nanoribbon (GNR) device can be controlled by gate voltage modulation. A vertical gate field shifts the potential on the top and bottom layers in opposite directions, resulting in a continuous change of band gap with applied gate voltage. This field simultaneously facilitates separation of photoexcited electron-hole pairs and gives rise to a photocurrent in a selected photon energy range. The photoresponse of a bilayer GNR device can thus be tuned by adjusting the applied gate voltage. In addition, the light frequency range can be changed by using nanoribbons of different widths. These findings provide a basis for the design of adjustable optoelectronic devices using two-dimensional materials.

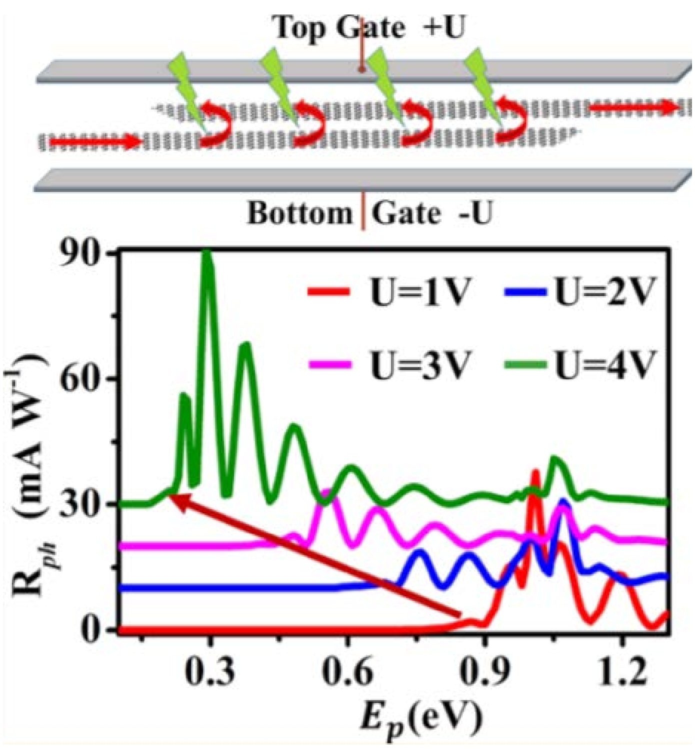

通过门电压调制实现的双层石墨烯纳米带器件的可调光响应

（中心作者：任志勇）

光电转换过程中，光激发产生的电子-空穴对的分离是产生光电流的重要步骤。一般来说，对于由p-n结构成的器件，界面处的内置电场可促进电子-空穴对的分离。另外，外加电场也可为电子-空穴对分离提供驱动力，例如由源极-漏极偏置电压或栅极电压提供的外部电场是驱动电子-空穴对分离的有效手段。最近，实验中发现通过施加外部电场可调控双层石墨烯的带隙[1]。进一步，该可调带隙可以调节光子能量的吸收范围，对光电器件的设计具有潜在的应用价值。

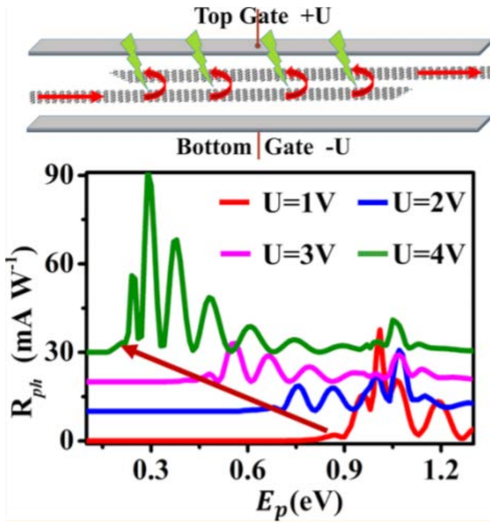

来自北京计算科学研究中心的任志勇等研究人员利用门压同时调控双层扶手型石墨烯纳米带的能隙和电子-空穴分离，研究了器件中光电流的可控性[2]。

他们采用非平衡格林函数（NEGF）的方法且在量子力学框架下引入电子-光子相互作用，对光电转换过程进行模拟[3]。结果表明，双层石墨烯纳米带器件的光响应可以通过门电压来调制。垂直方向的门电压使得顶层和底层石墨烯所在平面内的电势沿相反方向变化，从而导致双层石墨烯纳米带的带隙随施加的门电压连续变化。该垂直电场同时促进了光激发产生的电子-空穴对的分离，可在一定的能量范围内产生光电流。因此，可以通过调节门电压来调节双层石墨烯纳米带器件的光响应。另外，还可通过使用不同宽度的纳米带来调节吸收光的频率范围。这些发现为使用二维材料设计可调节光电器件提供了参考。

References:

[1] Ju, L.; Wang, L.; Cao, T.; Taniguchi, T.; Watanabe, K.; et al. Science 2017, 358, 907.

[2] Ruling, Wang; Fuzhen, Bi; Wencai, Lu and ChiYung Yam J. Phys. Chem. Lett. 2019, 10, 24, 7719–7724.

[3] Zhang, Y.; Meng, L.; Yam, C.; Chen, G. J. Phys. Chem. Lett. 2014, 5, 1272.

PHOTONIC BAND STRUCTURE CALCULATION FOR DISPERSIVE MATERIAL

(By **Wenqiang Xiao**, **Bo Gong**, Jiguang Sun, **Zhimin Zhang**)

Photonic crystals (PCs) are periodic structures composed of dielectric materials and exhibiting band gaps, which has many important applications in optical communications, filters, lasers, switches and optical transistors [1-3]. Effective calculations of the band structures are essential to identify novel optical phenomena and develop new devices. If the permittivity is independent of the frequency, the associated eigenvalue problem is linear. In contrast, dispersive materials lead to the challenging nonlinear eigenvalue problems.

Photonic band structures are posted as the eigenvalue problems of the Maxwell's equations [3]

$$\begin{cases} \nabla \times \dfrac{1}{\epsilon(x,\omega)} \nabla \times \mathbf{H} = \left(\dfrac{\omega}{c}\right)^2 \mathbf{H}, \\ \nabla \quad \mathbf{H} = 0, \end{cases}$$

where $\mathbf{H}$ is the magnetic field, ω is the frequency, $\epsilon(x, \omega)$ is the electric permittivity, and c is the speed of light in the vacuum.

In [4], a novel approach is proposed for the band structure calculation of dispersive materials. The band structure is formulated as the eigenvalue problem of a holomorphic Fredholm operator function. Then finite elements are used for discretization and the convergence is proved using the abstract approximation theory for the eigenvalue problem of the holomorphic operator function. A spectral indicator method (SIM) is developed to practically compute the eigenvalues. To our knowledge, this is the first effective approach that can treat permittivity depending arbitrarily on the frequency, being lossy or lossless, and crystals with irregular shapes.

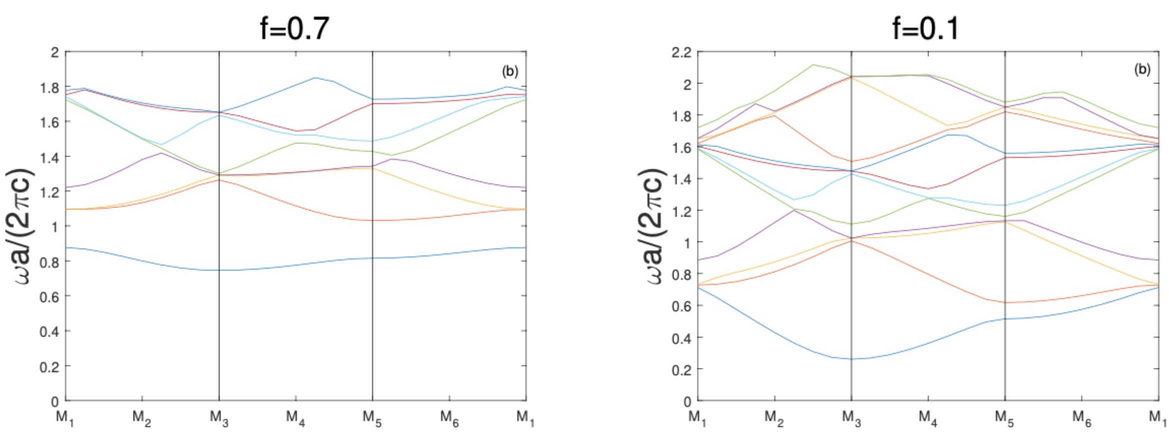

Fig. 1. Band structures(f is the filling factor). Left: lossless case. Right: lossy case.

Example. Consider metallic materials such that

$$\epsilon_b(\omega) = 1 - \frac{\omega_p^2}{\omega(\omega + i\gamma)},$$

where ω_p is the plasma frequency, γ is an inverse electronic relaxation time.

色散材料的光子带隙结构计算

（中心作者：肖文强、宫博、张智民）

光子晶体（PCs）是由介电材料构成的具有带隙的周期性结构，在光通信、滤波器、激光器、开关和光晶体管等方面有着重要的应用【1-3】。准确有效地计算光子晶体的光带结构，对于发现新的光学现象和发明新的光学器件至关重要。如果光子晶体材料不依赖于光波的频率，光带结构计算只需求解线性特征值问题，在这方面用很多工作。相比之下，如果材料依赖于频率，光带结构计算就需要求解非线性问题，挑战性非常高。只有少数工作，并且针对特殊的介电常数和结构。

非线性光带结构通常需要求解一类麦克斯韦方程的特征值问题【3】

$$\begin{cases} \nabla \times \dfrac{1}{\epsilon(x,\omega)} \nabla \times \mathbf{H} = \left(\dfrac{\omega}{c}\right)^2 \mathbf{H}, \\ \nabla \quad \mathbf{H} = 0, \end{cases}$$

其中，$\mathbf{H}$ 是磁场，ω 是频率，$\epsilon(x,\omega)$ 是依赖于频率的介电常数，c 代表真空中的光速。

最近的工作中【4】提出了一种新的办法来计算非线性材料光子晶体的光带结构。光带结构相关的麦克斯韦特征值问题先转化为一类解析算子函数的特征值问题。然后利用有限元方法对算子离散。最后发展了一类基于谱指示函数的方法来计算离散后的非线性特征值问题。这种方法是首个可以有效计算一般的非线性材料光带结构的方法，材料可以是吸收的，晶体的几何结构也可以是任意的。

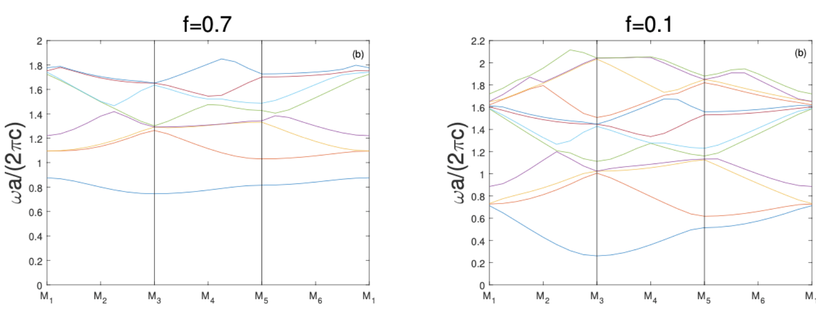

Fig. 1. Band structures(f is the filling factor). Left: lossless case. Right: lossy case.

例子：考虑如下的光子晶体。单个周期是单位正方形，中心是圆柱体金属材料，介电常数是关于频率的非线性函数：

$$\epsilon_b(\omega) = 1 - \frac{\omega_p^2}{\omega(\omega + i\gamma)},$$

其中 ω_p 是等离子体频率, γ 是电子弛豫时间的倒数。Fig.~1中给出了光带结构的计算结果。

References:

[1] V. Kuzmiak and A.A. Maradudin, Photonic band structures of two-dimensional systems fabricated from rods of a cubic crystal, Physical Review B, 55 (1997), 4298-4311

[2] A. Raman and S. Fan, Photonic band structure of dispersive metamaterials formulated as a Hermitian eigenvalue problem. Phys. Rev. Lett. 104 (2010), 087401.

[3] O. Toader and S. John, Photonic band gap enhancement in frequency-dependent dielectrics. Physical Review E 70 (2004), 046605.

[4] W. Xiao, B. Gong, J. Sun and Z. Zhang, Finite element calculation of photonic band structures for frequency dependent materials, arXiv:2007.11540, submitted to SIAM Journal on Numerical Analysis.

SWIMMING OF THE MOSQUITO LARVA: PRINCIPLES AND TRICKS OF LOCOMOTION AT INTERMEDIATE REYNOLDS NUMBERS

(By **Bowen Jin**, Haoxiang Luo, and **Yang Ding**)

For swimming, mosquito larva bends its cylindrical body nearly into a circle from one side to the other sequentially and generates a trajectory resembles figure-of-eight. This gait is drastically different from the undulatory gait used by other slender-body organisms, such as eel and nematode. Why the mosquito larva uses such gait while it is capable of using the undulatory gait? Previous studies show that this gait is fast: mosquito larva can move 0.8 body length per body deform cycle, which is comparable to large swimmers with undulatory gait and much larger compared to micro-swimmers using undulatory gait or helical propulsion (see Figure) [1]. But that is far from a satisfactory answer.

A study led by Yang Ding from CSRC sheds light on this question using numerical simulations. They found that, in contrast to undulatory swimmers who try to reduce rotation all the time to align their propulsion with the direction of motion, the mosquito larva purposely generates a significant rotation and timely generate the propulsion forces when the propulsion forces align with the direction of motion. The mosquito larva also modulates the speed of body deformation to increase the propulsion force since force scales greater than linear with velocity. As a result, the swimming speed is greater than the speed of the undulatory gait in the same condition (Reynolds number). Although the energetic efficiency of figure-of-eight gait is low, the power is small compared to the larva's metabolic rate.

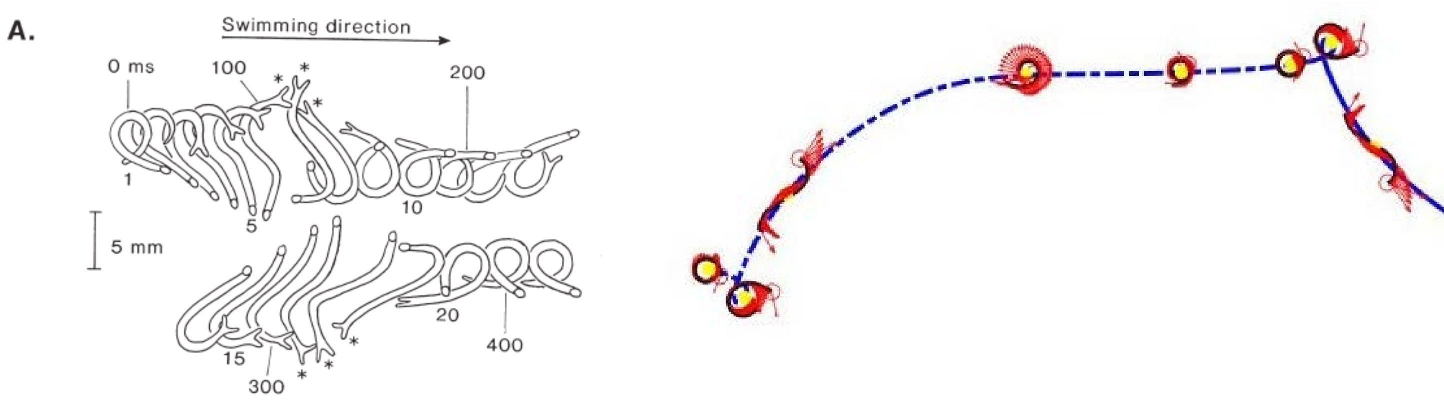

They showed that for micro-swimmers at low Reynolds number where the inertia effect is negligible, rotation is damped and difficult to generate. Besides, modulation of the speed of body deformation is not effective, as the forces scale linearly with velocities. Therefore, when Reynolds number is smaller than about 30, the figure-of-eight gait generates a displacement nearly in place. For large swimmers at high Reynolds numbers, the gait can be used. To achieve optimal speed, the body deformation needs to be adjusted to not over-rotate. While the speed of the figure-of-eight gait ($Re \sim 10^2 - 10^3$) is comparable to that of the undulatory gait ($Re \sim 10^3$) , the body deformation is much larger, and the frontal drag is larger. Therefore, the figure-of-eight gait is inefficient for swimmers at high Reynolds numbers.

Recently, centimeter-sized robots become available due to the advancement of material and manufacture technologies, such as the “print & fold” technology. This study shows that the figure-of-eight gait can provide high speed for swimming, especially for those robots with external power supplies, and provides practical guidance of gait optimization.

蚊子幼虫的游动：中雷诺数流体中运动的原理和技巧

（中心作者：靳博文、丁阳）

蚊子幼虫在运动过程中身体周期性的从一侧向另一侧弯曲成环状再打开，呈现出“8”字形的运动步态。这种步态与其他细长体生物，例如鳗鱼和线虫等所使用的波动步态完全不同。为什么蚊子幼虫会选择这样的步态而不是波动步态呢？之前的研究发现这样的步态可以实现快速移动：每个周期幼虫能够前进0.8个体长的距离，与采用波状运动的大生物速度相当，且比采用波状步态或螺旋推进的微游泳者速度更快[1]。然而这仅仅是答案的开始。

来自北京计算科学研究中心的丁阳团队使用数值模拟的方法阐释了这一问题。对于波状运动的游泳者而言，它们尽量减少身体的旋转以使推进与运动方向一致；而幼虫的运动方式有个明显的不同，幼虫在运动过程中有显著的身体旋转，并且当推进力与前进方向相同时会及时的产生推进力使其运动更远。同时，由于力与速度的非线性关系，幼虫通过调整身体形变的速度来提高推进力。因此，在同样的环境下，“8”字形步态比波状步态的速度更快。”8”字形运动是一种效率很低的运动，但与新陈代谢相比，运动所需能量只占很少一部分。

对于微游泳者而言，在低雷诺数下，惯性被忽略，所以身体旋转很难产生；而力与速度的线性关系也使得调整形变速度对力的调制的效果不是很明显。因此当雷诺数低于30时，幼虫几乎是在原地摆动。

对在大雷诺数环境下的大游泳者来说，可以采用这种“8”字形步态。当雷诺数过大时，需要调整身体的变形避免转过以获得最佳的速度。尽管“8”字形步态的速度（$Re \sim 10^2 - 10^3$）与波状步态（$Re \sim 10^3$）的速度相当，但是其变形和前缘阻力更大，所以在高雷诺数下效率很低。

最近，随着材料和制造技术的进步，例如“打印&折叠”技术的产生，使厘米机器人得到发展。本研究表明，机器人采用“8”字形步态能够产生更高速度的游动。除此之外，本研究还可以为步态优化提供实际指导。

References:

[1] John Brackenbury, 2000. Locomotory modes in the larva and pupa of *Chironomus plumosus (Diptera, Chironomidae)*, Journal of Insect Physiology 46, 1517–1527.

REGULARIZED 13-MOMENT EQUATIONS FOR INVERSE POWER LAW MODELS

(By Zhenning Cai and **Yanli Wang**)

Modeling of gas dynamics has been attracting people's attention for centuries. For low-density regime and large velocity slip or temperature jump at a solid wall due to gas-surface interaction, the interaction between gas molecules are either insufficient or severely ruined by gas-surface interactions, resulting in the failure of the continuum models. Although some microscopic models, such as Boltzmann equation, Enskog equation, or even molecular dynamics, have been validated to be accurate for most applications, they are usually too expensive to solve due to the high dimensionality. Since there is a large gap between the continuum models and the microscopic models, researchers have been trying to find models sitting in-between, which are cheaper to simulate than the kinetic models.

Since Euler equations and Navier-Stokes equations can be considered as zeroth-order and first-order approximations of the Boltzmann equation in the continuum limit Struchtrup (2005a), various attempts have been made to derive higher-order approximations. However, these attempts show that going beyond Navier-Stokes is quite nontrivial: Burnett and super Burnett equations are linearly unstable Bobylev (1982); Grad's method has the hyperbolicity problem and the convergence problem Cai et al. (2014), Müller & Ruggeri (1998); equations by maximum entropy are still difficult to solve numerically due to an ill-posed optimization problem hidden in the equations Tallec & Perlat (1997). These deficiencies have been severely restricting the applications of these models.

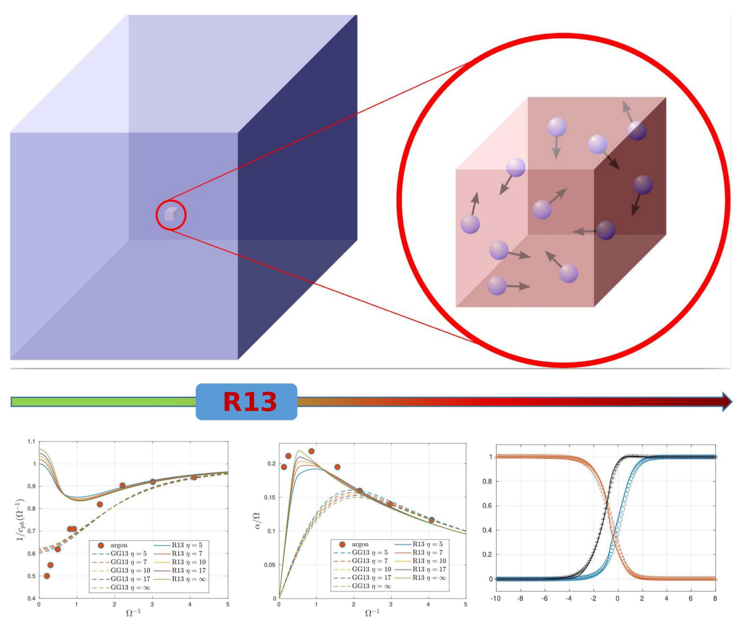

In spite of this, a number of new thoughts have been introduced for this classical modeling problem. In the current century, all these classical models are re-studied. Burnett equations have been fixed to regain linear stability Bobylev (2006, 2008); the hyperbolicity problem of Grad's equations is fixed in Cai et al. (2015); approximations of maximum-entropy equations have been proposed which have explicit analytical expressions McDonald & Torrilhon (2013). At the same time, Grad's old idea hidden in his notes Grad (1958) has been picked up to build new models called regularized moment equations Struchtrup & Torrilhon (2003). Although all these models are quite new, based on current studies, we find the regularized moment equations to be interesting due to its relatively complete theory (boundary conditions Torrilhon & Struchtrup (2008), H-theorem Struchtrup & Torrilhon (2017), Torrilhon (2012)) and a number of numerical studies Torrilhon (2006). However, the complete regularized 13-moment equations have been derived only for Maxwell molecules. In Torrilhon & Struchtrup (2004), it has been demonstrated by the example of plane shock structure that the equations derived for Maxwell molecules are not directly applicable to the hard-sphere model, which indicates that collision models needto be taken into account during the model derivation. This inspires us to go beyond Maxwell molecules, and study more realistic interaction models directly.

In this work, we will focus on inverse power potentials, which cover both Maxwell molecules and hard-sphere molecules (as the limit), and have been verified by experiments to be realistic for a number of gases (Torrens 1972, Table 8.1). As far as we know, the only regularized moment model derived for non-Maxwell monatomic molecules is Struchtrup & Torrilhon (2013), which is the fully linearized equations for hard-sphere molecules. Such a model cannot be applied in nonlinear regimes such as shock waves. In this work, we have extended the work Struchtrup & Torrilhon (2013) and write down equations for all inverse power law models linearized about the local Maxwellian. The long derivation of the R13 equations is done by our automated Mathematica code. Plane shock wave structures will be computed based on these 13-moment models to show better results than a simple alteration of the Maxwell model.

References:

[1] Bobylev, A. V. (1982), 'The Chapman-Enskog and Grad methods for solving the Boltzmann equation', Sov. Phys. Dokl. 27, 29–31.

[2] Bobylev, A. V. (2006), 'Instabilities in the Chapman-Enskog expansion and hyperbolic Burnett equations', J. Stat. Phys. 124(2–4), 371–399.

[3] Bobylev, A. V. (2008), 'Generalized Burnett hydrodynamics', J. Stat. Phys. 132, 569–580.

[4] Cai, Z., Fan, Y. & Li, R. (2014), 'On hyperbolicity of 13-moment system', Kin. Rel. Models 7(3), 415–432.

[5] Cai, Z., Fan, Y. & Li, R. (2015), 'A framework on moment model reduction for kinetic equation', SIAM J. Appl. Math. 75(5), 2001–2023.

[6] Grad, H. (1958), 'Principles of the kinetic theory of gases', Handbuch der Physik 12, 205–294.

[7] McDonald, J. & Torrilhon, M. (2013), 'Affordable robust moment closures for CFD based on the maximum-entropy hierarchy', J. Comput. Phys. 251, 500–523.

[8] Müller, I. & Ruggeri, T. (1998), Rational Extended Thermodynamics, Second Edition, Vol. 37 of Springer tracts in natural philosophy, Springer-Verlag, New York.

[9] Struchtrup, H. (2005a), 'Derivation of 13 moment equations for rarefied gas flow to second order accuracy for arbitrary interaction potentials', Multiscale Model. Simul. 3(1), 221–243.

[10] Struchtrup, H. & Torrilhon, M. (2003), 'Regularization of Grad's 13 moment equations: Derivation and linear analysis', Phys. Fluids 15(9), 2668–2680.

[11] Struchtrup, H. & Torrilhon, M. (2013), 'Regularized 13 moment equations for hard sphere molecules: Linear bulk equations', Phys. Fluids 25, 052001.

[12] Struchtrup, H. & Torrilhon, M. (2017), 'H-theorem, regularization, and boundary conditions for linearized 13 moment equations', Phys. Rev. Lett. 99, 014502.

[13] Tallec, P. L. & Perlat, J. P. (1997), Numerical analysis of Levermore's moment system, Rapport de recherche 3124, INRIA Rocquencourt.

[14] Torrens, I. M. (1972), Interatomic Potentials, Academic Press.

[15] Torrilhon, M. (2006), 'Two dimensional bulk microflow simulations based on regularized Grad's 13-moment equations', SIAM Multiscale. Model. Simul. 5(3), 695–728.

[16] Torrilhon, M. (2012), 'H-theorem for nonlinear regularized 13-moment equations in kinetic gas theory', Kin. Rel. Models 5(1), 185–201.

[17] Torrilhon, M. & Struchtrup, H. (2004), 'Regularized 13-moment equations: shock structure calculations and comparison to Burnett models', J. Fluid Mech. 513, 171–198.

[18] Torrilhon, M. & Struchtrup, H. (2008), 'Boundary conditions for regularized 13-moment-equations for micro-channel-flows', J. Comput. Phys. 227(3), 1982–2011.

CONTROLLING THE EMISSION FREQUENCY OF GRAPHENE NANORIBBON EMITTERS BASED ON SPATIALLY EXCITED TOPOLOGICAL BOUNDARY STATES

(By **Xiaoyan Wu**, Rulin Wang, Na Liu, **Hao Zou**, Bin Shao, **Lei Shao** and **ChiYung Yam**)

In recent years, advanced fabrication technologies have made it possible to control the interaction of nanoscale electronic components with light. High-speed on-chip communication and computing applications require these nano-emitters with the capability to tune the optical properties and the ability to be compatible with CMOS technology. To this end, the development of controllable, easily integrated, electrically triggered nano-emitters that can operate at various optical frequencies is significant. Graphene nanoribbons (GNRs) are emerging as promising candidates for nanoscale light emitting devices. Recently, formation of nanoscale emitters embedded in an armchair GNR has been realized.1 Chong et al. observed bright individual GNR luminescence via STM.[2] These studies indicate a promising route towards robust and controllable graphene-based light-emitting devices.

ChiYung Yam *et al*. at Beijing Computational Science Research Center design a nano-emitter with desirable frequencies based on GNR heterojunction.3 By connecting GNRs with different widths and lengths, topological boundary states can be formed and manipulated. Using first-principles-based atomistic simulations, they studied the luminescence properties of a STM GNR junction and explored the applications of these topological states as nanoscale light sources. Taking advantage of the ultrahigh resolution of the STM tip, direct injection of high energy carriers at selected boundary states can be achieved. In this way, the emission color can be controlled by precisely changing the tip position. The GNR heterojunction can therefore represent a robust and controllable light-emitting device that takes a step forward towards the fabrication of nanoscale graphene-based optoelectronic devices.

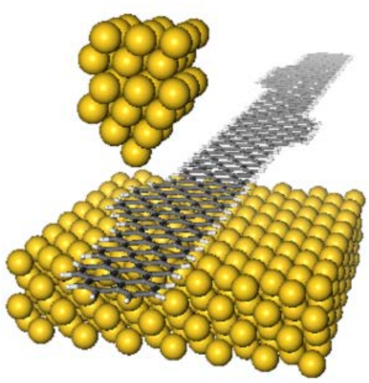

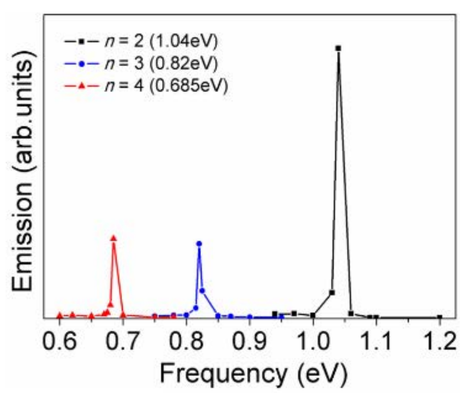

通过激发石墨烯纳米带不同位置处的拓扑边界态实现发光频率可调控的量子发光器件

（中心作者：武晓燕、邹浩、邵磊、任志勇）

近年来，先进的制造技术可实现对纳米尺寸的电子元件与光相互作用的控制从而得到纳米发光器件。而芯片上器件间的高速通信和计算要求纳米发射器具有可调节的光学特并且能很好的与芯片集成。因此设计一款可调控，易于集成且可在各种光频率下工作的电致激发的纳米发光器件具有重大意义。石墨烯纳米带以其优异的光电特性成为制作纳米发光器件的重要材料。最近，实验上实现了嵌入在扶手型石墨烯纳米带中的纳米发射器[1]。Chong等利用扫描隧道显微镜观察到了单条纳米带的明亮发光[2]。这些研究显示可基于石墨烯纳米带制造发光性能稳定且可控的纳米发光器件。

北京计算科学研究中心的研究小组基于石墨烯纳米带异质结设计了发光频率可调控的纳米发光器件[3]。通过连接不同宽度和长度的石墨烯纳米带，可以形成和调控拓扑边界态。该小组使用基于第一性原理的原子模拟，研究了扫描隧道显微镜隧道结中石墨烯纳米带的发光特性，并探索了这些拓扑态作为纳米光源的应用。研究发现，利用扫描隧道显微镜针尖的超高分辨率，可以在选定的边界态直接注入高能载流子。因此，可以通过精确地改变针尖位置来控制发射频率。该研究表明石墨烯纳米带异质结可作为一种性能稳定且可控的发光器件，使我们离基于石墨烯的光电器件的实现又近了一步。

References:

[1] Wang, S.; *et al*. Nano Lett. 2017, 17, 4277-4283.
[2] Chong, M. C.; *et al.* Nano Lett. 2017, 18, 175-181.
[3] Wu, Xiaoyan; *et al*. Phys. Chem. Chem. Phys. 2020, 22, 8277-8283.

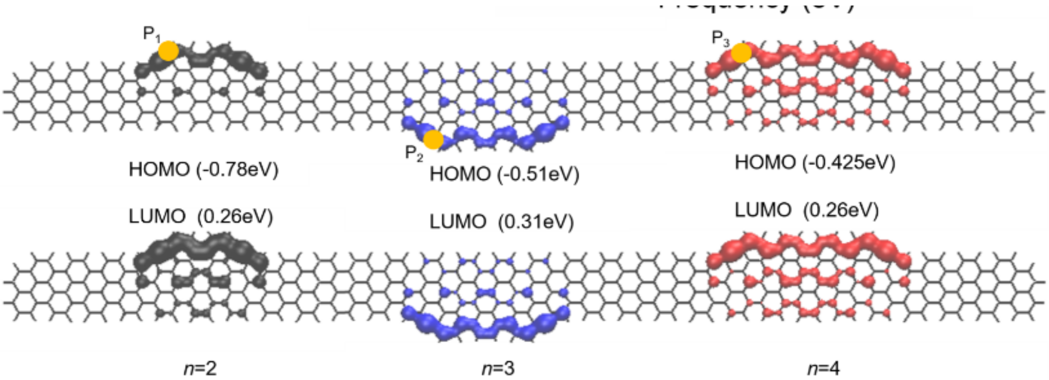

2019-2020学术年期间，中心承担中央组织部、科学技术部、国家基金委、博士后科学基金，以及中物院等在研项目共122项、年内结题项目38项。另外，2020年8月后中心将新启动项目15项。

During the 2019-2020 academic year, CSRC is undertakeing 122 projects from the Ministry of Science and Technology of China, National Natural Science Foundation of China, China Academy of Engineering Physics, China Postdoctoral Science Foundation and so on. 38 projects were concluded during the academic year. In addition, 15 new projects will be started after August 2020.

No.	项目负责人 PI	经费来源 SOURCE	项目类别 CATEGORY	项目名称 PROJECT TITLE	起止时间 FROM AND TO
1	林海青 Hai-Qing Lin	科学技术部 MOST	国家重点研发计划 National Key Research and Development Project	低维固态极性结构中量子态调控及其原型器件研究	2017.07 - 2022.06
2	游建强 Jian-Qiang You	科学技术部 MOST	国家重点研发计划 National Key Research and Development Project	高品质腔与固体量子态的耦合及其量子调控	2016.07 - 2021.06
3	黄　兵 Bing Huang	军委科技委 Science and Technology Commission, CMC	基础加强计划重点基础研究项目 Key Basic Research Program of Basic Strengthening Plan	非平衡态下半导体材料缺陷的基础科学问题研究	2018.01 - 2021.12
4	管鹏飞 Peng-Fei Guan	国防科技工业局 State Administration of Science, TIND	国防基础科研核科学挑战专题 Scientific Challenge Project	辐照条件多尺度计算与模拟研究	2018.01 - 2021.12
5	魏苏淮 Su-Huai Wei	工业和信息化部 Ministry of Industry and Information Technology of China	国家重点研发计划 National Key Research and Development Project	环境友好型高稳定性太阳能电池的材料设计与器件研究	2016.07 - 2020.06
6	魏苏淮 Su-Huai Wei	北京市科学技术委员会 Beijing Municipal Commission of Science and Technology	-	铜铟镓硒电池的碱金属后处理及相关技术研究	2018.06 - 2020.05
7	胡淑贤 Shu-Xian Hu	中国工程物理研究院 China Academy of Engineering Physics	院长基金 Dean's Fund	锕系化合物的多组态量子化学研究	2018.01 - 2020.12
8	林海青 Hai-Qing Lin	国家自然科学基金委员会 NSFC	联合基金项目 NSAF	科学计算与物理系统模拟研究	2020.01 - 2022.12

No.	项目负责人 PI	经费来源 SOURCE	项目类别 CATEGORY	项目名称 PROJECT TITLE	起止时间 FROM AND TO
9	赵　楠 Nan Zhao	国家自然科学基金委员会 NSFC	联合基金项目重点项目 Key Program of Joint Fund	基于原子自旋的惯性传感物理基础与小型化系统综合优化研究	2021.01 - 2024.12
10	魏苏淮 Su-Huai Wei	国家自然科学基金委员会 NSFC	重大项目 Major projects	微纳器件中非平衡物理过程研究	2020.01 - 2024.12
11	王　奇 Qi Wang	国家自然科学基金委员会 NSFC	重大研究计划重点项目 Key Program of Major Research Plan	多相物质体系的计算建模算法设计与数值分析	2017.01 - 2019.12
12	高世武 Shiwu Gao	国家自然科学基金委员会 NSFC	重点项目 Key Program	表面激发态和非绝热动力学方法及应用	2020.01 - 2024.12
13	林海青 Hai-Qing Lin	国家自然科学基金委员会 NSFC	重点项目 Key Program	海森堡模型和Kitaev模型的元激发、激发谱和量子相变	2018.01 - 2022.12
14	孙昌璞 Chang-Pu Sun	国家自然科学基金委员会 NSFC	重点项目 Key Program	有限开放系统的量子相干效应及其应用	2016.01 - 2020.12
15	汤雷翰 Lei-Hang Tang	国家自然科学基金委员会 NSFC	重点项目 Key Program	活性系统的热耗散及长时动力学	2017.01 - 2021.12
16	魏苏淮 Su-Huai Wei	国家自然科学基金委员会 NSFC	重点项目 Key Program	透明导电体的物理机理研究与新材料设计	2017.01 - 2021.12
17	张智民 Zhimin Zhang	国家自然科学基金委员会 NSFC	数学天元基金 Mathematics Tianyuan Fund	麦克斯韦传输特征值问题零散度约束的高效谱方法研究	2020.01 - 2020.12
18	刘海广 Hai-Guang Liu	国家自然科学基金委员会 NSFC	国际(地区)合作与交流项目 International (Regional) Cooperation and Exchange Program	利用X射线自由电子激光研究分子结构和动力学机理	2018.07 - 2020.06
19	Stefano Chesi	国家自然科学基金委员会 NSFC	面上项目 General Program	半导体纳米结构的空穴自旋的相干性质	2016.01 - 2019.12
20	管鹏飞 Peng-Fei Guan	国家自然科学基金委员会 NSFC	面上项目 General Program	非晶合金中β-弛豫结构起源的计算模拟研究	2016.01 - 2019.12
21	黄　兵 Bing Huang	国家自然科学基金委员会 NSFC	面上项目 General Program	晶格匹配的层状合金做为新型高效光源材料的理论探索	2016.01 - 2019.12
22	刘海广 Hai-Guang Liu	国家自然科学基金委员会 NSFC	面上项目 General Program	X射线自由电子激光在单分子成像中的应用及相关计算方法与理论研究	2016.01 - 2019.12

续表

No.	项目负责人 PI	经费来源 SOURCE	项目类别 CATEGORY	项目名称 PROJECT TITLE	起止时间 FROM AND TO
23	刘利民 Li-Min Liu	国家自然科学基金委员会 NSFC	面上项目 General Program	水溶液条件下光电催化材料理论设计及其性能优化	2016.01 - 2019.12
24	王 奇 Qi Wang	国家自然科学基金委员会 NSFC	面上项目 General Program	活性的、各向异性流体的数学建模分析与计算	2016.01 - 2019.12
25	徐辛亮 Xin-Liang Xu	国家自然科学基金委员会 NSFC	面上项目 General Program	宏观热涨落体系的非平衡态涨落定理	2016.01 - 2019.12
26	Rubem Mondaini	国家自然科学基金委员会 NSFC	面上项目 General Program	关联超流体中的赝能隙相变研究	2017.01 - 2020.12
27	丁 阳 Yang Ding	国家自然科学基金委员会 NSFC	面上项目 General Program	波状运动中的力矩规律在解释生物驱动控制和设计机器人柔性材料中的应用	2017.01 - 2020.12
28	胡广辉 Guang-Hui Hu	国家自然科学基金委员会 NSFC	面上项目 General Program	基于固定入射方向的反媒介理论和算法研究	2017.01 - 2020.12
29	任志勇 Chi-Yung Yam	国家自然科学基金委员会 NSFC	面上项目 General Program	纳米等离子体太阳能电池的光学-电学相结合研究	2017.01 - 2020.12
30	魏苏淮 Su-Huai Wei	国家自然科学基金委员会 NSFC	面上项目 General Program	复杂半导体清洁能源材料的理论研究	2017.01 - 2020.12
31	张东波 Dong-Bo Zhang	国家自然科学基金委员会 NSFC	面上项目 General Program	低维材料电子性质的应变调控：自洽密度泛函紧束缚广义布洛赫方法	2017.01 - 2020.12
32	蔡勇勇 Yong-Yong Cai	国家自然科学基金委员会 NSFC	面上项目 General Program	高振荡色散方程的多尺度计算方法及分析	2018.01 - 2021.12
33	高 翔 Xiang Gao	国家自然科学基金委员会 NSFC	面上项目 General Program	低能电子-离子散射过程中的Breit效应理论研究	2018.01 - 2021.12
34	李 勇 Yong Li	国家自然科学基金委员会 NSFC	面上项目 General Program	光力系统中光学非互易性传输的理论研究	2018.01 - 2021.12
35	杨 文 Wen Yang	国家自然科学基金委员会 NSFC	面上项目 General Program	适用于连续模型的通用格林函数方法及载流子局域输运和干涉现象的理论研究	2018.01 - 2021.12
36	游建强 Jian-Qiang You	国家自然科学基金委员会 NSFC	面上项目 General Program	超越玻恩-马科夫近似的固态量子比特系统的量子动力学研究	2018.01 - 2021.12

No.	项目负责人 PI	经费来源 SOURCE	项目类别 CATEGORY	项目名称 PROJECT TITLE	起止时间 FROM AND TO
37	喻　进 Jin Yu	国家自然科学基金委员会 NSFC	面上项目 General Program	蛋白因子和分子机器在DNA上的信号探测和信息识别	2018.01 - 2021.12
38	张继伟 Ji-Wei Zhang	国家自然科学基金委员会 NSFC	面上项目 General Program	多尺度非局部模型的理论分析和高效数值方法	2018.01 - 2021.12
39	汪　玲 Ling Wang	国家自然科学基金委员会 NSFC	面上项目 General Program	矩阵乘积态的切空间投影法研究强关联系统的自旋动力学结构因子	2019.01 - 2022.12
40	张瑞勤 Rui-Qin Zhang	国家自然科学基金委员会 NSFC	面上项目 General Program	氮化碳表面非金属原子梯度掺杂对光生载流子产生和分离影响的计算研究	2019.01 2022.12
41	张智民 Zhimin Zhang	国家自然科学基金委员会 NSFC	面上项目 General Program	电磁场方程及其特征值问题高效高精度数值方法	2019.01 - 2022.12
42	Rubem Mondaini	国家自然科学基金委员会 NSFC	面上项目 General Program	强关联系统中d波配对的非平衡探索研究	2020.01 - 2023.12
43	Stefano Chesi	国家自然科学基金委员会 NSFC	面上项目 General Program	基于半导体量子点的自旋量子比特的长距耦合	2020.01 - 2023.12
44	胡淑贤 Shu-Xian Hu	国家自然科学基金委员会 NSFC	面上项目 General Program	辐照下氧化铀/水界面表面腐蚀机理的量子化学研究	2020.01 - 2023.12
45	刘海广 Hai-Guang Liu	国家自然科学基金委员会 NSFC	面上项目 General Program	应用时间分辨串行晶体衍射和分子动力学模拟方法研究氯离子输运视紫 质蛋白结构和动力学	2020.01 - 2023.12
46	王　奇 Qi Wang	国家自然科学基金委员会 NSFC	面上项目 General Program	热力学一致模型的计算建模保结构算法设计分析与实现	2020.01 - 2023.12
47	徐辛亮 Xin-Liang Xu	国家自然科学基金委员会 NSFC	面上项目 General Program	活性物质集体运动的涌现及其非平衡态物理特性	2020.01 - 2023.12
48	康　俊 Jun Kang	国家自然科学基金委员会 NSFC	面上项目 General Program	摩尔超晶格平带产生与调控机制的大规模第一性原理研究	2021.01 - 2024.12
49	李　勇 Yong Li	国家自然科学基金委员会 NSFC	面上项目 General Program	基于量子光学方法的手性分子检测、分离与转化研究	2021.01 - 2024.12

续表

No.	项目负责人 PI	经费来源 SOURCE	项目类别 CATEGORY	项目名称 PROJECT TITLE	起止时间 FROM AND TO
50	任志勇 Chi-Yung Yam	国家自然科学基金委员会 NSFC	面上项目 General Program	纳米光电器件的时域模拟方法的发展与应用	2021.01 - 2024.12
51	王冀鲁 Ji-Lu Wang	国家自然科学基金委员会 NSFC	面上项目 General Program	粘性浅水波方程的高精度数值方法	2021.01 - 2024.12
52	杜　宇 Yu Du	国家自然科学基金委员会 NSFC	青年科学基金项目 Young Scientists Fund	求解高波数Helmholtz问题的PPR方法和弱有限元方法	2017.01 - 2019.12
53	胡自玉 Zi-Yu Hu	国家自然科学基金委员会 NSFC	青年科学基金项目 Young Scientists Fund	二维材料的新型结构相和其边缘态的量子调控的理论研究	2017.01 - 2019.12
54	李　俊 Jun Li	国家自然科学基金委员会 NSFC	青年科学基金项目 Young Scientists Fund	核磁共振体系的量子控制模型及其应用	2017.01 - 2019.12
55	刘卯鑫 Mao-Xin Liu	国家自然科学基金委员会 NSFC	青年科学基金项目 Young Scientists Fund	多量子比特与玻色场耦合系统量子相变研究	2017.01 - 2019.12
56	尚宝双 Bao-Shuang Shang	国家自然科学基金委员会 NSFC	青年科学基金项目 Young Scientists Fund	金属玻璃塑性局域重组方向敏感性研究	2017.01 - 2019.12
57	胡　麟 Lin Hu	国家自然科学基金委员会 NSFC	青年科学基金项目 Young Scientists Fund	非平衡态下二维宽带隙半导体中缺陷和掺杂性质的研究和调控	2018.01 - 2020.12
58	胡淑贤 Shu-Xian Hu	国家自然科学基金委员会 NSFC	青年科学基金项目 Young Scientists Fund	含氮冠醚三价次锕系离子和镧系离子配合物成键及电子结构的理论研究	2018.01 - 2020.12
59	康　雷 Lei Kang	国家自然科学基金委员会 NSFC	青年科学基金项目 Young Scientists Fund	典型狄拉克材料的非线性光学性质的理论研究	2018.01 - 2020.12
60	庞国飞 Guo-Fei Pang	国家自然科学基金委员会 NSFC	青年科学基金项目 Young Scientists Fund	分数阶导数对流-弥散方程参数识别的多重精度高斯过程回归算法	2018.01 - 2020.12
61	吴　威 Wei Wu	国家自然科学基金委员会 NSFC	青年科学基金项目 Young Scientists Fund	量子开放系统动力学的数值研究	2018.01 - 2020.12
62	袁少杰 Shao-Jie Yuan	国家自然科学基金委员会 NSFC	青年科学基金项目 Young Scientists Fund	超导量子比特的弱测量及其量子力学时间对称性的研究	2018.01 - 2020.12
63	张春芳 Chun-Fang Zhang	国家自然科学基金委员会 NSFC	青年科学基金项目 Young Scientists Fund	芳香烃超导材料制备中涉及的化学反应的理论研究	2018.01 - 2020.12

No.	项目负责人 PI	经费来源 SOURCE	项目类别 CATEGORY	项目名称 PROJECT TITLE	起止时间 FROM AND TO
64	张闻钊 Wen-Zhao Zhang	国家自然科学基金委员会 NSFC	青年科学基金项目 Young Scientists Fund	开放量子系统中光机械振子辐射压冷却的理论研究	2018.01 - 2020.12
65	陈　虎 Hu Chen	国家自然科学基金委员会 NSFC	青年科学基金项目 Young Scientists Fund	无界域上分数阶和非局部扩散方程的高精度数值方法研究	2019.01 - 2021.12
66	晋力京 Li-Jing Jin	国家自然科学基金委员会 NSFC	青年科学基金项目 Young Scientists Fund	多模光力超导电路中非线性效应的增强和探测	2019.01 - 2021.12
67	李　季 Ji Li	国家自然科学基金委员会 NSFC	青年科学基金项目 Young Scientists Fund	基于矩阵分解的相位恢复非凸优化算法研究	2019.01 - 2021.12
68	李　晓 Xiao Li	国家自然科学基金委员会 NSFC	青年科学基金项目 Young Scientists Fund	非局部相场方程的保持能量稳定与最大模稳定的高效数值方法	2019.01 - 2021.12
69	罗智煌 Zhi-Huang Luo	国家自然科学基金委员会 NSFC	青年科学基金项目 Young Scientists Fund	利用核自旋系统进行拓扑相量子模拟的实验研究	2019.01 - 2021.12
70	房一楠 Yi-Nan Fang	国家自然科学基金委员会 NSFC	青年科学基金项目 Young Scientists Fund	对称性度量在多比特量子随机基准中的应用	2021.01 - 2023.12
71	郭震林 Zhen-Lin Guo	国家自然科学基金委员会 NSFC	青年科学基金项目 Young Scientists Fund	带表面活性剂的两相流相场模型建模与数值求解	2021.01 - 2023.12
72	黄卫杰 Wei-Jie Huang	国家自然科学基金委员会 NSFC	青年科学基金项目 Young Scientists Fund	表面扩散流的保结构高效数值算法	2021.01 - 2023.12
73	莫崇杰 Chong-Jie Mo	国家自然科学基金委员会 NSFC	青年科学基金项目 Young Scientists Fund	温稠密物质X射线光谱的第一性原理研究	2021.01 - 2023.12
74	孙庆德 Qing-De Sun	国家自然科学基金委员会 NSFC	青年科学基金项目 Young Scientists Fund	高光吸收材料的物理机理研究	2021.01 - 2023.12
75	王建峰 Jian-Feng Wang	国家自然科学基金委员会 NSFC	青年科学基金项目 Young Scientists Fund	拓扑半金属的等离激元及其在太赫兹领域应用的理论研究	2021.01 - 2023.12
76	Kyle John Welch	国家自然科学基金委员会 NSFC	外国青年学者基金项目 Fund for International Young Scientists	Emergent complexity in the collective motion of simple, self-propelled agents	2018.01 - 2019.12

续表

No.	项目负责人 PI	经费来源 SOURCE	项目类别 CATEGORY	项目名称 PROJECT TITLE	起止时间 FROM AND TO
77	Santanu Sinha	国家自然科学基金委员会 NSFC	外国青年学者基金项目 Fund for International Young Scientists	Multiphase flow in porous media: a new computational approach	2018.01 - 2019.12
78	Stefano Chesi	国家自然科学基金委员会 NSFC	外国青年学者基金项目 Fund for International Young Scientists	Magnetic phases and superradiant-like dynamics of nuclear spins in a quantum dot	2018.01 - 2019.12
79	Tirthankar Dutta	国家自然科学基金委员会 NSFC	外国青年学者基金项目 Fund for International Young Scientists	Theoretical Study of Interfacial Magnetism and Transport of Metals and Insulators	2018.01 - 2019.12
80	Jorge Botana Alcalde	国家自然科学基金委员会 NSFC	外国青年学者基金项目 Fund for International Young Scientists	Design of mixed-anion structures for industrial applications	2019.01 - 2020.12
81	Rubem Mondaini	国家自然科学基金委员会 NSFC	外国青年学者基金项目 Fund for International Young Scientists	Out-of-equilibrium systems: Thermalization, Many-body localization and topological Time-crystals	2019.01 - 2020.12
82	Georg Engelhardt	国家自然科学基金委员会 NSFC	外国青年学者基金项目 Fund for International Young Scientists	Spectroscopy of molecular excitation dynamics- far beyond linear response	2020.01.2020.12
83	Rubem Mondaini	国家自然科学基金委员会 NSFC	外国青年学者基金项目 Fund for International Young Scientists	Giant magnetoresistance and correlated physics in twisted bilayer graphene: large scale numerical study using quantum-classical Hamiltonians	2021.01 - 2022.12
84	秦慧慧 Hui-Hui Qin	国家自然科学基金委员会 NSFC	理论物理专款 Theoretical Physics Fund	量子系统非对称性度量研究和量子非局域性关联研究	2019.01 - 2019.12
85	闻　波 Bo Wen	国家自然科学基金委员会 NSFC	理论物理专款 Theoretical Physics Fund	基于极化子增强二氧化钛光催化机理的理论研究	2019.01 - 2019.12
86	胡高科 Gao-Ke Hu	国家自然科学基金委员会 NSFC	理论物理专款 Theoretical Physics Fund	非周期性边界系统的有限尺度标度理论	2020.01 - 2020.12
87	刘　磊 Lei Liu	国家自然科学基金委员会 NSFC	理论物理专款 Theoretical Physics Fund	基于非线性傅里叶变换研究光纤通信中的两类可积非线性薛定谔方程	2020.01 - 2020.12
88	刘玉海 Yu-Hai Liu	国家自然科学基金委员会 NSFC	理论物理专款 Theoretical Physics Fund	单尺度解禁闭量子临界性及相关物理的数值研究	2020.01 - 2020.12

No.	项目负责人 PI	经费来源 SOURCE	项目类别 CATEGORY	项目名称 PROJECT TITLE	起止时间 FROM AND TO
89	莫崇杰 Chong-Jie Mo	国家自然科学基金委员会 NSFC	理论物理专款 Theoretical Physics Fund	温稠密物质中X射线汤姆逊散射谱第一性原理计算方法的研究	2020.01 - 2020.12
90	叶　冲 Chong Ye	国家自然科学基金委员会 NSFC	理论物理专款 Theoretical Physics Fund	手性对映体测定、对映体分离和对映体转化的光学方法研究	2020.01 - 2020.12
91	陈　升 Sheng-Chen	中国博士后科学基金 CPSF	博士后创新人才支持计划 Creative Talents Plan	若干奇性问题的高效谱方法	2018.07 - 2020.06
92	王建平 Jian-Ping Wang	中国博士后科学基金 CPSF	博士后创新人才支持计划 Creative Talents Plan	非铅半导体钙钛矿量子点发光材料的理论设计	2018.07 - 2020.06
93	Georg Engelhardt	中国博士后科学基金 CPSF	博士后国际交流计划引进项目 International Exchange Program for Incoming Postdoctoral Fellows		2018.10 - 2020.09
94	冼　殷 Yin Xian	中国博士后科学基金 CPSF	博士后国际交流计划引进项目 International Exchange Program for Incoming Postdoctoral Fellows		2018.10 - 2020.09
95	马小磊 Xiao-Lei Ma	中国博士后科学基金 CPSF	博士后国际交流计划引进项目 International Exchange Program for Incoming Postdoctoral Fellows		2019.06 - 2021.05
96	杨雪清 Xue-Qing Yang	中国博士后科学基金 CPSF	博士后国际交流计划引进项目 International Exchange Program for Incoming Postdoctoral Fellows		2019.11 - 2021.10
97	黄卫杰 Wei-Jie Huang	中国博士后科学基金 CPSF	博士后国际交流计划派出项目 International Exchange Program for Outgoing Postdoctoral Fellows		2019.07 - 2021.06
98	景晓波 Xiao-Bo Jin	中国博士后科学基金 CPSF	博士后国际交流计划派出项目 International Exchange Program for Outgoing Postdoctoral Fellows		2019.07 - 2021.06

续表

No.	项目负责人 PI	经费来源 SOURCE	项目类别 CATEGORY	项目名称 PROJECT TITLE	起止时间 FROM AND TO
99	李　季 Ji Li	中国博士后科学基金 CPSF	博士后国际交流计划学术交流项目 International Exchange Program	SIAM Conference on Computational Science and Engineering (CSE19)	2019.01 - 2019.12
100	邵　灿 Can Shao	中国博士后科学基金 CPSF	博士后国际交流计划学术交流项目 International Exchange Program	APS March Meeting	2019.01 - 2019.12
101	赵兴举 Xing-Ju Zhao	中国博士后科学基金 CPSF	博士后国际交流计划学术交流项目 International Exchange Program	APS March Meeting	2019.01 - 2019.12
102	王　燕 Yan Wang	中国博士后科学基金 CPSF	特别资助 Special Support	固态去湿问题的数学分析与数值模拟	2018.07 - 2020.06
103	吴　威 Wei Wu	中国博士后科学基金 CPSF	特别资助 Special Support	自旋环境中退相干行为的数值研究	2018.07 - 2020.06
104	张闻钊 Wen-Zhao Zhang	中国博士后科学基金 CPSF	特别资助 Special Support	基于光机械系统的超灵敏探测研究	2018.07 - 2020.06
105	马小磊 Xiao-Lei Ma	中国博士后科学基金 CPSF	特别资助（站前） Special Support	关于active matter中压强的研究	2019.06 - 2021.05
106	徐小绪 Xiao-Xu Xu	中国博士后科学基金 CPSF	特别资助（站前） Special Support	无相位反散射问题的唯一性和数值算法	2019.06 - 2021.05
107	陶　琪 Qi Tao	中国博士后科学基金 CPSF	特别资助（站前） Special Support	求解空间高阶导数方程超弱局部间断有限元方法的误差估计及超收敛研究	2020.08 - 2022.07
108	刘玉海 Yu-Hai Liu	中国博士后科学基金 CPSF	特别资助（站中） Special Support	自发对称破缺量子自旋霍尔态相关物理问题的数值研究	2020.08 - 2022.07
109	莫崇杰 Chong-Jie Mo	中国博士后科学基金 CPSF	特别资助（站中） Special Support	温稠密物质X射线光谱的第一性原理方法研究	2020.08 - 2022.07
110	霍明夏 Ming-Xia Huo	中国博士后科学基金 CPSF	面上一等资助First Class	基于量子光学系统的量子模拟器的研究及应用	2018.06 - 2020.05

No.	项目负责人 PI	经费来源 SOURCE	项目类别 CATEGORY	项目名称 PROJECT TITLE	起止时间 FROM AND TO
111	刘　震 Zhen Liu	中国博士后科学基金 CPSF	面上一等资助First Class	高压下离子化合物与惰性气体反应机理的第一性原理研究	2018.06 - 2020.05
112	Georg Engelhardt	中国博士后科学基金 CPSF	面上一等资助First Class	开放量子系统的调控	2018.12 - 2020.11
113	王　威 Wei Wang	中国博士后科学基金 CPSF	面上一等资助 First Class	特征值问题的大规模、高精度快速算法研究	2018.12 - 2020.11
114	张煜然 Yu-Ran Zhang	中国博士后科学基金 CPSF	面上一等资助 First Class	量子拓扑态的多体纠缠性质的研究	2018.12 - 2020.11
115	莫崇杰 Chong-Jie Mo	中国博士后科学基金 CPSF	面上一等资助 First Class	温稠密物质中X射线汤姆逊散射谱的理论模拟研究	2019.11 - 2021.10
116	王坤坤 Kun-Kun Wang	中国博士后科学基金 CPSF	面上一等资助 First Class	非厄米系统中Leggett-Gary不等式的实验研究	2019.11 - 2021.10
117	董海霞 Hai-Xia Dong	中国博士后科学基金 CPSF	面上二等资助 Second Class	三维Stokes界面问题的高效数值方法及其理论分析	2017.11 - 2019.10
118	江　成 Cheng Jiang	中国博士后科学基金 CPSF	面上二等资助 Second Class	宇称-时间-对称的光力系统中的非线性效应研究	2017.11 - 2019.10
119	李　季 Ji Li	中国博士后科学基金 CPSF	面上二等资助 Second Class	相位恢复数值算法研究：凸优化与低秩模型	2017.11 - 2019.10
120	王建峰 Jian-Feng Wang	中国博士后科学基金 CPSF	面上二等资助 Second Class	设计并寻找理想的拓扑半金属和拓扑超导材料	2017.11 - 2019.10
121	王鹏德 Peng-De Wang	中国博士后科学基金 CPSF	面上二等资助 Second Class	两类非局部发展方程的保结构数值方法	2017.11 - 2019.10
122	陈　虎 Hu Chen	中国博士后科学基金 CPSF	面上二等资助 Second Class	无界域上分数阶扩散方程的高精度数值方法研究	2018.06 - 2020.05
123	张　鹏 Peng Zhang	中国博士后科学基金 CPSF	面上二等资助 Second Class	锂离子电池正极材料充放电反应机理研究与新材料设计	2018.06 - 2020.05

续表

No.	项目负责人 PI	经费来源 SOURCE	项目类别 CATEGORY	项目名称 PROJECT TITLE	起止时间 FROM AND TO
124	Ben Aicha Ibtissem	中国博士后科学基金 CPSF	面上二等资助 Second Class	单组测量数据的时域反问题的唯一性和稳定性	2019.05 - 2021.04
125	Pankaj Bhalla	中国博士后科学基金 CPSF	面上二等资助 Second Class	拓扑量子物质中的信息传递	2019.05 - 2021.04
126	陈　升 Sheng-Chen	中国博士后科学基金 CPSF	面上二等资助 Second Class	几类奇异摄动问题的高精度谱/谱元法	2019.05 - 2021.04
127	宫　博 Bo Gong	中国博士后科学基金 CPSF	面上二等资助 Second Class	求解一类带有模式转换的随机最优控制问题的数值方法	2019.05 - 2021.04
128	李珍珍 Zhen-Zhen Li	中国博士后科学基金 CPSF	面上二等资助 Second Class	表面吸附模型中自旋声子耦合作用的研究	2019.05 - 2021.04
129	邵　灿 Can Shao	中国博士后科学基金 CPSF	面上二等资助 Second Class	低维强关联系统的非平衡超快动力学研究	2019.05 - 2021.04
130	赵腾飞 Teng-Fei Zhao	中国博士后科学基金 CPSF	面上二等资助 Second Class	关于外域上非线性Schrodinger方程的数学研究	2019.05 - 2021.04
131	程永喜 Yong-Xi Chen	中国博士后科学基金 CPSF	面上二等资助 Second Class	多轨道杂质系统中多体效应依赖的热电输运特性	2019.11 - 2021.10
132	刘　磊 Lei Liu	中国博士后科学基金 CPSF	面上二等资助 Second Class	运用非线性傅里叶变换分析和计算光纤脉冲的演化和调制	2019.11 - 2021.10
133	刘玉海 Yu-Hai Liu	中国博士后科学基金 CPSF	面上二等资助 Second Class	拓展的Kane-Mele模型的深入数值研究	2019.11 - 2021.10
134	王云华 Yun-Hua Wang	中国博士后科学基金 CPSF	面上二等资助 Second Class	二维材料中压电铁电效应和关联效应的理论研究	2019.11 - 2021.10
135	洪　旗 Qi Hong	中国博士后科学基金 CPSF	面上二等资助 Second Class	复杂流体相场模型高效、高精度保结构算法的研究与应用	2020.07 - 2022.06
136	鲁少华 Shao-Hua Lu	中国博士后科学基金 CPSF	面上二等资助 Second Class	新型碳/硅基二维催化材料的理论设计	2020.07 - 2022.06
137	王丽修 Li-Xiu Wang	中国博士后科学基金 CPSF	面上二等资助 Second Class	H（$curl^2$）协调谱元的构造及其应用	2020.07 - 2022.06

2019-2020学术年期间，中心合计发表论文约368篇，其中归属中心（包括第一单位及通讯作者第一单位）论文207篇，其他合作论文161篇。

During the 2019-2020 academic year, CSRC has published a total of about 368 papers.

SIMULATION OF PHYSICAL SYSTEMS DIVISION 物理系统模拟研究部

1	Room-temperature valleytronic transistor; Li, Lingfei; Shao, Lei; Liu, Xiaowei; Gao, Anyuan; Wang, Hao; Zheng, Binjie; Hou, Guozhi; Shehzad, Khurram; Yu, Linwei; Miao, Feng; Shi, Yi; Xu, Yang; Wang, Xiaomu; NATURE NANOTECHNOLOGY, (2020)
2	Large out-of-plane piezoelectricity of oxygen functionalized MXenes for ultrathin piezoelectric cantilevers and diaphragms; Tan, Jie; Wang, Yunhua; Wang, Zongtan; He, Xiujie; Liu, Yulan; Wang, Biao; Katsnelson, Mikhail I.; Yuan, Shengjun; NANO ENERGY, 65, (2019)
3	Resonant Photovoltaic Effect in Doped Magnetic Semiconductors; Bhalla, Pankaj; MacDonald, Allan H.; Culcer, Dimitrie; PHYSICAL REVIEW LETTERS, 124, 8 (2020)
4	Plasmonically enabled two-dimensional material-based optoelectronic devices; Wang, Hao; Li, Shasha; Ai, Ruoqi; Huang, He; Shao, Lei; Wang, Jianfang; NANOSCALE, 12, 15 (2020)
5	Electrostatic force driven helium insertion into ammonia and water crystals under pressure; Bai, Yihong; Liu, Zhen; Botana, Jorge; Yan, Dadong; Lin, Hai-Qing; Sun, Jian; Pickard, Chris J.; Needs, Richard J.; Miao, Mao-Sheng; COMMUNICATIONS CHEMISTRY, 2, (2019)
6	Kondo resonance assisted thermoelectric transport through strongly correlated quantum dots; Cheng, YongXi; Li, ZhenHua; Wei, JianHua; Luo, HongGang; Lin, HaiQing; Yan, YiJing; SCIENCE CHINA-PHYSICS MECHANICS & ASTRONOMY, 63, 9 (2020)
7	THz Emission by Frequency Down-conversion in Topological Insulator Quantum Dots; Huang, Yongwei; Lou, Wenkai; Cheng, Fang; Yang, Wen; Chang, Kai; PHYSICAL REVIEW APPLIED, 12, 3 (2019)
8	phq: A Fortran code to compute phonon quasiparticle properties and dispersions; Zhang, Z.; Zhang, D. -B.; Sun, T.; Wentzcovitch, R. M.; COMPUTER PHYSICS COMMUNICATIONS, 243, (2019)
9	Twist-induced preferential distribution of dopants in single-crystalline Si nanowires; Zhao, Xing-Ju; Seifert, Gotthard; Zhu, Junyi; Zhang, Dong-Bo; PHYSICAL REVIEW B, 100, 17 (2019)

SIMULATION OF PHYSICAL SYSTEMS DIVISION 物理系统模拟研究部

10	Analysis of time-resolved single-particle spectrum on the one-dimensional extended Hubbard model; Shao, Can; Tohyama, Takami; Luo, Hong-Gang; Lu, Hantao; PHYSICAL REVIEW B, 101, 4 (2020)
11	Anomalous caustics and Veselago focusing in 8-Pmmn borophene p-n junctions with arbitrary junction directions; Zhang, Shu-Hui; Yang, Wen; NEW JOURNAL OF PHYSICS, 21, 10 (2019)
12	Lattice dynamics of twisted ZnO nanowires under generalized Born-von Karman boundary conditions; Liu, Zhao; Yam, Chi-Yung; Gao, Shiwu; Sun, Tao; Zhang, Dong-Bo; NEW JOURNAL OF PHYSICS, 22, 2 (2020)
13	Unconventional deformation potential and half-metallicity in zigzag nanoribbons of 2D-Xenes; Shi, Jin-Lei; Zhao, Xing-Ju; Seifert, Gotthard; Wei, Su-Huai; Zhang, Dong-Bo; PHYSICAL CHEMISTRY CHEMICAL PHYSICS, 22, 14 (2020)
14	Strain induced spin-splitting and half-metallicity in antiferromagnetic bilayer silicene under bending; Shi, Jin-Lei; Wang, Yunhua; Zhao, Xing-Ju; Zhang, Yu-Zhong; Yuan, Shengjun; Wei, Su-Huai; Zhang, Dong-Bo; PHYSICAL CHEMISTRY CHEMICAL PHYSICS, 22, 20 (2020)
15	Data processing over single-port homodyne detection to realize superresolution and supersensitivity; Xu, J. H.; Chen, A. X.; Yang, W.; Jin, G. R.; PHYSICAL REVIEW A, 100, 6 (2019)
16	Velocity-determined anisotropic behaviors of RKKY interaction in 8-Pmmn borophene; Zhang, Shu-Hui; Shao, Ding-Fu; Yang, Wen; JOURNAL OF MAGNETISM AND MAGNETIC MATERIALS, 491, (2019)
17	Possible cluster pairing correlation in the checkerboard Hubbard model: a quantum Monte Carlo study; Wu, Yongzheng; Fang, Shichao; Liu, Guangkun; Zhang, Yan; JOURNAL OF PHYSICS-CONDENSED MATTER, 31, 37 (2019)
18	Carrier free long-range magnetism in Mo doped one quintuple layer Bi2Te3 and Sb2Te3; Zhang, Xiaodong; Zhu, Junyi; JOURNAL OF PHYSICS-CONDENSED MATTER, 32, 6 (2020)
19	Comment on Quantum fidelity approach to the ground-state properties of the one-dimensional axial next-nearest-neighbor Ising model in a transverse field; Nemati, Somayyeh; Fumani, Fatemeh Khastehdel; Mahdavifar, Saeed; PHYSICAL REVIEW E, 102, 1 (2020)
20	Interlayer vibration of twisted bilayer graphene: A first-principles study; Song, Hong-Quan; Liu, Zhao; Zhang, Dong-Bo; PHYSICS LETTERS A, 383, 22 (2019)
21	Ab-Initio Simulations of Monolayer InSe and MoS2 Strain Effect: From Electron Mobility to Photoelectric Effect; Luo, Kun; Yang, Wen; Pan, Yu; Yin, Huaxiang; Zhao, Chao; Wu, Zhenhua; JOURNAL OF ELECTRONIC MATERIALS, 49, 1 (2020)
22	Recent Progress in Optical-Resonance-Assisted Movement Control of Nanomotors; Jiapeng Zheng;Shiu Hei Lam;He Huang;Lei Shao; ADVANCED INTELLIGENT SYSTEMS, (2020)
23	Self-organized bosonic domain walls; Xingchuan Zhu, Shiying Dong, Yang Lin, Rubem Mondaini, Huaiming Guo, Shiping Feng, and Richard T. Scalettar; PHYSICAL REVIEW RESEARCH, 2, 1 (2020)

QUANTUM PHYSICS AND QUANTUM INFORMATION DIVISION 量子物理与量子信息实验室

1	Non-Hermitian bulk-boundary correspondence in quantum dynamics; Xiao, Lei; Deng, Tianshu; Wang, Kunkun; Zhu, Gaoyan; Wang, Zhong; Yi, Wei; Xue, Peng; NATURE PHYSICS, 16, 7 (2020)
2	Magnetic Noise Enabled Biocompass; Xiao, Dawu; Hu, Wen-Hui; Cai, Yunfeng; Zhao, Nan; PHYSICAL REVIEW LETTERS, 124, 12 (2020)
3	Observation of Critical Phenomena in Parity-Time-Symmetric Quantum Dynamics; Xiao, Lei; Wang, Kunkun; Zhan, Xiang; Bian, Zhihao; Kawabata, Kohei; Ueda, Masahito; Yi, Wei; Xue, Peng; PHYSICAL REVIEW LETTERS, 123, 23 (2019)
4	Precise characterization of atomic-scale corrosion of single crystal diamond in H2 plasma based on MEMS/NEMS; Wu, Haihua; Zhang, Zilong; Sang, Liwen; Li, Tiefu; You, Jianqiang; Imura, Masataka; Koide, Yasuo; Liao, Meiyong; CORROSION SCIENCE, 170, (2020)
5	Fixed Points and Dynamic Topological Phenomena in a Parity-Time-Symmetric Quantum Quench; Qiu, Xingze; Deng, Tian-Shu; Hu, Ying; Xue, Peng; Yi, Wei; ISCIENCE, 20, (2019)
6	Theory of the magnon Kerr effect in cavity magnonics; Zhang, GuoQiang; Wang, YiPu; You, JianQiang; SCIENCE CHINA-PHYSICS MECHANICS & ASTRONOMY, 62, 8 (2019)
7	Experimental preparation of topologically ordered states via adiabatic evolution; Luo, ZhiHuang; Li, Jun1; Li, ZhaoKai; Hung, Ling-Yan; Wan, Yidun; Peng, XinHua; Du, JiangFeng; SCIENCE CHINA-PHYSICS MECHANICS & ASTRONOMY, 62, 8 (2019)
8	Nonreciprocity via Nonlinearity and Synthetic Magnetism; Xu, Xun-Wei; Li, Yong; Li, Baijun; Jing, Hui; Chen, Ai-Xi; PHYSICAL REVIEW APPLIED, 13, 4 (2020)
9	Photon-Dressed Bloch-Siegert Shift in an Ultrastrongly Coupled Circuit Quantum Electrodynamical System; Wang, Shuai-Peng; Zhang, Guo-Qiang; Wang, Yimin; Chen, Zhen; Li, Tiefu; Tsai, J. S.; Zhu, Shi-Yao; You, J. Q.; PHYSICAL REVIEW APPLIED, 13, 5 (2020)
10	Closed-Loop Nuclear Magnetic Resonance Gyroscope Based on Rb-Xe; Zhang, Ke; Zhao, Nan; Wang, Yanhua; SCIENTIFIC REPORTS, 101, (2020)
11	Overcoming standard quantum limit using a momentum measuring interferometer; Davuluri, Sankar; Li, Yong; OPTICS LETTERS, 45, 8 (2020)
12	Nonreciprocal interference and coherent photon routing in a three-port optomechanical system; Du, Lei; Chen, Yao-Tong; Wu, Jin-Hui; Li, Yong; OPTICS EXPRESS, 28, 3 (2020)
13	Dual-gate transistor amplifier in a multimode optomechanical system; Chen, Yao-Tong; Du, Lei; Liu, Yi-Mou; Zhang, Yan; OPTICS EXPRESS, 28, 5 (2020)
14	Topological band theory for non-Hermitian systems from the Dirac equation; Ge, Zi-Yong; Zhang, Yu-Ran; Liu, Tao; Li, Si-Wen; Fan, Heng; Nori, Franco; PHYSICAL REVIEW B, 100, 5 (2019)

QUANTUM PHYSICS AND QUANTUM INFORMATION DIVISION 量子物理与量子信息实验室

15	Quantum illumination assistant with error-correcting codes; Zhang, Wen-Zhao; Ma, Yu-Han; Chen, Jin-Fu; Sun, Chang-Pu; NEW JOURNAL OF PHYSICS, 22, 1 (2020)
16	High bandwidth three-axis magnetometer based on optically polarized Rb-85 under unshielded environment; Yang, Hongying; Zhang, Ke; Wang, Yanhua; Zhao, Nan; JOURNAL OF PHYSICS D-APPLIED PHYSICS, 53, 6 (2020)
17	Prominent enhancement on the radiative branching ratio of the doubly excited resonant states due to the Breit interaction induced ion-core energy inversion; Wu, Chensheng; Xie, Lu-You; Hu, Zhimin; Gao, Xiang; JOURNAL OF QUANTITATIVE SPECTROSCOPY & RADIATIVE TRANSFER, 246, (2020)
18	Enantio-discrimination via light deflection effect; Chen, Yu-Yuan; Ye, Chong; Zhang, Quansheng; Li, Yong; JOURNAL OF CHEMICAL PHYSICS, 152, 20 (2020)
19	Utilizing competitions between optical parametric amplifications and dissipations to manipulate photon transport; Yan, Cong-Hua; Jia, W. Z.; Jia, Xin-Hong; Yuan, Hao; Li, Yong; Yuan, Haidong; PHYSICAL REVIEW A, 100, 2 (2019)
20	Optimal unidirectional amplification induced by optical gain in optomechanical systems; Song, L. N.; Zheng, Qiang; Xu, Xun-Wei; Jiang, Cheng; Li, Yong; PHYSICAL REVIEW A, 100, 4 (2019)
21	Phase-controlled single-photon nonreciprocal transmission in a one-dimensional waveguide; Wang, Zhihai; Du, Lei; Li, Yong; Liu, Yu-xi; PHYSICAL REVIEW A, 100, 5 (2019)
22	Experimental orthogonalization of highly overlapping quantum states with single photons; Zhu, Gaoyan; Kalman, Orsolya; Wang, Kunkun; Xiao, Lei; Qu, Dengke; Zhan, Xiang; Bian, Zhihao; Kiss, Tamas; Xue, Peng; PHYSICAL REVIEW A, 100, 5 (2019)
23	Experimental quantum cloning in a pseudo-unitary system; Zhan, Xiang; Wang, Kunkun; Xiao, Lei; Bian, Zhihao; Zhang, Yongsheng; Sanders, Barry C.; Zhang, Chengjie; Xue, Peng; PHYSICAL REVIEW A, 101, 1 (2020)
24	Experimental demonstration of one-sided device-independent self-testing of any pure two-qubit entangled state; Bian, Zhihao; Majumdar, A. S.; Jebarathinam, C.; Wang, Kunkun; Xiao, Lei; Zhan, Xiang; Zhang, Yongsheng; Xue, Peng; PHYSICAL REVIEW A, 101, 2 (2020)
25	Relativistic eigenchannel R-matrix studies of the strong intrashell electron correlations in highly charged Ar13+ ions; Dou, Li-Jun; Jin, Rui; Sun, Rui; Xie, Lu-You; Huang, Zhong-Kui; Li, Jia-Ming; Ma, Xin-Wen; Gao, Xiang; PHYSICAL REVIEW A, 101, 3 (2020)
26	Subfemtosecond glory hologrammetry for vectorial optical waveform reconstruction; Tao, Jianfei; Cai, J.; Xia, Q. Z.; Liu, J.; PHYSICAL REVIEW A, 101, 4 (2020)
27	Experimental entropic test of state-independent contextuality via single photons; Qu, Dengke; Kurzynski, Pawel; Kaszlikowski, Dagomir; Raeisi, Sadegh; Xiao, Lei; Wang, Kunkun; Zhan, Xiang; Xue, Peng; PHYSICAL REVIEW A, 101, 6 (2020)
28	Experimental demonstration of quantum-to-quantum Bernoulli factory; Zhan, Xiang; Wang, Kunkun; Xiao, Lei; Bian, Zhihao; Xue, Peng; PHYSICAL REVIEW A, 102, 1 (2020)

29	Effective two-level models for highly efficient inner-state enantioseparation based on cyclic three-level systems of chiral molecules; Ye, Chong; Zhang, Quansheng; Chen, Yu-Yuan; Li, Yong; PHYSICAL REVIEW A, 100, 4 (2019)
30	Determination of enantiomeric excess with chirality-dependent ac Stark effects in cyclic three-level models; Ye, Chong; Zhang, Quansheng; Chen, Yu-Yuan; Li, Yong; PHYSICAL REVIEW A, 100, 3 (2019)
31	Electrical readout/characterization of single crystal diamond (SCD) cantilever resonators; Wu, Haihua; Zhang, Zilong; Sang, Liwen; Li, Tiefu; You, Jianqiang; Lu, Yingjie; Koide, Yasuo; Liao, Meiyong; DIAMOND AND RELATED MATERIALS, 103, (2020)
32	Directional quantum random walk induced by coherence; Chen, Jin-Fu; Ma, Yu-Han; Sun, Chang-Pu; FRONTIERS OF PHYSICS, 15, 2 (2020)
33	A Perturbative View from the Master Equation: Electromagnetically Induced Transparency Revisited; Wang, Xin; APPLIED SCIENCES-BASEL, 9, 21 (2019)
34	Unidirectional gyroscope using optomechanics to avoid mode-locking; Davuluri, Sankar; Li, Yong; JOURNAL OF OPTICS, 21, 11 (2019)
35	Boosting the performance of quantum Otto heat engines; Chen, Jin-Fu; Sun, Chang-Pu; Dong, Hui; PHYSICAL REVIEW E, 100, 3 (2019)
36	Achieve higher efficiency at maximum power with finite-time quantum Otto cycle; Chen, Jin-Fu; Sun, Chang-Pu; Dong, Hui; PHYSICAL REVIEW E, 100, 6 (2019)
37	Photonic discrete-time quantum walks [Invited]; Zhu, Gaoyan; Xiao, Lei; Huo, Bingzi; Xue, Peng; CHINESE OPTICS LETTERS, 18, 5 (2020)
38	Quantifying algebraic asymmetry of Hamiltonian systems; Qin, Hui-Hui; Fei, Shao-Ming; Sun, Chang-Pu; JOURNAL OF PHYSICS A-MATHEMATICAL AND THEORETICAL, 53, 3 (2020)
39	Photon echo using imperfect x-ray pulse with phase fluctuation; Chen, Jin-Fu; Dong, Hui; Sun, Chang-Pu; PHYSICA SCRIPTA, 94, 10 (2019)
40	Quantifying quantum non-Markovianity based on quantum coherence via skew information; Shao, Lian-He; Zhang, Yu-Ran; Luo, Yu; Xi, Zhengjun; Fei, Shao-Ming; LASER PHYSICS LETTERS, 17, 1 (2020)
41	Variation of the transition energies and oscillator strengths for the 3C and 3D lines of the Ne-like ions under plasma environment; Wu, Chensheng; Chen, Shaomin; Chang, T. N.; Gao, Xiang; JOURNAL OF PHYSICS B-ATOMIC MOLECULAR AND OPTICAL PHYSICS, 52, 18 (2019)
42	Optimizations of a parametric-modulation atomic magnetometer in a nuclear magnetic resonance gyroscope; Tang, Feng; Li, Ai-xian; Zhang, Ke; Wang, Yanhua; Zhao, Nan; JOURNAL OF PHYSICS B-ATOMIC MOLECULAR AND OPTICAL PHYSICS, 52, 20 (2019)

QUANTUM PHYSICS AND QUANTUM INFORMATION DIVISION 量子物理与量子信息实验室

43	Experimental optimization of atomic magnetometer in nuclear magnetic resonance gyroscope; Zhang, Ke; Luo, Zhihuang; Tang, Feng; Zhao, Nan; Wang, Yanhua; JAPANESE JOURNAL OF APPLIED PHYSICS, 59, 3 (2020)
44	Saturation effect of atomic magnetic resonance; Yang, Hongying; Wang, Yanhua; Zhao, Nan; AIP ADVANCES, 10, 5 (2020)
45	Double-passage mechanical cooling in a coupled optomechanical system; Mu, Qing-Xia; Lang, Chao; Zhang, Wen-Zhao; CHINESE PHYSICS B, 28, 11 (2019)
46	Dissipative quantum phase transition in a biased Tavis-Cummings model*; Chen, Zhen; Qiu, Yueyin; Zhang, Guo-Qiang; You, Jian-Qiang; CHINESE PHYSICS B, 29, 4 (2020)
47	Confinement Induced Resonance with Weak Bare Interaction in a Quasi 3+0 Dimensional Ultracold Gas; Xiao, Dawu; Zhang, Ren; Zhang, Peng; FEW-BODY SYSTEMS, 60, 4 (2019)
48	Fast enantioconversion of chiral mixtures based on a four-level double- model; Ye, Chong; Zhang, Quansheng; Chen, Yu-Yuan; Li, Yong; PHYSICAL REVIEW RESEARCH, (2020)
49	Conserved quantities in parity-time symmetric systems; Bian, Zhi-Hao; Xiao, Lei; Wang, Kun-kun; Zhan Xiang; Franck Assogba Onanga; Frantisek Ruzicka; Yi, Wei; Yogesh N. Joglekar; Xue, Peng; PHYSICAL REVIEW RESEARCH, (2020)
50	Direct experimental test of forward and reverse uncertainty relations; Xiao, Lei; Fan, Bo-wen; Wang, Kun-kun; Xue, Peng; Arun Kumar Pati; PHYSICAL REVIEW RESEARCH, (2020)

MATERIALS AND ENERGY DIVISION 材料与能源研究部

1	Response to Comment on “Prediction of Novel p-Type Transparent Conductors in Layered Double Perovskites: A First-Principles Study”; Jian Xu, Jian-Bo Liu, Jianfeng Wang, Bai-Xin Liu, and Bing Huang; ADVANCED FUNCTIONAL MATERIALS, 30, 31 (2020)
2	Plasmon-Induced Electron−Hole Separation at the Ag/TiO2(110) Interface; Jie Ma, and Shiwu Gao; ACS NANO, 13, 12 (2019)
3	Fast surface dynamics enabled cold joining of metallic glasses; Jiang Ma, Can Yang, Xiaodi Liu, Baoshuang Shang, Quanfeng He, Fucheng Li, Tianyu Wang, Dan Wei, Xiong Liang, Xiaoyu Wu, Yunjiang Wang, Feng Gong, Pengfei Guan, Weihua Wang, Yong Yang; SCIENCE ADVANCES, 5, 11 (2019)
4	Defect Modulation of Z-Scheme TiO2/Cu2O Photocatalysts for Durable Water Splitting; Wei, Tingcha; Zhu, Ya-Nan; An, Xiaoqiang; Liu, Li-Min; Cao, Xingzhong; Liu, Huijuan; Qu, Jiuhui; ACS CATALYSIS, 9, 9 (2019)

5	Atomic layer deposited Pt-Ru dual-metal dimers and identifying their active sites for hydrogen evolution reaction; Zhang, Lei; Si, Rutong; Liu, Hanshuo; Chen, Ning; Wang, Qi; Adair, Keegan; Wang, Zhiqiang; Chen, Jiatang; Song, Zhongxin; Li, Junjie; Banis, Mohammad Norouzi; Li, Ruying; Sham, Tsun-Kong; Gu, Meng; Liu, Li-Min; Botton, Gianluigi A.; Sun, Xueliang; NATURE COMMUNICATIONS, 10, (2019)
6	Realization of Lieb lattice in covalent-organic frameworks with tunable topology and magnetism; Bin Cui, Xingwen Zheng, Jianfeng Wang, Desheng Liu, Shijie Xie, Bing Huang; NATURE COMMUNICATIONS, (2020)
7	Design of Multifunctional Quinternary Metal-Halide Perovskite Compounds Based on Cation−Anion Co-Ordering; Yang Huang, Tao Zhang, Jing Wang, Shao-Gang Xu, Peng Zhang, Shiyou Chen, Wan-Jian Yin, Xiuwen Zhang, and Su-Huai Wei; CHEMISTRY OF MATERIALS, (2020)
8	Tunable magnetism of a single-carbon vacancy in graphene; Yu Zhang, Fei Gao, Shiwu Gao, Lin He; SCIENCE BULLETIN, (2020)
9	Elastic avalanches reveal marginal behavior in amorphous solids; Shang, Baoshuang; Guan, Pengfei; Barrat, Jean-; PROCEEDINGS OF THE NATIONAL ACADEMY OF SCIENCES, 117, 1 (2020)
10	Prediction of room-temperature half-metallicity in layered halide double perovskites; Xu, Jian; Xu, Changsong; Liu, Jian-Bo; Bellaiche, Laurent; Xiang, Hongjun; Liu, Bai-Xin; Huang, Bing; NPJ COMPUTATIONAL MATERIALS, 5, (2019)
11	Serial and parallel spin circuits at the molecular scale with two atomic-vacancies in graphene: Amplification of spin-filtering effect; Wen, Shizheng; Gao, Shiwu; Yam, ChiYung; CARBON, 154, (2019)
12	Anomalous Dirac Plasmons in 1D Topological Electrides; Wang, Jianfeng; Sui, Xuelei; Gao, Shiwu; Duan, Wenhui; Liu, Feng; Huang, Bing; PHYSICAL REVIEW LETTERS, 123, 20 (2019)
13	Formation of Bloch Flat Bands in Polar Twisted Bilayers without Magic Angles; Zhao, Xing-Ju; Yang, Yang; Zhang, Dong-Bo; Wei, Su-; PHYSICAL REVIEW LETTERS, 124, 8 (2020)
14	Transition from Positive to Negative Photoconductance in Doped Hybrid Halide Perovskites; Md Azimul Haque, Jin-Ling Li, Ahmed L. Abdelhady, Makhsud I. Saidaminov, Derya Baran, Osman M. Bakr, Su-Huai Wei, and Tom Wu; ADVANCED OPTICAL MATERIALS, (2019)
15	Revealing the ultra-low-temperature relaxation peak in a model metallic glass; B. Wang, L.J. Wang, B.S. Shang, X.Q. Gao, Y. Yang, H.Y. Bai, M.X. Pan, W.H. Wang, P.F. Guan; ACTA MATERIALIA, (2020)
16	Designing Dirac semimetals with a honeycomb Na3Bi-lattice via isovalent cation substitution; Xinbo Chen, Weida Chen, Shu Yu, Shaogang Xu, Ximing Rong, Pu Huang, Xiuwen Zhang and Su-Huai Wei; JOURNAL OF MATERIALS CHEMISTRY C, (2019)
17	Phonon-Assisted Hopping through Defect States in MoS2: A Multiscale Simulation; Kang, Jun; JOURNAL OF PHYSICAL CHEMISTRY LETTERS, (2020)

MATERIALS AND ENERGY DIVISION 材料与能源研究部

18	Hole-induced Spontaneous Mutual Annihilation of Dislocation Pair; Yelong Wu, Guangde Chen, Jinying Yu,§ Dan Wang, Chao Ma,Chen Li, Stephen J. Pennycook, Yanfa Yan, and Su-Huai Wei; JOURNAL OF PHYSICAL CHEMISTRY LETTERS, (2019)
19	Soft-Mode Parameter as an Indicator for the Activation Energy Spectra in Metallic Glass; Shan Zhang, Chaoyi Liu, Yue Fan, Yong Yang, and Pengfei Guan; JOURNAL OF PHYSICAL CHEMISTRY LETTERS, 11, 7 (2020)
20	Water-Hydrogen-Polaron Coupling at Anatase TiO2(101) Surfaces: A Hybrid Density Functional Theory Study; Ya-Nan Zhu, Gilberto Teobaldi, and Li-Min Liu; JOURNAL OF PHYSICAL CHEMISTRY LETTERS, 11, 11 (2020)
21	Segregation-sandwiched stable interface suffocates nanoprecipitate coarsening to elevate creep resistance; Y. H. Gao, P. F. Guan, R. Su, H. W. Chen, C. Yanga, C. He, L. F. Cao, H. Song, J. Y. Zhang, X.F. Zhang, G. Liu, J. F. Nie, J. Sun and E. Ma; MATERIALS RESEARCH LETTERS, (2020)
22	Deep-ultraviolet nonlinear optical crystals by design: A computer-aided modeling blueprint from first principles; Lei Kang, Fei Liang, Zheshuai Lin and Bing Huang; SCIENCE CHINA-MATERIALS, (2020)
23	Revealing a hidden dynamic signature of the non-Arrhenius crossover in metallic glass-forming liquids; Nannan Ren, Lina Hu, Lijin Wang, Pengfei Guan; SCRIPTA MATERIALIA, 181, (2020)
24	Destruction of the Uranyl Moiety in a U(V) "Cation-Cation" Interaction; Hu, Shu-Xian; Jian, Jiwen; Li, Jun; Gibson, John K.; INORGANIC CHEMISTRY, (2019)
25	A general rule for transition metals doping on magnetic properties of Fe-based metallic glasses; Chen, Hui; Zhou, Shaoxiong; Dong,; JOURNAL OF ALLOYS AND COMPOUNDS, (2020)
26	Accurate and effective computation of the multi-phonon nonradiative transition; Su-Huai Wei; SCIENCE CHINA-PHYSICS MECHANICS & ASTRONOMY, 63, 11 (2020)
27	Band-Structure Engineering of ZnxCd1−xSySe1−y Quaternary Alloys as the Window Layer for CdTe Solar Cells; Rong Wang, Mu Lan, Jingxiu Yang, and Su-Huai Wei; PHYSICAL REVIEW APPLIED, (2020)
28	Coupled Transport of Water and Ions through Graphene Nanochannels; Yunzhen Zhao, Decai Huang, Jiaye Su, and Shiwu Gao; JOURNAL OF PHYSICAL CHEMISTRY C, (2020)
29	Giant enhancement of solid solubility in monolayer alloys by selective orbital coupling; Du, Shiqiao; Wang, Jianfeng; Kang, Lei; Huang,; PHYSICAL REVIEW B, (2020)
30	Realistic dimension-independent approach for charged-defect calculations in semiconductors; Jin Xiao, Kaike Yang, Dan Guo, Tao Shen, Hui-Xiong Deng, Shu-Shen Li, Jun-Wei Luo, and Su-Huai Wei; PHYSICAL REVIEW B, 101, 16 (2020)
31	Chemical trend of a Cu impurity in Zn chalcogenides; Yang Yang , Peng Zhang, Jingxiu Yang, and Su-Huai Wei; PHYSICAL REVIEW B, 101, 17 (2020)

32	A systematic study of the negative thermal expansion in zinc-blende and diamond-like semiconductors; Kaike Yang, Jin Xiao, Jun-Wei Luo, Shu-Shen Li, Su-Huai Wei and Hui-Xiong Deng; NEW JOURNAL OF PHYSICS, 21, 12 (2019)
33	Site Dependent Reactivity of Pt Single Atoms on Anatase TiO2 (101) in Aqueous Environment; Bo Wen, Wen-Jin Yin, Annabella Selloni, Li-Min Liu; PHYSICAL CHEMISTRY CHEMICAL PHYSICS, (2019)
34	Unconventional deformation potential and halfmetallicity in zigzag nanoribbons of 2D-Xenes; Jin-Lei Shi, Xing-Ju Zhao, Gotthard Seifert, Su-Huai Wei and Dong-Bo Zhang; PHYSICAL CHEMISTRY CHEMICAL PHYSICS, (2020)
35	Sound attenuation in stable glasses; Wang, Lijin; Berthier, Ludovic; Flenner, Elijah; Guan, Pengfei; Szamel, Grzegorz; SOFT MATTER, 15, 35 (2019)
36	Structure and reactivity of highly reduced titanium oxide surface layers on TiO2: A first-principles study; Wen, Bo; Liu, Li-Min; Selloni, Annabella; JOURNAL OF CHEMICAL PHYSICS, 151, 18 (2019)
37	Sn3O4 exfoliation process investigated by density functional theory and modern scotch-tape experiment; Freire, Rafael L. H.; Masteghin, Mateus G.; Da Silva, Juarez L. F.; Orlandi, Marcelo O.; COMPUTATIONAL MATERIALS SCIENCE, 170, (2019)
38	Mechanical behavior of metallic nanowires with twin boundaries parallel to loading axis; Hao, Longhu; Liu, Qi; Fang, Yunyi; Huang, Ming; Li, Wei; Lu, Yan; Luo, Junfeng; Guan, Pengfei; Zhang, Ze; Wang, Lihua; Han, Xiaodong; COMPUTATIONAL MATERIALS SCIENCE, 169, (2019)
39	Evaluation of chemical bonding and electronic structures in trisodium actinate for actinide series from thorium to curium; Zhong-Fei Xu, Shu-Xian Hu, Yu Yang, Ping Zhang; COMPUTATIONAL MATERIALS SCIENCE, (2020)
40	Probing the Electronic Structure and Chemical Bonding of Uranium Nitride Complexes of NU-XO (X = C, N, O); Qin, Jian-Wei; Zhang, Peng; Pu, Zhen; Hu, Yin; Zhang, Ping; Shuai, Mao-Bing; Hu, Shu-Xian; JOURNAL OF PHYSICAL CHEMISTRY A, 123, 32 (2019)
41	First-principles study of electronic and diffusion properties of intrinsic defects in 4H-SiC; Yan, Xiaolan; Li, Pei; Kang, Lei; Wei, Su-Huai; Huang,; JOURNAL OF APPLIED PHYSICS, (2020)
42	First-principles study of the band gap tuning and doping control in CdSexTe1-x alloy for high efficiency solar cell; Yang, Jingxiu; Wei, Su-Huai; CHINESE PHYSICS B, 28, 8 (2019)
43	Revisit of the band gaps of rutile SnO2 and TiO2: a first-principles study; Cai, Xuefen; Zhang, Peng; Wei, Su-Huai; JOURNAL OF SEMICONDUCTORS, 40, 9 (2019)
44	Strain tunable band structure of a new 2D carbon allotrope C568; Qiang Gao, Hasan Sahin, and Jun Kang; JOURNAL OF SEMICONDUCTORS, (2020)
45	Defect Dynamic Model of the Synergistic Effect in Neutron- and γ Ray-Irradiated Silicon NPN Transistors; Yu Song, Hang Zhou, Xue-Fen Cai, Yang Liu, Ping Yang, Guang-Hui Zhang, Ying Zhang, Mu Lan, and Su-Huai Wei; ACS APPLIED MATERIALS & INTERFACES, (2020)

COMPLEX SYSTEMS DIVISION 复杂系统研究部

1	Emergence of collective oscillations in adaptive cells; Shou-Wen Wang, Lei-Han Tang; NATURE COMMUNICATIONS, 10, 5613 (2019)
2	Discontinuities in Driven Spin-BosonSystems due to Coherent Destruction of Tunneling: Breakdown of the Floquet-Gibbs Distribution; Georg Engelhardt, Gloria Platero, Jianshu Cao; PHYSICAL REVIEW LETTERS, 123, (2019)
3	GDP release from the open conformation of Gα requires allosteric signaling from the agonist bound human β2 adrenergic receptor; Vikash Kumar, Hannah Hoag, Safaa Sader, Nicolas Scorese, Haiguang Liu, Chun Wu; JOURNAL OF CHEMICAL INFORMATION AND MODELING, (2020)
4	Model Reconstruction from Small-Angle X-Ray Scattering Data Using Deep Learning Methods; Hao He,Can Liu, Haiguang Liu; ISCIENCE, 23, 3 (2020)
5	Prediction of disulfide bond engineering sites using a machine learning method; Xiang Gao, Xiaoqun Dong, Xuanxuan Li, Zhijie Liu, Haiguang Liu; SCIENTIFIC REPORTS, 10, (2020)
6	Neighborhood Preference of Amino Acids in Protein Structures and its Applications in Protein Structure Assessment; Siyuan Liu, Xilun Xiang, Xiang Gao, Haiguang Liu; SCIENTIFIC REPORTS, 10, (2020)
7	Binding of agonist WAY-267,464 and antagonist WAY-methylated to oxytocin receptor probed by all-atom molecular dynamics simulations; A.I. Uba, C. Radicella, C. Readmond, N. Scorese, S. Liao, H. Liu, C. Wu; LIFE SCIENCES, 252, (2020)
8	SAS-cam: a program for automatic processing and analysis of small-angle scattering data; Hongjin Wu, Yiwen Li, Guangfeng Liu, Haiguang Liu, Na Li; JOURNAL OF APPLIED CRYSTALLOGRAPHY, 53, (2020)
9	EM-detwin: A Program for Resolving Indexing Ambiguity in Serial Crystallography Using the Expectation-Maximization Algorithm; Yingchen Shi, Haiguang Liu; CRYSTALS, 10, 7 (2020)
10	SPIND-TC: An indexing method for two-color X-ray diffraction data; Xuanxuan Li, Chufeng Li, Haiguang Liu; ACTA CRYSTALLOGR. SECT. A FOUND. ADV, 76, (2020)

APPLIED AND COMPUTATIONAL MATHEMATICS DIVISION 应用与计算数学研究部

1	A new finite element approach for the Dirichlet eigenvalue problem; Wenqiang Xiao, Bo Gong, Jiguang Sun, and Zhimin Zhang; APPLIED MATHEMATICS LETTERS, 105, (2020)
2	A linear energy andentropy-production-rate preserving scheme for thermodynamically consistent crystal growth models; Yucan Zhao, Jun Li, Jia Zhao,Qi Wang; APPLIED MATHEMATICS LETTERS, 98, (2019)

3	Supplementary variable method for structure-preserving approximations to partial differential equations with deduced equations; Qi Hong, Jun Li, Qi Wang; Applied Mathematics Letters, 110, (2020)
4	A locking-free weak Galerkin finite element method for Reissner-Mindlin plate on polygonal meshes; Xiu Ye, Shangyou Zhang, Zhimin Zhang; COMPUTERS AND MATHEMATICS WITH APPLICATIONS, 80, (2020)
5	Error analysis of a finite element method with GMMP temporal discretisation for a time-fractional diffusion equation; Chaobao Huang, Martin Stynes; COMPUTERS AND MATHEMATICS WITH APPLICATIONS, 79, (2020)
6	A discrete comparison principle for the time-fractional diffusion equation; Hu Chen,Martin Stynes; COMPUTERS AND MATHEMATICS WITH APPLICATIONS, 80, (2020)
7	A patient specific predicative model for human albumin based on deep neural networks; Cheng Lei, Yu Wang, Jia Zhao, Kexun Li, Hua Jiang, Qi Wang; COMPUTER METHODS AND PROGRAMS IN BIOMEDICINE, (2020)
8	A shifted-inverse adaptive multigrid method for the elastic eigenvalue problem; Bo Gong, Jiayu Han, Jiguang Sun, Zhimin Zhang; COMPUTER PHYSICS COMMUNICATIONS, 27, 1 (2020)
9	Linear second order energy stable schemes of phase field models with nonlocal constraints for crystal growth; Xiaobo Jing, Qi Wang; COMPUTERS & MATHEMATICS WITH APPLICATIONS, 79, 3 (2020)
10	Why fractional derivatives with nonsingular kernels should not be used Kai Diethelm Roberto Garrappa, Andrea Giusti, Martin Stynes; FRACTIONAL CALCULUS AND APPLIED ANALYSIS, 23, 3 (2020)
11	Dynamic phase diagram of an auto-regulated gene in fast switching conditions; Chen Jia, Ramon Grima; JOURNAL OF CHEMICAL PHYSICS, 152, 17 (2020)
12	Small protein number effects in autoregulated bursty gene expression; Chen Jia, Ramon Grima; JOURNAL OF CHEMICAL PHYSICS, 152, 8 (2020)
13	Discrete-velocity vector-BGK models based numerical methods for the incompressible Navier-Stokes equations; Jin Zhao; COMMUNICATIONS IN COMPUTATIONAL PHYSICS, (2020)
14	An arbitrary Lagrangian-Eulerian RKDG method for multi-material flows on adaptive unstructured meshes; Xiaolong Zhao, Xijun Yu, Meilan Qiu, Fang Qing, Shijun Zou; COMPUTERS AND FLUIDS, 207, 207 (2020)
15	Stochastic gene expression kinetics with positive-plus-negative feedback; Chen Jia, Le Yi Wang, George G. Yin, Michael Q. Zhang; PHYSICAL REVIEW E, 100, 5 (2019)
16	A new analysis of a numerical method for the time-fractional Fokker-Planck equation with general forcing; Can Huang, Kim Ngan Le,Martin Stynes; IMA JOURNAL OF NUMERICAL ANALYSIS, 40, (2020)

APPLIED AND COMPUTATIONAL MATHEMATICS DIVISION 应用与计算数学研究部

17	High-order dual-parametric finite element methods for cavitation computation in nonlinear elasticity; Weijie Huang, Weijun Ma, Liang Wei, Zhiping Li; NUMERICAL METHODS FOR PARTIAL DIFFERENTIAL EQUATIONS, 36, 5 (2020)
18	Superconvergence of the direct discontinuous Galerkin method for a time-fractional initial-boundary value problem; Chaobao Huang, Martin Stynes; NUMERICAL METHODS FOR PARTIAL DIFFERENTIAL EQUATIONS, 35, (2019)
19	Superconvergence points for the spectral interpolation of Riesz fractional derivatives; Beichuan Deng, Zhimin Zhang, Xuan Zhao; JOURNAL OF SCIENTIFIC COMPUTING, 81, (2019)
20	Finite element methods based on two families of second-order numerical formulas for the fractional cable model with smooth solutions; Baoli Yin, Yang Liu, Hong Li, Zhimin Zhang; JOURNAL OF SCIENTIFIC COMPUTING, 84, 2 (2020)
21	Structure-Preserving numerical approximations to thermodynamically consistent non-isothermal models of binary viscous fluid flows; Shouwen Sun, Jun Li, Jia Zhao, Qi Wang; JOURNAL OF SCIENTIFIC COMPUTING, 83, 50 (2020)
22	Superconvergence of a finite element method for the multi-term time-fractional diffusion problem; Chaobao Huang, Martin Stynes; JOURNAL OF SCIENTIFIC COMPUTING, 82, (2020)
23	Barrier function local and global analysis of an L1 finite element method for a multiterm time-fractional initial-boundary value problem; Xiangyun Meng, Martin Stynes; JOURNAL OF SCIENTIFIC COMPUTING, 84, 5 (2020)
24	Convergence analysis of Crank-Nicolson Galerkin-Galerkin FEMs for miscible displacement in porous media; Wentao Cai, Jilu Wang, Kai Wang; JOURNAL OF SCIENTIFIC COMPUTING, 83, (2020)
25	Error bounds of the finite difference time domain methods for the Dirac equation in the semiclassical regime; Ying Ma, Jia Yin; JOURNAL OF SCIENTIFIC COMPUTING, 81, 3 (2019)
26	A new proof of scattering theory for the 3D radial focusing energy-critical NLS with combined terms; Chengbin Xu, Tengfei Zhao; JOURNAL OF DIFFERENTIAL EQUATIONS, 286, 11 (2020)
27	Spectral-Galerkin approximation and optimal error estimate for biharmonic eigenvalue problems in circular/spherical/elliptical domains; Jing An, Huiyuan Li, Zhimin Zhang; NUMERICAL ALGORITHMS, 84, (2020)
28	A direct discontinuous Galerkin finite element method for convection-dominated two-point boundary value problems; Guanglong Ma, Martin Stynes; NUMERICAL ALGORITHMS, 83, (2020)
29	Local ultraconvergence of linear and bilinear finite element method for second order elliptic problems; Wenming He, Runchang Lin, Zhimin Zhang; JOURNAL OF COMPUTATIONAL AND APPLIED MATHEMATICS, 372, (2020)

30	Superconvergence analysis of linear FEM based on polynomial preserving recovery for Helmholtz equation with high wave number; Yu Du, Haijun Wu, Zhimin Zhang; JOURNAL OF COMPUTATIONAL AND APPLIED MATHEMATICS, 372, (2020)
31	Optimal spatial H^1-norm analysis of a finite element method for a time-fractional diffusion equation; Chaobao Huang, Martin Stynes; JOURNAL OF COMPUTATIONAL AND APPLIED MATHEMATICS, 367, (2020)
32	Fast acoustic source imaging using multi-frequency sparse data, Inverse Problems; A. Alzaalig, G. Hu, X. Liu, J. Sun; INVERSE PROBLEMS, 36, (2020)
33	Uniqueness and factorization method for inverse elastic scattering with a single incoming wave; J. Elschner and G. Hu; INVERSE PROBLEMS, 35, (2020)
34	Bayesian Approach to Inverse Time-harmonic Acoustic Scattering with Phaseless Far-field Data; Zhipeng Yang, Xinping Gui, Ju Ming, Guanghui Hu; INVERSE PROBLEMS, 36, 6 (2020)
35	A spectrally accurate approximation to subdiffusion equations using the Log orthogonal functions; Sheng Chen, Jie Shen, Zhimin Zhang, Zhi Zhou; SIAM JOURNAL ON SCIENTIFIC COMPUTING, 42, 2 (2020)
36	Limit theorems for generalized density-dependent Markov chains and bursty gene regulatory networks; Xian Chen, Chen Jia; JOURNAL OF MATHEMATICAL BIOLOGY, 80, 4 (2020)
37	An alternative finite difference stability analysis for a multiterm time-fractional initial-boundary value problem; Xiaohui Liu, Martin Stynes; EAST ASIAN JOURNAL ON APPLIED MATHEMATICS, 10, 3 (2020)
38	A Jacobi-Galerkin spectral method for computing the ground and first excited states of the nonlinear fractional Schrödinger equation; Ying Ma, Lizhen Chen; EAST ASIAN JOURNAL ON APPLIED MATHEMATICS, 2, (2020)
39	Kinetic foundation of zero-inflated negative binomial models for single-cell RNA sequencing data; Chen Jia; SIAM JOURNAL ON APPLIED MATHEMATICS, 80, 3 (2020)
40	Uniqueness in inverse electromagnetic scattering problem with phaseless far-field data at a fixed frequency; Xiaoxu Xu, Bo Zhang, Haiwen Zhang; IMA JOURNAL OF APPLIED MATHEMATICS, 85, 4 (2020)
41	Uniqueness in inverse acoustic and electromagnetic scattering with phaseless near-field data at a fixed frequency; Xiaoxu Xu, Bo Zhang, Haiwen Zhang; INVERSE PROBLEMS & IMAGING, 14, 3 (2020)
42	A partial data inverse problem for the Convection-diffusion equation; Suman Kumar Sahoo, Manmohan Vashisth; PROBLEMS AND IMAGING, (2020)
43	A curl-conforming weak Galerkin method for the quad-curl problem; Jiguang Sun, Qian Zhang, Zhimin Zhang; BIT NUMERICAL MATHEMATICS, 59, (2019)

APPLIED AND COMPUTATIONAL MATHEMATICS DIVISION 应用与计算数学研究部

44	Convergence analysis of a finite difference scheme for a two-point boundary value problem with a Riemann-Liouville-Caputo fractional derivative; José Luis Gracia, Eugene O'Riordan, Martin Stynes; BIT NUMERICAL MATHEMATICS, 60, 2 (2020)
45	Approximation of the multi-dimensional incompressible Navier-Stokes equations by discrete-velocity vector-BGK models; Jin Zhao, Zhimin Zhang, Wen-An Yong; JOURNAL OF MATHEMATICAL ANALYSIS AND APPLICATIONS, 486, (2020)
46	Single logarithmic conditional stability in determining unknown boundaries; J. Elschner, G. Hu, M. Yamamoto; APPLICABLE ANALYSIS, 99, (2020)
47	Uniqueness to inverse acoustic and electromagnetic scattering from locally perturbed rough surfaces; Y. Zhao, G. Hu, B. Yan; APPLICABLE ANALYSIS, (2020)
48	Determining the time dependent matrix potential in a wave equation from partial boundary data; Rohit Kumar Mishra, Manmohan Vashisth; APPLICABLE ANALYSIS, (2020)
49	Convergence analysis of finite element approximation for 3-D magnetoheating coupling model; Lixiu Wang, Changhui Yao, Zhimin Zhang; INTERNATIONAL JOURNAL OF NUMERICAL ANALYSIS AND MODELING, 17, 1 (2020)
50	Existence, uniqueness and regularity of the solution of the time-fractional Fokker-Planck equation with general forcing; Kim Ngan Le, William McLean, Martin Stynes; COMMUNICATIONS ON PURE AND APPLIED ANALYSIS, 18, 5 (2019)
51	Moderate maximal inequalities for the Ornstein-Uhlenbeck process; Chen Jia, Guohuan Zhao; PROCEEDINGS OF THE AMERICAN MATHEMATICAL SOCIETY, 148, 8 (2020)
52	A class of efficient spectral methods and error analysis for nonlinear Hamiltonian systems; Jing An, Waixiang Cao, Zhimin Zhang; COMMUNICATIONS IN MATHEMATICAL SCIENCES, 18, 2 (2020)
53	Uniqueness to Some Inverse Source Problems for the Wave Equation in Unbounded Domains; G. Hu, Y. Kian,Y. Zhao; ACTA MATHEMATICAE APPLICATAE SINICA-ENGLISH SERIES, 36, 1 (2020)
54	Optimal H1 spatial convergence of a fully discrete finite element method for the time-fractional Allen-Cahn equation; Chaobao Huang, Martin Stynes; ADVANCES IN COMPUTATIONAL MATHEMATICS, 46, 63 (2020)
55	C^1-conforming quadrilateral spectral element method for fourth-order equations; Huiyuan Li, Weikun Shan, Zhimin Zhang; COMMUNICATIONS ON APPLIED MATHEMATICS AND COMPUTATION, 1, (2019)

MECHANICS DIVISION 力学研究部

1	3D computational models explain muscle activation patterns and energetic functions of internal structures in fish swimming; Ming, Tingyu; Jin, Bowen; Song, Jialei; Luo, Haoxiang; Du, Ruxu; Ding, Yang; PLOS COMPUTATIONAL BIOLOGY, 15, 9 (2019)
2	Regularized 13-moment equations for inverse power law models; Cai, Zhenning; Wang, Yanli; JOURNAL OF FLUID MECHANICS, 894, (2020)
3	An exactly force-balanced boundary-conforming arbitrary-Lagrangian-Eulerian method for interfacial dynamics; Cheng, Zekang; Li, Jie; Loh, Ching Y.; Luo, Li-Shi; JOURNAL OF COMPUTATIONAL PHYSICS, 408, (2020)
4	Lattice Boltzmann equation with Overset method for moving objects in two-dimensional flows; Lallemand, Pierre; Luo, Li-Shi; JOURNAL OF COMPUTATIONAL PHYSICS, 407, (2020)
5	A comparative study of interface-conforming ALE-FE scheme and diffuse interface AMR-LB scheme for interfacial dynamics; Zhang, Changjuan; Fakharic, Abbas; Li, Jie; Luo, Li-Shi; Qian, Tiezheng; JOURNAL OF COMPUTATIONAL PHYSICS, 395, (2019)
6	Burnett spectral method for the spatially homogeneous Boltzmann equation; Cai, Zhenning; Fan, Yuwei; Wang, Yanli; COMPUTERS & FLUIDS, 200, (2020)
7	Numerical Study on the Leakage and Diffusion Characteristics of Low-Solubility and Low-Volatile Dangerous Chemicals from Ship in Inland Rivers; Shuifen Zhan, Mingchao Wang, Min Wang, Qianqian Shao, Zefang Zhang, Wenxin Jiang and Xuemin Chen; CMES-COMPUTER MODELING IN ENGINEERING & SCIENCES, 123, 1 (2020)
8	Mesh Curving and Refinement Based on Cubic Bézier Surface for High-order Discontinuous; Shu-Jie Li; NUMERICAL GEOMETRY, GRID GENERATION AND SCIENTIFIC COMPUTING, (2019)
9	Mesh Curving and Refinement Based on Cubic Bézier Surface for High-order Discontinuous Galerkin Methods; Shu-Jie Li; COMPUTATIONAL MATHEMATICS AND MATHEMATICAL PHYSICS, 59, 12 (2019)
10	Roads to Smart Artificial Microswimmers; Alan C. H. Tsang, Ebru Demir, Yang Ding,On Shun Pak; ADVANCED INTELLIGENT SYSTEMS, (2020)
11	Adaptive exponential time integration of the Navier-Stokes equations; Shu-Jie Li, L. Ju, S. Hang; AIAA-2020-2033, (2020)
12	Time Advancement of the Navier-Stokes Equations: p-Adaptive Exponential Methods; Shu-Jie Li; JOURNAL OF FLOW CONTROL, MEASUREMENT & VISUALIZTION, 8, 2 (2020)

ALGORITHMS DIVISION 计算方法研究部

1	Pressure-promoted irregular CoMoP2 nanoparticles activated by surface reconstruction for oxygen evolution reaction electrocatalysts; Xu, Shishuai; Gao, Xiang; Deshmukh, Amol; Zhou, Junshuang; Chen, Ning; Peng, Wenfeng; Gong, Yutong; Yao, Zhiqiang; Finkelstein, Kenneth D.; Wan, Biao; Gao, Faming; Wang, Mingzhi; Chen, Mingyang; Gou, Huiyang; JOURNAL OF MATERIALS CHEMISTRY A, 8, 4 (2020)
2	Au-Ag synergistic effect in CF3-ketone alkynylation catalyzed by precise nanoclusters; Sun, Lili; Shen, Kangqi; Sheng, Hongting; Yun, Yapei; Song, Yongbo; Pan, Dianhui; Du, Yuanxin; Yu, Haizhu; Chen, Mingyang; Zhu, Manzhou; JOURNAL OF CATALYSIS, 378, (2019)
3	One-core-atom loss in a gold nanocluster promotes hydroamination reaction of alkynes; Wang, Liqun; Shen, Kangqi; Chen, Mingyang; Zhu, Yan; NANOSCALE, 11, 29 (2019)
4	Tunable Photoresponse by Gate Modulation in Bilayer Graphene Nanoribbon Devices; Wang, Rulin; Bi, Fuzhen; Lu, Wencai; Yam, ChiYung; JOURNAL OF PHYSICAL CHEMISTRY LETTERS, 10, 24 (2019)
5	Suppressed Carrier Recombination in Janus MoSSe Bilayer Stacks: A Time-Domain Ab Initio Study; Song, Bing; Liu, Limin; Yam, ChiYung; JOURNAL OF PHYSICAL CHEMISTRY LETTERS, 10, 18 (2019)
6	Selectivity switch in transformation of CO2 from ethanol to methanol on Cu embedded in the defect carbon; Li, Shuohao; Saranya, Govindarajan; Chen, Mingyang; Zhu, Yan; SCIENCE CHINA-CHEMISTRY, 63, 5 (2020)
7	An accurate and efficient algorithm for the time-fractional molecular beam epitaxy model with slope selection; Chen, Lizhen; Zhang, Jun; Zhao, Jia; Cao, Waixiang; Wang, Hong; Zhang, Jiwei; COMPUTER PHYSICS COMMUNICATIONS, 245, (2019)
8	Controlling the emission frequency of graphene nanoribbon emitters based on spatially excited topological boundary states; Wu, Xiaoyan; Wang, Rulin; Liu, Na; Zou, Hao; Shao, Bin; Shao, Lei; Yam, ChiYung; PHYSICAL CHEMISTRY CHEMICAL PHYSICS, 22, 16 (2020)
9	Direct solver for the Cahn-Hilliard equation by Legendre-Galerkin spectral method; Chen, Lizhen; JOURNAL OF COMPUTATIONAL AND APPLIED MATHEMATICS, 358, (2019)
10	A Jacobi-Galerkin Spectral Method for Computing the Ground and First Excited States of Nonlinear Fractional Schrodinger Equation; Ma, Ying; Chen, Lizhen; EAST ASIAN JOURNAL ON APPLIED MATHEMATICS, 10, 2 (2020)
11	The Electronic Structure and Optical Properties of Two-Dimensional BiOX-YO3 (X=Cl, Br, and I; Y=Mo, W) Heterostructures; Tang, Zhen-Kun; Luo, Lin-Tao; Deng, Xiao-Hui; Zhang, Deng-Yu; Chen, Mingyang; PHYSICA STATUS SOLIDI B-BASIC SOLID STATE PHYSICS, 256, 11 (2019)
12	Subnano Ruthenium Species Anchored on Tin Dioxides Surface for Efficient Alkaline Hydrogen Evolution Reaction; Wujie Dong, Yajing Zhang, Jie Xu,Jun-WenYin,ShuyingNong,ChenlongDong,ZichaoLiu,BoweiDong,Li-MinLiu,Rui Si, MingyangChen, Jun Luo,Fuqiang Huang; CELL REPORTS PHYSICAL SCIENCE, 1, 3 (2020)

WORKSHOPS & CONFERENCES (2019-2020) 中心主办、合办的学术会议

时间 Date	会议名称 Title
2020.7.30 - 31	CSRC-ICTP Joint Workshop on Big Data, Machine Learning and Complexity Research CSRC-ICTP大数据、机器学习和复杂性研究联合研讨会
2020.7.27 - 31	1st International Workshop on Frontiers in Biomechanics and Bio-Inspired Robotics 第一届生物力学和仿生机器人前沿国际研讨会
2020.5.29 - 6.2	Kinetic Theory in CFD and Other Applications CFD中的动力学理论及其他应用
2019.12.14 - 16	The 7th International Workshop on Frontiers in Quantum Physics and Quantum Information: The workshop on topology and dynamics in non-Hermitian systems 第七届量子物理与量子信息前沿国际研讨会：非厄米系统拓扑与动力学
2019.10.27 - 30	Workshop on Modelling，Algorithm and Analysis on Complex Fluid Dynamics 复杂流体力学问题建模、算法与分析研讨会
2019.10.27	Workshop on Complex Systems and Social Computing 复杂系统与社会计算研讨会

TUTORIALS (2019-2020) 培训班

时间 Date	会议名称 Title
2020.7.27 - 31	机器学习和大数据在复杂性科学中的应用暑期培训班
2019.12.14 - 16	非厄米系统动力学演化及其拓扑性质培训班
2019.10.14 - 18	微游泳体短期培训课程
2019.09.23 - 26	材料与能源前沿科学：激发态和动力学培训班
2019.08.23 - 27	强场物理培训班

如需了解更多会议详情，请浏览：
For more details about Workshops & Conferences in CSRC, please visit：
http://www.csrc.ac.cn/events/WorkshopsConferences/

CSRC SEMINAR 专题报告

中心积极邀请国内外相关领域重要学者举行专题报告，活跃学术氛围，激发学术思维。2019-2020学术年期间中心共举办专题讲座73期（总910期）。

CSRC invites national and overseas leading researchers to give academic seminars. During academic year 2019-2020, CSRC has already held 73 seminars.

序号	DATE\日期	SPEAKER\报告人	INSITUTE\单位	TITLE/报告题目
1	2019-8-5	夏可宇 Ke-Yu Xia	南京大学现代工程与应用科学学院 College of Engineering and Applied Sciences, Nanjing University	When Chiral Light Meets Chiral Matter: Optical Nonreciprocity and Isolation
2	2019-8-6	李继春 Ji-Chun Li	美国内华达大学拉斯维加斯分校 University of Nevada-Las Vegas, USA	Analysis and Application of Some Numerical Methods for Maxwell’s Equations with Random Inputs
3	2019-8-8	Jiang-Guo (James) Liu	美国科罗拉多州立大学 Colorado State University, USA	Developing Finite Element Solvers for Poroelasticity in the 2-Field Approach
4	2019-8-12	邓伟华 Wei-Hua Deng	兰州大学数学与统计学院 School of Mathematics and Statistics, Lanzhou University	Heterogeneous and Nonergodic Diffusion: Multiscale Modelling and Simulation
5	2019-8-19	Mourad Choulli	法国洛林大学 University of Lorraine, France	Multidimensional Borg-Levinson Type Theorems
6	2019-8-19	Peter Nordlander	美国莱斯大学 Rice University, USA	Plasmonic Nanostructures: Artificial Molecules
7	2019-8-22	周珍楠 Zhen-Nan Zhou	北京大学 Peking University	Numerical Methods for Some Nonlinear Transport Equations in Biology
8	2019-8-23	张浩然 Hao-Ran Chang	四川师范大学 Sichuan Normal University	Generalized Passarino-Veltman Reduction at Finite Temperature and Chemical Potential
9	2019-8-27	凤小兵 Xiao-Bing Feng	美国田纳西大学 The University of Tennessee, USA	Recent Developments in Numerical Methods for Stochastic Stokes and Navier-Stokes Equations
10	2019-8-27	何洪兴 Hong-Xing He	美国休斯敦大学 University of Houston, USA	Direct Phasing of Protein Crystals
11	2019-8-29	崔　凯 Kai Cui	中科院力学所 Institute of Mechanics, CAS	高压捕获翼:一种全新的高超音速气动布局
12	2019-8-30	王剑威 Jian-Wei Wang	北京大学物理学院 School of Physics, Peking University	Integrated Photonics Quantum Technologies

序号	DATE\日期	SPEAKER\报告人	INSITUTE\单位	TITLE/报告题目
13	2019-9-3	徐红星 Hong-Xing Xu	武汉大学物理科学与技术学院 School of Physics and Technology, Wuhan University	Ultrasensing Optical Spectroscopy of Plasmonic Nanocavity
14	2019-9-4	谢和虎 He-Hu Xie	中国科学院数学与系统科学研究院 Academy of Mathematics and Systems Science, Chinese Academy of Sciences	High Efficient Numerical Method for Nonlinear Eigenvalue Problems
15	2019-9-5	陆　帅 Shuai Lu	复旦大学 Fudan University	Increasing Stability in the Inverse Source Problem with Attenuation and Many Frequencies
16	2019-9-10	Balázs Kovács	University of Tuebingen	L^2 Error Estimates for Wave Equations with Dynamic Boundary Conditions
17	2019-9-11	Yun-Long Xiao	南洋理工大学物理与数学科学学院 School of Physical and Mathematical Sciences, Nanyang Technological University, Singapore	The Complementary Information Principle of Quantum Mechanics
18	2019-9-12	徐　劼 Jie Xu	中国科学院计算数学与科学工程计算研究所 Institute of Computational Mathematics and Scientific/ Engineering Computing, CAS	Approximations on SO(3) by Wigner D-matrix and applications
19	2019-9-17	李有泉 You-Quan Li	浙江大学物理系 Department of Physics, Zhejiang University	Quantum Severalty: Fast Protein Folding, Speed up versus Suppression
20	2019-9-17	盛志强 Zhi-Qiang Sheng	北京应用物理与计算数学研究所 Institute of Applied Physics and Computational Mathematics	A nonlinear finite volume scheme preserving maximum principle for diffusion equation
21	2019-9-17	吴朔男 Shuo-Nan Wu	北京大学数学科学学院 School of Mathematical Sciences, Peking University	Robust discretization and solver for convection-dominated PDEs with applications to MHD multi-physics systems
22	2019-9-19	Yshai Avishai	本·古里安大学 Physics Department, Ben Gurion University, Israel	Klein Scattering, Tunnelling and Bound-states in Graphene
23	2019-9-25	Dimitrie Culcer	新南威尔士大学 University of New South Wales, Australia	Resonant Photovoltaic Effect in Doped Magnetic Topological Materials
24	2019-9-26	管习文 Xi-Wen Guan	中国科学院武汉物理与数学研究所 Wuhan Institute of Physics and Mathematics, CAS	Spin Charge Separation with Quantum Criticality
25	2019-9-27	Norbert J. Mauser	沃尔夫冈泡利研究所 & 维也纳大学 Wolfgang Pauli Institute & University of Vienna	Computational Semi-relativistic Quantum Mechanics: the Pauli Equation

CSRC SEMINAR 专题报告

序号	DATE\日期	SPEAKER\报告人	INSITUTE\单位	TITLE/报告题目
26	2019-9-29	黄旻怡 Min-Yi Huang	浙江理工大学数学科学系 Zhejiang Sci-Tech University	PT-对称量子系统的嵌入性质及模拟问题
27	2019-10-9	Qing Peng	密歇根大学安娜堡分校 University of Michigan, Ann Arbor, USA	Mystery of the Formation of <100> Loops in Irradiated Iron
28	2019-10-10	杜　洁 Jie Du	清华大学 Tsinghua University	High-order Bound-preserving Discontinuous Galerkin Method for Stiff Multispecies Detonation
29	2019-10-14	李瑞光 Ray-Kuang Lee	国立清华大学 Institute of Photonics Technologies, National Tsing Hua University, Hsinchu, Taiwan	10dB Vacuum Noise Squeezing and its Application to the Gravitational Wave Detector and On-chip Quantum Circuits
30	2019-10-15	Zaven Altounian	麦吉尔大学 Department of Physics, McGill University, Canada	General Motors and NdFeB Magnets
31	2019-10-16	Rosario Fazio	International Center for Theoretical Physics (ICTP), Italy	Topological Fractional Pumping in Optical Lattice
32	2019-10-21	Yuriy Maistrenko	FZ Jülich (Germany), TU Lodz (Poland), and NASU (Ukraine)	New Trends in Complex Networks: Chimera States and Solitary Oscillators
33	2019-10-21	Francis Filbet	图卢兹第三大学 Université Paul Sabatier, Toulouse III, France	Asymptotically Stable Particle-In-Cell Methods for the Vlasov-Poisson System with a Strong External Magnetic
34	2019-10-22	毛士鹏 Shi-Peng Mao	中国科学院数学与系统科学研究院 Academy of Mathematics and Systems Science, CAS	Analysis of Finite Element Methods for Incompressible Magnetohydrodynamic Flows with Magnetic Vector Potential Formulations
35	2019-10-25	赵宏凯 Hong-Kai Zhao	加州大学尔湾分校 Department of Mathematics, University of California, Irvine	Intrinsic Complexity: From Approximation of Random Vectors and Random Fields to Solutions of PDEs
36	2019-10-29	吕　博 Bo Lü	天津大学 Tianjin University	Focus on the Surface Andreev Bound States of Unconventional Superconductors
37	2019-10-30	张文献 Wen-Xian Zhang	武汉大学 School of Physics and Technology, Wuhan University	Generation and Storage of Massively Entangled States in a Spin-1 BEC
38	2019-11-4	冉仕举 Shi-Ju Ran	首都师范大学 Department of Physics, Capital Normal University	Efficient Encoding of Matrix Product States into Quantum Circuits of One- and Two-Qubit Gates

序号	DATE\日期	SPEAKER\报告人	INSITUTE\单位	TITLE/报告题目
39	2019-11-5	崔　明 Ming Cui	北京工业大学应用数理学院 College of Applied Sciences, Beijing University of Technology	Numerical Methods for Nonlinear Aerosol Dynamic Equations
40	2019-11-7	George Japaridze	格鲁吉亚国家科学院，安德罗尼卡什维利物理研究所 Georgian National Academy of Sciences, Andronikashvili Institute of Physics	Ground State Phase Diagram of the Spin S=1/2 XXZ Heisenberg Chain with Alternating Dzyaloshinskii-Moriya Interaction
41	2019-11-11	张　威 Wei Zhang	中国人民大学 Renmin University of China	具有SU(N)自旋对称性的哈伯德模型中的平带铁磁相
42	2019-11-12	杨欢欢 Huan-Huan Yang	汕头大学 Department of Mathematics, Shantou University	Problems in Patient-Specific Modeling of Electrocardiology
43	2019-11-12	Yuki Ueda	香港理工大学 Department of Applied Mathematics, The Hong Kong Polytechnic University	The Inf-Sup Condition and Error Estimate of the Nitsche Method for Evolutionary Diffusion-Advection-Reaction Equations
44	2019-11-12	Lev Shchur	朗道理论物理研究所 Landau Institute for Theoretical Physics	Acceptance Rate is a Thermodynamic Function in Local Monte Carlo Algorithms
45	2019-11-14	刘　歆 Xin Liu	中国科学院数学与系统科学研究院 Academy of Mathematics and Systems Science, CAS	Parallelizable Approaches for Nonsmooth Optimization Problems with Orthogonality Constraints
46	2019-11-14	徐立伟 Li-Wei Xu	电子科技大学数学科学学院 School of Mathematical Sciences, University of Electronic Science and Technology of China	New Results on Coupling Methods for Scattering Problems on Unbounded Domains
47	2019-11-15	周　知 Zhi Zhou	香港理工大学 Department of Applied Mathematics, The Hong Kong Polytechnic University	Numerical Analysis of Subdiffusion with a Time-Dependent Coefficient
48	2019-11-18	郭领阵 Ling-Zhen Guo	德国马克思·普朗克光学研究所 Max Planck Institute for the Science of Light (MPL), Erlangen, Germany	Non-Markovian Quantum Optics: Spontaneous Emission of a Giant Artificial Atom
49	2019-11-19	Georgios Akrivis	希腊约阿尼纳大学 Department of Computer Science and Engineering, University of Ioannina, Greece	On the Unconditional Stability of Implicit-Explicit BDF Methods
50	2019-11-26	周　涛 Tao Zhou	中国科学院数学与系统科学研究院 Academy of Mathematics and Systems Science, CAS	时间分数阶相场模型的能量稳定性

CSRC SEMINAR 专题报告

序号	DATE\日期	SPEAKER\报告人	INSITUTE\单位	TITLE/报告题目
51	2019-11-27	李东方 Dong-Fang Li	华中科技大学 Huazhong University of Science and Technology	A Novel Numerical Approach to Time-Fractional Parabolic Equations with Nonsmooth Solutions
52	2019-11-28	田　圃 Pu Tian	吉林大学生命科学学院 College of Life Sciences, Jilin University	Generalized Solvation Free Energy, Neural Network Implementation and Application in Structural Model Assessment, Refinement and Design
53	2019-11-28	陈伟强 Wei-Qiang Chen	南方科技大学 Southern University of Science and Technology	Classification of Topological Phases in One Dimensional Interacting Non-Hermitian Systems and Emergent Unitarity
54	2019-12-2	Sebastian Franz	德累斯顿工业大学 Technical University of Dresden, Germany	Variational Methods for Evolutionary Systems
55	2019-12-2	乔中华 Zhong-Hua Qiao	香港理工大学 The Hong Kong Polytechnic University	Semi-Implicit Methods for Phase Field Equations
56	2019-12-10	黄秋梅 Qiu-Mei Huang	北京工业大学 Beijing University of Technology	Discontinuous Galerkin Methods for Nonlinear Delay Differential Equations
57	2019-12-11	刘继军 Ji-Jun Liu	东南大学 Southeast University	Image Restoration from Noisy Incomplete Frequency Data by Alternative Iteration Scheme
58	2019-12-13	钟　勇 Yong Zhong	华南理工大学 South China University of Technology	仿生机器鱼的设计与控制研究
59	2019-12-13	范　桁 Heng Fan	中国科学院物理研究所 Institute of Physics, CAS	超导量子计算进展及谷歌量子优势解析
60	2019-12-13	刘海文 Hai-Wen Liu	北京师范大学物理学系 Department of Physics, Beijing Normal University	Discrete Scale Invariance in Topological Semimetal
61	2019-12-16	Ming-Tao Xia	加州大学洛杉矶分校 University of California, Los Angeles	PDE Models of Adder Mechanisms in Cellular Proliferation
62	2019-12-19	王　成 Cheng Wang	麻省大学达特茅斯分校 University of Massachusetts Dartmouth	A Weakly Nonlinear, Energy Stable Scheme for the Strongly Anisotropic Cahn-Hilliard System
63	2019-12-23	汤华中 Hua-Zhong Tang	北京大学数学科学学院 School of Mathematical Sciences, Peking University	相对论流体力学方程组的可容许状态集与保物理约束的数值方法

序号	DATE\日期	SPEAKER\报告人	INSITUTE\单位	TITLE/报告题目
64	2019-12-24	曹礼群 Li-Qun Cao	中国科学院数学与系统科学研究院 LSEC, NCMIS, ICMSEC, Academy of Mathematics and Systems Science, CAS	Multiscale Analysis and Algorithms in Electrodynamics of Novel Materials and Devices
65	2019-12-24	Jian-Lin Xia	普渡大学 Purdue University	Analytical Low-rank Compression via Proxy Point Selection and Contour Integration
66	2019-12-26	赵润东 Run-Dong Zhao	杜克大学 Duke University	Relativistic Energy Band Theory and Its Code Development in the FHI-aims Code Package
67	2019-12-27	张　元 Yuan Zhang	郑州大学物理学院 School of Physics, Zhengzhou University	表面增强拉曼中的分子集体效应
68	2020-1-6	Yue Yu	理海大学 Lehigh University, USA	A Multiscale/Multiphysics Coupling Framework for Bioprosthetic Heart Valves (BHVs) Damage
69	2020-1-7	高河伟 He-Wei Gao	清华大学 Tsinghua University	CT with Non-Standard Trajectory: from Concept to Product
70	2020-1-15	王　峙 Zhi Wang	科罗拉多大学 University of Colorado	Restoring E vs k Band Structure Dispersion in Low Symmetric, Disordered Systems
71	2020-1-17	刘刚钦 Gang-Qin Liu	中国科学院物理研究所 Institute of Physics, CAS	高压下的自旋量子传感
72	2020-1-17	赵　楠 Nan Zhao	北京计算科学研究中心 Beijing Computational Science Research Center	基于热原子的磁强计和核磁共振陀螺物理研究
73	2020-1-20	郭海龙 Hai-Long Guo	墨尔本大学 University of Melbourne	Hessian Recovery Based Finite Element Methods for the Cahn-Hilliard Equation

如需了解更多报告信息，请浏览：
For more details about Seminars in CSRC, please visit:
http://www.csrc.ac.cn/events/seminars/

To facilitate scientific interactions between CSRC scientists and scientists elsewhere, CSRC has developed partnerships with several universities and research institutions around the world. Besides engaging in long-term scientific collaborations, CSRC staff also host conferences, workshops, and seminars with collaborators. Through these activities, CSRC is working towards extending the frontier in computational science research and improving its competitive edge and prestige.

北京计算科学研究中心非常重视与科研机构及高校的合作，在积极组织承办国内外学术会议之时，也鼓励科研人员与国内外其他科研机构之间的互访交流，扩展学术视野和扩大学术影响。目前已与国际数所科研机构签署了合作协议，为打造中心作为国际一流的开展计算科学及相关学科交叉研究的综合平台而不断努力。

INTERNATIONAL PARTNERSHIP 国际及地区合作伙伴

UNIVERSITY OF GOTHENBURG, SWEDEN
瑞典哥德堡大学

UNIVERSITY OF OSLO, NORWAY
挪威奥斯陆大学

INSTITUTE FOR QUANTUM COMPUTING, UNIVERSITY OF WATERLOO, CANADA
加拿大滑铁卢大学

NORWEGIAN UNIVERSITY OF SCIENCE AND TECHNOLOGY, NORWAY
法国原子能与可替代能源委员会

UNIVERSITY OF WARWICK, UK
英国华威大学

CENTER FOR SIMULATIONAL PHYSICS, THE UNIVERSITY OF GEORGIA, USA
美国乔治亚大学

NTNU
NORWEGIAN UNIVERSITY OF SCIENCE AND TECHNOLOGY, NORWAY
挪威科技大学

THE HONG KONG UNIVERSITY OF SCIENCE AND TECHNOLOGY, CHINA
香港科技大学

COLLEGE OF SCIENCES, OLD DOMINION UNIVERSITY, USA
美国奥多明尼昂大学

RIKAGAKU KENKYUSHO/INSTITUTE OF PHYSICAL AND CHEMICAL RESEARCH, JAPAN
日本理化学研究所

DEPARTMENT OF PHYSICS, NATIONAL TAIWAN NORMAL UNIVERSITY, CHINA
国立台湾师范大学

DEPARTMENT OF PHYSICS, THE CHINESE UNIVERSITY OF HONG KONG, CHINA
香港中文大学

HEARNE INSTITUTE FOR THEORETICAL PHYSICS, LOUISIANA STATE UNIVERSITY, USA
美国路易斯安那州立大学

KOREA INSTITUTE FOR ADVANCED STUDY, SOUTH KOREA
韩国高等科学院

Since its establishment, more than 5000 visiting scholars from over 20 countries and regions have visited CSRC. CSRC faculty members went out for academic eschange for more than 1800 times. During the academic year 2019-2020, CSRC has hosted over 200 visiting scholars.

CSRC warmly welcomes scientists around the world to visit for collaboration and exchange. CSRC frequently hosts academic activities such as conferences, workshops, and seminars together with its counterparts. Living allowance and housing subsidies are provided during visitor's stay at CSRC.

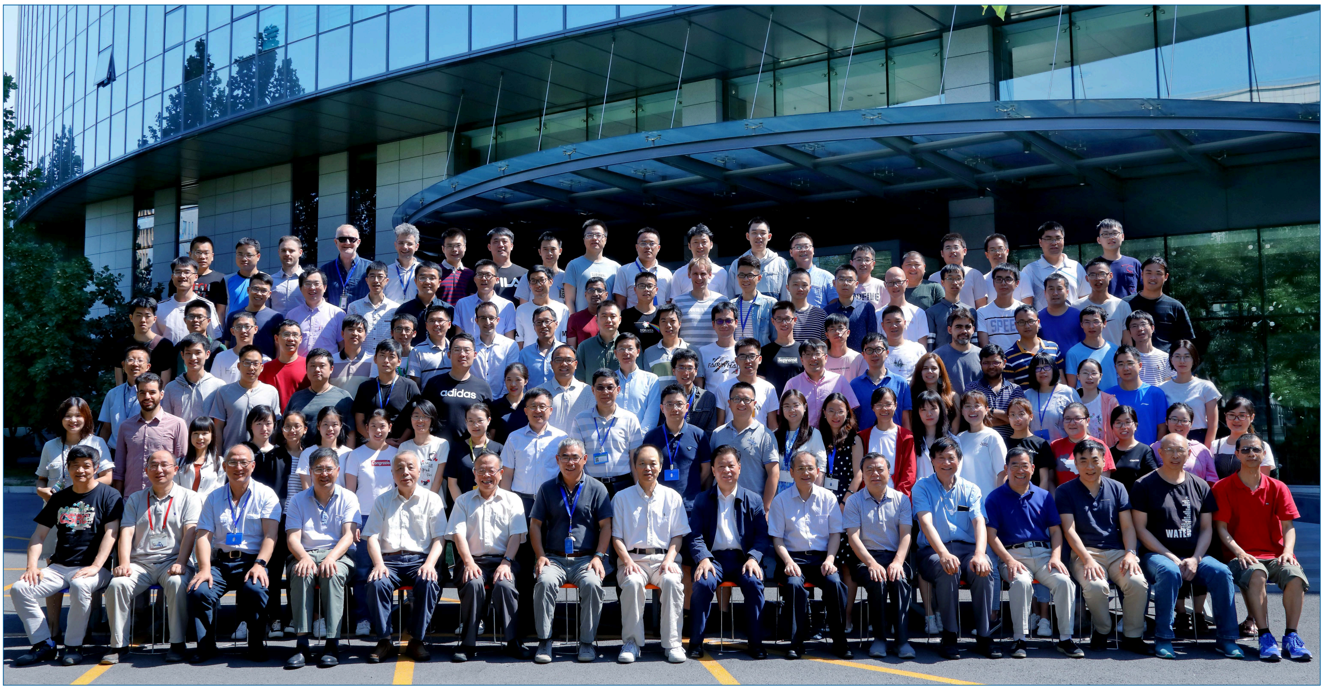

中心在加强与科研机构及高校的合作交流，积极组织承办国内外学术会议之余，也鼓励科研人员与国内外其他科研机构之间的互访交流。成立至今，中心接待了来自20多个国家和地区的访问学者超过5000余人次，中心科研人员外出参加学术交流活动超过2000余人次。2019-2020学术年期间，中心来访学者超过了200人次；同时年初因疫情影响，访问交流逐渐向线上等多元化模式发展。

中心欢迎国内外各机构相关专业的科研人员和教师，以访问学者和客座研究人员的形式来访，进行短期或长期合作研究。中心也与同行们一起举办学术活动如会议、讲习班等。在中心访问期间，中心将提供一定的生活和住房补贴。

〖 中心办公楼效果图 〗 CSRC building

〖 中关村软件园一二期鸟瞰图 〗 ZPark

〖 大厅 〗 Lobby

〖 中庭院 〗 Courtyard

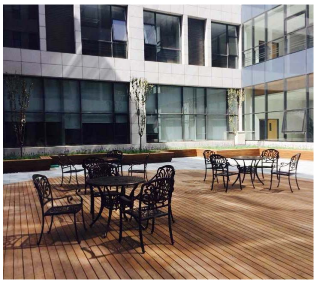

〖 学术报告厅 〗 Auditorium

Seminar Rom 〖 学术会议室 〗

Common 〖 学术讨论区 〗

〖 博士后办公室 〗 Postdoc Office

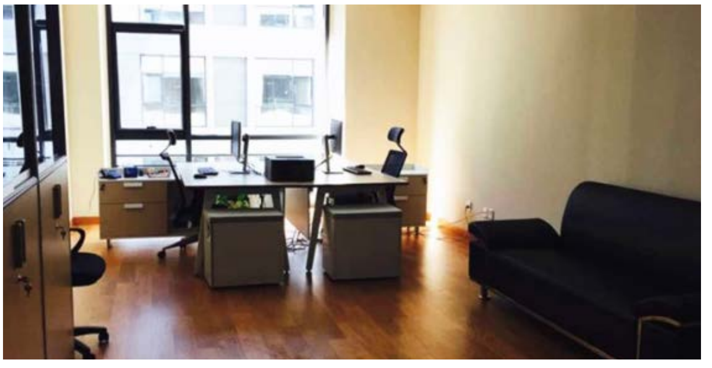

Visitor Office 〖 客座教授办公室 〗

〖 访问学者办公室 〗 Visitor Office

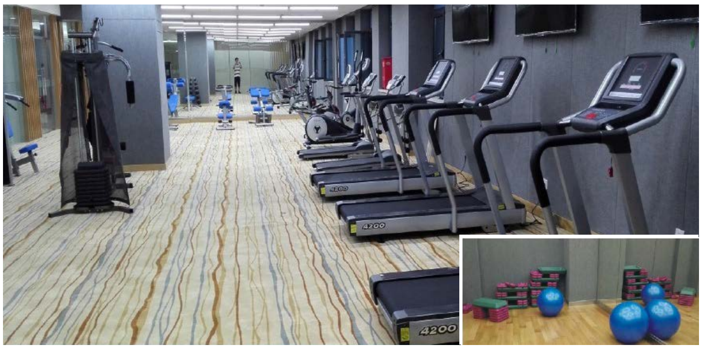

〖 健身房 〗 Gym

〖 餐厅 〗 Canteen

天河二号-计科中心集群系统

CLUSTER TIANHE2-JK

The CSRC is equipped with the state of art high performance computing facilities, which include a dedicated in-house 14,000+ core cluster TianHe2-JK in addition to many smaller clusters.

For more details about CSRC Computing, please visit: http://www.csrc.ac.cn/en/facility/cmpt/

14112cores

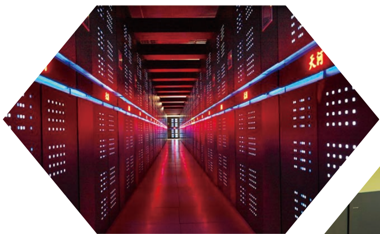

131.1TB Memory

1440TB disks
2304TB back-up disks

80Gb/s QDR